Molecular principles of mTORC1 localization and signaling

Doctoral thesis

for

the award of the doctoral degree

of the Faculty of Mathematics and Natural Sciences

of the University of Cologne

submitted by

Aishwarya Atul Acharya

accepted in the year 2025

“Imagination is more important than knowledge. Knowledge is limited. Imagination encircles the world.”

– *Albert Einstein*

“The Universe is under no obligation to make sense to you.”

– *Neil deGrasse Tyson*

Abstract

Nutrient sensing is essential for proper cellular function — to ensure that supply meets demand and to adjust the metabolic program from anabolism to catabolism if resources are scarce. The mammalian/mechanistic target of Rapamycin complex 1 (mTORC1) is a growth-promoting signaling complex that is critical for sensing nutrient availability and regulating cellular processes accordingly. Information about nutrient availability is conveyed from a complex upstream regulatory network to mTORC1 via two small GTPases — Rags and Rheb, which primarily influence mTORC1 lysosomal localization and activity, respectively.

A large amount of research effort investigating the intricate mechanisms by which mTORC1 is recruited to the lysosomal membrane has culminated in a model which proposes that the nucleotide-binding state of the Rag GTPases is responsive to nutrient sufficiency, such that mTORC1 is recruited to lysosomes by Rags in their active configuration and delocalized away from lysosomes when Rags are in their inactive configuration due to nutrient insufficiency. However, how mTORC1 is released from lysosomes under basal conditions, conceivably an imperative for sustaining the activity of mTORC1 toward its non-lysosomal substrates, remains elusive. Here, I show that mTORC1 regulates its own lysosomal localization in an activity-dependent manner by impacting the GATOR1-RagA axis. Specifically, inactive mTORC1 triggers locking of the Rags in their active conformation, impairing release from lysosomes unless prior activation has taken place. This reveals that mTORC1 itself triggers a molecular fail-safe mechanism to prevent the release of non-activated complexes, thus preventing its futile cycling, and suggests that mTORC1 activity and localization bilaterally regulate each other.

A key input to mTORC1 is its direct activator Rheb, which lies downstream of the Tuberous Sclerosis Complex (TSC), a potent inhibitor of the pathway. Past work has indicated that in TSC loss-of-function models, not only mTORC1 activity but also its localization is affected, but the underlying molecular cause was not fully decoded. Here, I demonstrate that hyperactive Rheb drives the forced lysosomal localization of mTORC1 by functioning as a secondary anchor on the lysosomal landscape.

In sum, this work unravels two important facets of mTORC1 regulation that affect its localization and signaling.

Table of Contents

1 Introduction

Awareness of one's own resources is a crucial aspect of life at each level of organization of a biological system— cell, tissue, organ, and organism. The ability of cells to perceive steady-state amounts of intracellular and extracellular nutrients as well as to detect fluctuations in said amounts lies at the very crux of maintaining proper cellular function. Indeed, even the simplest of prokaryotic organisms have developed strategies for sensing the availability of biomolecules in their environment, to determine if conditions are favorable for growth and survival [1]. In eukaryotes, from unicellular organisms such as yeast to multicellular organisms such as humans, concomitant with the increase in complexity across evolution, several conserved nutrient sensing and signaling pathways have emerged to acquire and convey information about a myriad of intrinsic and extrinsic factors. These pathways are tightly regulated through diverse mechanisms and, in turn, regulate a host of downstream processes to ensure that homeostatic balance is maintained between resource availability and cellular needs. One such pathway that lies at the nexus of nutrient sensing is the mTORC1 signaling pathway.

1.1 mTORC1 is a nodal kinase complex

The mechanistic/mammalian target of Rapamycin complex 1 (mTORC1) is often regarded as the 'master regulator of growth and metabolism [2-4]. This is not entirely unfounded, as it integrates an array of upstream cues about nutrient availability and environmental stresses and induces a corresponding physiological response in the cell by regulating a host of downstream processes. Overall, active mTORC1 promotes anabolism and suppresses catabolism.

The earliest studies identified the yeast homolog Tor1 in yeast, and later this was identified in humans as the target for the immunosuppressant macrolide, Rapamycin, which gave it its name [5].

1.1.1 Composition of mTORC1

mTOR forms the catalytic component of two complexes — mTORC1 and mTORC2 — which have similar architectures but are distinct in their accessory proteins, sensitivity to

Rapamycin and cellular function. mTORC1 is nucleated by three core proteins— mTOR, RAPTOR and mLST8.

mTOR is a serine/threonine kinase belonging to the PI3K-related protein kinases (PIKK) family of proteins. It comprises of the following domains: N-terminal HEAT (huntingtin, elongation factor 3, a subunit of protein phosphatase 2A and TOR) repeats, FAT (FRAP, ATM and TRRAP) domain, the FKBP12–rapamycin binding (FRB) domain, the catalytic kinase domain; and the C- terminal FATC domain.

RAPTOR is the unique accessory component of mTORC1, which is involved in substrate recruitment by binding to the TOS motifs (TOR signaling motifs) that are embedded in the sequences of several canonical substrates. It is also responsible for mediating interaction with the Rag GTPases, thus enabling proper subcellular localization.

mLST8 (mammalian lethal with SEC13 protein 8) is the second component that is shared between mTORC1 and mTORC2. It has been shown to enhance mTOR-RAPTOR interaction, but its loss does not affect complex activity [6,7].

DEPTOR (DEP domain-containing mTOR interacting protein) is an intrinsic kinase inhibitor of both mTORC1 and mTORC2; however, DEPTOR deletion only results in increased mTORC1 activity [8]. When DEPTOR is bound to mTOR, it attains a non-activated conformation [9]. It is also a substrate for both mTORC1 and mTORC2, and its mTORC1-mediated phosphorylation causes its degradation [8,10].

PRAS40 (proline-rich AKT substrate 40 kDa) is another endogenous inhibitor of mTORC1 that is recruited via RAPTOR. It has a TOS motif and exerts its inhibitory activity by competitively blocking other substrates from binding to the TOS recognition site on RAPTOR [11,12]. PRAS40 is also directly phosphorylated by mTORC1, causing its release [13].

mTORC2 shares mTOR, mLST8 and DEPTOR with mTORC1; in addition, the complex comprises of RICTOR (rapamycin-insensitive companion of mTOR), mSIN1 (MAPK-interacting protein 1), and PROTOR1/2 [14,15]. RICTOR and mSIN1 are the unique, defining components of mTORC2. Further, the rapamycin insensitivity of mTORC2 arises from the structural attributes of RICTOR and mSIN1 [16]. However, it is important to note that chronic

Rapamycin treatment has been shown to inhibit mTORC2 in certain cell lines. mTORC2 is primarily involved in regulating cell proliferation and survival via regulation of AGC kinase family proteins. The rest of this thesis primarily focuses on mTORC1.

1.1.2 Structure of mTORC1

mTORC1 exists as a dimer in the cell, with two copies each of mTOR and RAPTOR; the dimers form a lozenge structure with a cavity in the center. The dimerization occurs along the mTOR HEAT repeats and the mTOR-RAPTOR interface [17,18]. Structural evidence has shown that inhibition by FKBP12-Rapamycin and PRAS40 occurs due to their binding to the FRB domain that occludes substrate entry into the active site of mTOR, by narrowing the cleft of the active site from ~20 Å to ~10 Å (ref. [6]).

1.1.3 Catalytic activity of mTORC1

The active site of mTOR contains a substrate-binding pocket formed of the activation loop, the FATC domain and portions of the mLST8 binding site. The FRB domain and mLST8 collectively confer specificity by narrowing the catalytic cleft, and preventing binding of non-specific proteins [6,17]. Further, the FRB domain of mTOR acts as a secondary substrate binding site that cooperates with the TOS recognition site on RAPTOR to recruit mTORC1 targets that contain the TOS-motif [12]. Another feature of mTORC1 kinase activity is that it is proline-directed, with mTOR sites containing mainly a proline residue at position +1. Based on all known phosphosites, mTOR target sites are more likely to be a serine than a threonine residue [19].

1.1.4 Subcellular distribution of mTORC1

mTORC1 was found to localize to lysosomes in nutrient sufficient conditions [20]. However, this localization is not static; rather, a population of mTORC1 was found to dynamically shuttle between the lysosomal surface and the cytosol due to merely transient associations of mTORC1 with lysosomes [21]. Further, only around 50% of the total mTORC1 population was lysosomal at any given time in nutrient-replete conditions [21]. Changes in subcellular localization is one of the main processes by which mTORC1 activity is regulated. Further sections will elaborate on the precise mechanisms (known so far) by which this takes place.

In addition to lysosomes, presence of mTORC1 has also been noted at other organelles such as the Golgi, mitochondria, and the ER [22-24]. A nuclear pool of mTOR has also been detected, and although other known components and regulators of mTORC1 have also been found in the same compartment, the composition and precise function of nuclear mTORC1 remains elusive, although it has been implicated in transcriptional regulation [25-28]. Additionally, mTORC1 has been found in proximity of focal adhesions (FAs) [29].

1.1.5 Pharmacological inhibition of mTORC1

Rapamycin (Sirolimus) was the original prototype that led to the development of the first generation of mTORC1 inhibitors, known as 'rapalogs'. Rapamycin is a naturally-derived macrolide first isolated from *Streptomyces hygroscopicus,* a soil bacterium found on the island of Rapa Nui with immunosuppressive properties [30,31]. Its mode of action for inhibition of mTORC1 is unique: it forms a gain-of-function complex with FKBP12 (FK506-binding protein), an endogenous protein, which allosterically binds to the FRB domain of mTOR in an irreversible manner. In doing so, it sterically hinders access of substrates to the catalytic site. However, the inhibition brought about by Rapamycin is considered to be incomplete: while certain larger substrates (such as S6K) are completely inhibited, other smaller substrates (such as 4E-BP1) are partially inhibited, while others (such as TFEB) are completely insensitive. This differential effect of Rapamycin on different *bona fide* mTORC1 substrates has been associated with the specific sequences of the target peptides [32].

The second generation of inhibitors, comprised of ATP-competitive inhibitors like Torin1, bind to the catalytic site of mTOR thus leading to complete inhibition of both mTORC1 and mTORC2 [33].

1.2 Key molecular players in the mTORC1 signaling pathway

The regulation of mTORC1 activity occurs through coordinated action of a number of proteins that, according to the predominant model, occupy a position in one of the following two signaling arms. This section aims to introduce the key molecules involved in the pathway, while their role in nutrient sensing will be elaborated on in Section 1.3.

1.2.1 The Rag GTPase signaling arm

This signaling arm upstream of mTORC1 converges on the Rag GTPases, and is considered to primarily control the localization of mTORC1 to the lysosomal limiting membrane. Of note, this axis plays a pivotal role in enabling amino acid sensing by mTORC1.

Rag GTPases

The Rag (ras-related GTP binding) GTPases are the key factors that recruit mTORC1 to the lysosomal surface in amino acid-replete conditions [20,34]. Unlike other small GTPases, they are obligate heterodimers, with one 'small' Rag (A or B) coupled with one 'large' Rag (C or D) [35]. The Rag paralogues exhibit very high sequence homology, with RagA and RagB showing 90% similarity, and RagC and RagD showing 80% identity. This led to the assumption that the paralogues were functionally redundant; however, recent studies have highlighted functional distinctions between members of each pair [36,37]. In their active conformation in nutrient-sufficient conditions, RagA/B is GTP-bound and RagC/D is GDP-bound; conversely, the Rags adopt an inactive configuration wherein RagA/B is GDP-bound and RagC/D is GTP-bound in cases of nutrient insufficiency [20,34]. The nucleotide loading of the Rags is tightly controlled by GAPs (GTPase-activating proteins) and GEFs (Guanine nucleotide exchange factors), mentioned below. Unlike the majority of Ras-related proteins, the Rags to not contain any lipid modification through which they can achieve membrane anchorage. Therefore, for localizing to lysosomes, they rely on binding to the LAMTOR complex.

LAMTOR

The LAMTOR complex (also referred to as the Ragulator complex) is a pentameric complex composed of LAMTOR1 (late endosomal/lysosomal adaptor and MAPK and MTOR activator 1; also known as p18), LAMTOR2 (p14), LAMTOR3 (MP1), LAMTOR4 (C1ORF59) and LAMTOR5 (HBXIP) [38]. It docks onto the lysosomal membrane through myristoylation and palmitoylation modifications present on its N-terminal tail [39,40]. The complex is structured in a way that LAMTOR2–LAMTOR3 and LAMTOR4–LAMTOR5 heterodimers are wrapped together by the N- and C-termini of LAMTOR1. Initially, the LAMTOR complex was considered a GEF for RagA [41]; however, this claim was later rectified in a publication which showed that LAMTOR controlled RagC loading by

stimulating release of GTP, but not GDP, thus acting in a non-canonical fashion to push the Rag GTPases into their active state [42].

SLC38A9

SLC38A9 (solute carrier family 38 member 9, also known as neutral amino acid transporter 9) is an AA transporter that resides on the lysosomal membrane. With respect to its transporter activity, intralysosomal Arg stimulates the efflux of Leu and other non-polar essential amino acids from the lysosomal lumen [43-47]. Structurally, it comprises of 11 transmembrane domains and an N-terminal cytosolic tail that contacts LAMTOR and the Rags; this contact enables its function as a non-canonical GEF for RagA[42,48].

v-ATPase

v-ATPase is the lysosomal vacuolar H+-ATPase, that pumps protons into the lysosomal lumen by utilizing ATP. This generation of acidic pH is necessary for activation of many lysosomal resident hydrolases [49]. The v-ATPase extensively interacts with the Rag-LAMTOR complex on the lysosomal membrane to bring about amino acid-dependent activation of RagA/B in an 'inside-out' mechanism [50,51].

GATOR1

The GATOR1 (GAP activity towards the Rags 1) complex is a trimeric protein complex comprised of DEPDC5 (DEP domain-containing 5), NPRL2 (nitrogen permease related-like 2), and NPRL3 (nitrogen permease related-like32), which has been designated as the GAP for RagA/B, and thus negatively regulates mTORC1 activity [52]. The GAP activity of GATOR1 stems from the 'arginine finger' residue that is contained by NPRL2. DEPDC5 acts as an intrinsic inhibitor of the complex, suppressing its GAP activity toward RagA/B [53].

GATOR2

GATOR2 is a complex that lies upstream of GATOR1 and negatively regulates it, thus activating the mTORC1 pathway. It is composed of five subunits: MIOS (meiosis regulator for oocyte development), WDR24 (WD repeat domain 24), WDR59 (WD repeat domain59), SEH1L (seh1 like nucleoporin) and SEC13 (sec13 homolog nuclear pore and

COPII coat complex component). Mechanistically, the WDR24 E3 ligase activity triggers NPRL2 ubiquitination, thus inhibiting it GATOR1 GAP activity [54].

KICSTOR

The KICSTOR complex, composed of KPTN (Kaptin), ITFG2 (integrin-α FG-GAP repeat containing 2) and SZT2 (C12orf66 and seizure threshold 2), is thought to have a role in scaffolding GATOR1 to the lysosomal membrane, in proximity to the Rag-LAMTOR complex [55,56]. In vitro, it has been shown to be dispensable for GATOR1 GAP activity.

FLCN-FNIP1/2

The FLCN (folliculin) – FNIP1/2 (FLCN-interacting proteins 1 and 2) complex is the designated GAP for the RagC/D GTPases. Stimulating the GAP activity of RagC/D induces a switch to its GDP-bound, active conformation; thus FLCN-FNIP1/2 is a positive regulator of mTORC1 activity.

1.2.2 The TSC-Rheb signaling arm

This signaling arm upstream of mTORC1 has predominantly been considered the growth factor signaling arm of the pathway which is involved in stimulating mTORC1 activity.

Rheb

Rheb (Ras homologue enriched in brain), a small GTPase belonging to the Ras superfamily of GTPases, is the direct upstream activator of mTORC1 that induces its catalytically active state by binding directly to the mTOR subunit [6,57]. More specifically, when RHEB is GTP-loaded, its binding to mTOR induces a conformational change within the FAT domain that increases the proximity between the catalytic residues within the active site and the phosphate groups of ATP. This facilitates substrate phosphorylation. Conversely, when mTOR is not bound to RHEB, the greater distance between the catalytic residue of mTOR and the bound ATP impedes catalytic activity from taking place [6,57]. This highlights the prominent role of Rheb in stimulating the mTORC1 pathway. It is important to note that while Rheb can bind to mTOR even when lacking GTP, it can stimulate mTORC1 activity only when GTP-bound.

Although highly similar to other small GTPases, due to subtle structural differences in the

Switch I and II regions, Rheb exhibits a much lower intrinsic GTPase activity [57]. Another feature of Ras proteins is that they contain a carboxy-terminal hypervariable region (HVR) followed by the CAAX motif (where A is an aliphatic amino acid, and X is a C-terminal amino acid) [58]. Rheb also has a CAAX motif (CSVM), but due to the lack of basic amino acid residues or palmitoylated cysteines in the HVR, instead of being targeted to the plasma membrane, Rheb obtains a farnesylation moiety. This farnesylation of Rheb occurs post-translationally in a two-step reaction involving the enzymes Rce1 and Icmt1 [58]. Rheb farnesylation allows it to anchor to endomembranes such as lysosomes, which has been reported as necessary for its potential to activate mTORC1 [59,60]. The biochemical properties of farnesylation also endow Rheb with the ability to weakly interact with membranes, thus allowing for only transient interactions [61].

In mammals, two different RHEB genes have been identified: RHEB1 and RHEB2, the latter coding for the protein RhebL1 (or Rheb2). The genes share 54% identity and 74% similarity, and both Rheb and RhebL1 proteins undergo similar post-translational processing. RhebL1 has been reported to activate mTORC1, thus indicating functional overlap between the homologs [62,63].

Rheb is directly regulated by its upstream negative regulator, the TSC complex, which inhibits Rheb function by exerting GAP activity.

TSC

The TSC (tuberous sclerosis complex) is a heterotrimeric complex consisting of TSC1 (hamartin), TSC2 (tuberin) and TBC1D7 in a 2:2:1 stoichiometry [64,65]. The TSC2 subunit harbors GAP activity toward Rheb; it contains a GAP domain at the C-terminal end that employs an arginine thumb to induce GTP hydrolysis [66,67]. Although it does not exhibit GAP activity, TSC1 has been reported as crucial for TSC complex function, as it facilitates proper folding of TSC2 and prevents its proteasomal degradation [68,69]. TBC1D7 participates in the complex via an interaction with TSC1, and has been shown to increase complex stability [70].

TSC operates downstream of several signaling pathways such as PI3K-AKT, RAS-ERK and AMPK, and thus acts as a receiver for several signaling inputs [71,72]. Further, it becomes

activated when cells are subjected to several kinds of stresses, such as hypoxia (via REDD1), amino acid or growth factor starvation, energetic stress, osmostress, or pH changes [72,73]. Thus, it integrates multiple inputs and conveys an inhibitory signal to mTORC1 through Rheb.

To carry out its inhibitory function, TSC undergoes translocation to lysosomes upon nutrient starvation or stress stimuli, where it then exerts its GAP activity toward Rheb and subsequently downregulates mTORC1 [74-76]. GAP-independent inhibition of mTORC1 by TSC through steric hindrance has also been described as a mechanism of TSC-driven mTORC1 downregulation [77]. Thus far, five different modes of lysosomal anchoring of the TSC complex have been described: (1) through binding of TSC2 to the inactive Rag dimer [78], (2) through TSC2-Rheb interaction [76], (3) through the binding of TSC1 to lysosomal PIPs (phosphatidylinositol phosphates) [79], (4) through G3BPs and their interaction with LAMP1/2 proteins located on lysosomes [80], and (5) through the TSC:WIPI3 interaction [81]. A systematic study of the relative contribution of each of the anchoring machineries is still pending, and whether they are different for distinct stimuli remains unclear.

1.2.3 Convergence of the two arms

The model of mTORC1 activation acting as a ‘coincidence detector’ was first proposed in 2008 with the discovery of the Rag GTPases and their role in the mTOR pathway [20]. According to the model, the Rag GTPases recruit mTORC1 to lysosomes when amino acids are available, without affecting mTORC1 activity. At the lysosomal surface, mTORC1 encounters Rheb which is active only if inputs from growth factor signaling are stimulatory [76]. Thus, mTORC1 is activated only when both criteria are fulfilled.

While this concept is promising in its simplicity, the past decade of research since its conception has shown that the two signaling arms are not entirely discrete, and each is involved in sensing of multiple upstream stimuli. Thus, the ‘coincidence detector’ model requires updating.

1.3 Nutrient inputs that regulate the mTORC1 pathway

1.3.1 Amino acid sensing

Amino acid availability directly impacts Rag GTPase nucleotide loading through the action of several of its regulators. When amino acids are depleted, GATOR2 is inhibited due to binding of several amino acid sensors [82]. This allows GATOR1 to exert its GAP activity toward RagA/B GTPase, causing a switch from its GTP- to GDP-bound state. Due to crosstalk between the two subunits of the Rag dimer, in the absence of amino acids, RagC also switches from its GDP- to GTP- bound state [83]. Another possible explanation for this switch has been recently described: GATOR1 makes contacts not just with RagA but also RagC, and through a spatial constraint mechanism coordinates nucleotide-loading of both subunits [53]. Thus, the inactive configuration of the Rag dimer is achieved, which has reduced affinity for mTORC1, causing its delocalization away from lysosomes, and hence lack of proximity to its direct upstream activator Rheb, leading to diminished mTORC1 signaling.

In this state of amino acid starvation, the FLCN-FNIP1/2 complex is recruited to the lysosomal membrane due to increased interaction with RagA-GDP [84]. Despite its lysosomal localization and proximity to its substrate (GTP-bound RagC), it remains in a state where its GAP activity is repressed [21]. This is termed as the LFC (lysosomal folliculin complex).

Upon restimulation with amino acids, the inhibition on GATOR2 is released, which in turn relieves the GATOR1-mediated inhibition on RagA/B. Further, through the GEF activities of SLC38A9, in concert with the LAMTOR and v-ATPase, loading of RagA/B with GTP is induced [42,48]. Additionally, upon amino acid stimulation, SLC38A9 causes the destabilization of the LFC, activating FLCN GAP activity toward RagC [43]. When RagA is GTP-bound and RagC is GDP-bound, the Rag-RAPTOR binding affinity is higher thus causing recruitment of mTORC1 to the lysosomal membrane, where it can be fully activated by Rheb.

In addition to amino acid sensing via the Rag GTPases, amino acid depletion also causes localization of the TSC complex to lysosomes through binding with inactive RagA [78]. This exemplifies the crosstalk that exists between the two upstream signaling branches.

GATOR2 acts as a platform where several amino acid sensors bind in an inhibitory manner

in response to absence of a particular amino acid. For instance, Sestrin2 and SAR1B directly bind and sense the presence of leucine, albeit with different affinities; in the absence of leucine, both these sensors bind to GATOR2 and inhibit its activity. The amino acid sensors that have been discovered till date, as well as the amino acids that they sense are illustrated in Figure 1. Also illustrated are the Rag-independent amino acid mechanisms that impact on mTORC1 signaling.

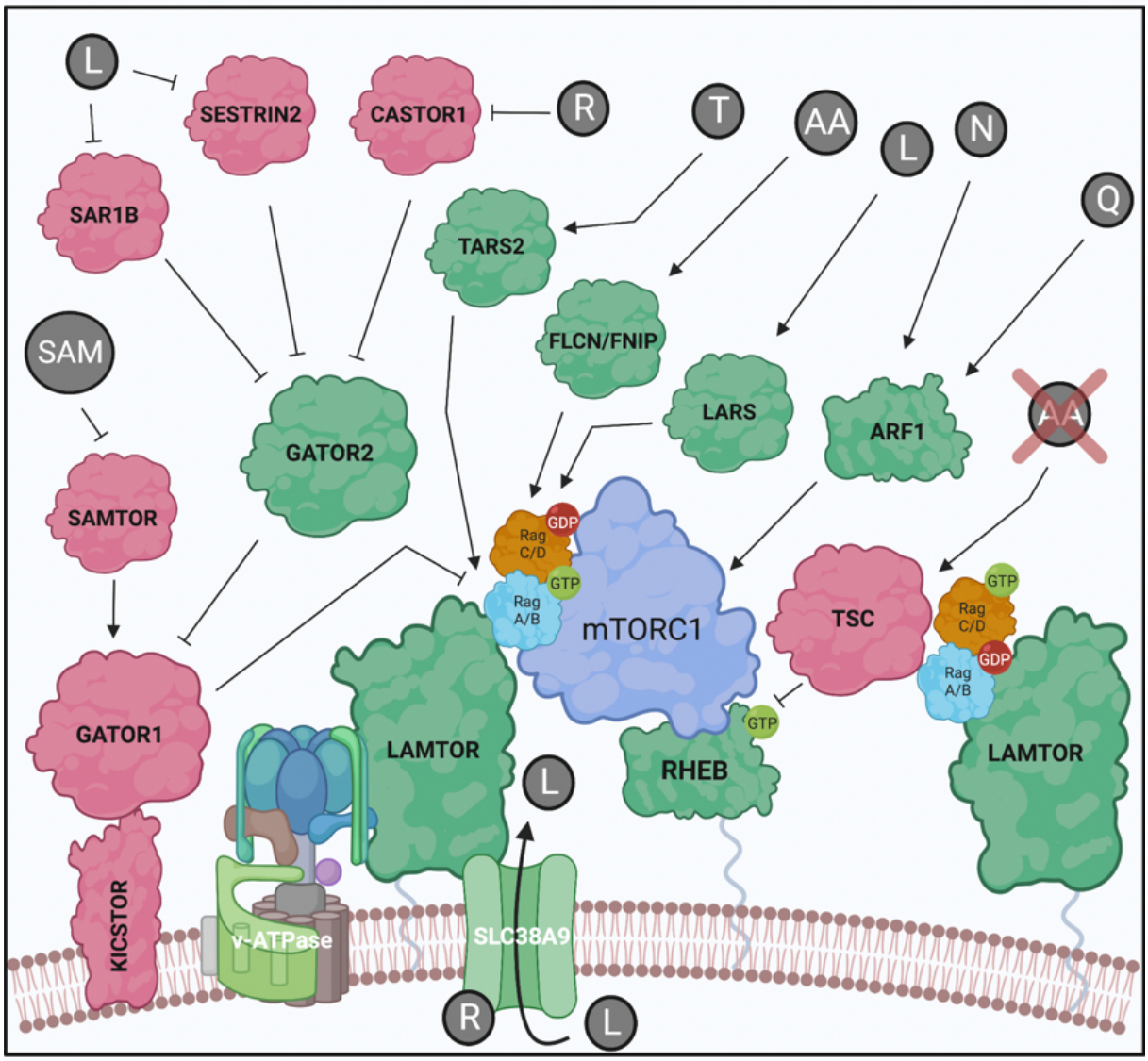

Figure 1: Amino acid sensors and their inputs to mTORC1. Adapted from Fernandes and Demetriades, 2021 [2].

1.3.2 Glucose Sensing

Glucose starvation is primarily sensed by AMPK via altered ATP/AMP ratios within the cell [85]. When activated, AMPK further phosphorylates several proteins in the mTORC1 signaling pathway. AMPK-dependent TSC phosphorylation at two distinct residues causes its

activation, leading to suppressed mTORC1 activity. It also directly phosphorylates RAPTOR at two different sites which results in 14-3-3 binding to RAPTOR, and consequent mTORC1 inhibition [86]. More recently, AMPK-dependent phosphorylation of the WDR24 subunit of GATOR2 was uncovered, which reduced GATOR2 stability and thus caused a decline in mTORC1 signaling in a Rag GTPase-dependent manner [87].

Independently of AMPK, DHAP (dihydroxyacetone phosphate), an intermediate of the glycolytic pathway was shown to be sensed by mTORC1 [88]. Further, aldolase, an enzyme involved in metabolizing Fructose-1,6-bisphosphate (FBP) was found to also sense it and impact mTORC1 activity in a manner independent of AMPK [89].

1.3.3 Growth Factor Signaling

The TSC-Rheb axis receives a majority of the inputs from growth factor (GF) and insulin signaling. Downstream of PI3K signaling, active AKT directly phosphorylates TSC2 at 5 different phospho-acceptor sites upon insulin stimulation, promoting its delocalization from the lysosomal membrane and preventing its inhibition of Rheb [76]. AKT also activates mTORC1 directly via phosphorylating PRAS40 and releasing its self-inhibitory action toward the complex [11]. ERK, RSK and WNT signaling pathways also all converge on the TSC to regulate mTORC1 function [90].

Further, highlighting the feedback mechanisms that exist within cells, mTORC1 can in turn regulate PI3K-AKT signaling through S6K1-driven degradation of IRS1, thus attenuating signaling through that pathway [91], as well as through activation of Grb10, another downstream substrate that negatively regulates the insulin/IGF-1 receptor [92].

1.4 Processes regulated by mTORC1

Overall, when active, mTORC1 functions to promote anabolism while suppressing catabolism by regulating multiple substrates, some of which are stated below.

Protein synthesis is one of the key processes regulated by mTORC1. The main route through which mTORC1 does so is by promoting phosphorylation of its canonical substrates: the eukaryotic initiation factor 4E-binding proteins (4E-BPs) and p70 S6 kinase 1 (S6K1). Both substrates are considered canonical and regulated in a RHEB-dependent manner, with

substrate recruitment taking place through RAPTOR-mediated binding. Phosphorylation of 4E-BP1 on multiple sites drives its release from eIF4E (eukaryotic translation initiation factor 4E) and thus relieves it of its inhibition, allowing 5' cap-dependent translation [93]. mTORC1 also mediates phosphorylation of S6K1 and triggers its activity in concert with PDK1, causing phosphorylation of the ribosomal protein S6, a component of the 40S subunit of the ribosome. Phosphorylation of LARP1, another mTORC1 substrate, allows the formation of a functional eIF4F complex by releasing its inhibitory binding from 5'UTRs of transcripts, thus promoting translation [94,95]. S6K1 is also involved in regulation of PDCD4 (programmed cell death protein 4) that suppresses eIF4A (eukaryotic initiation factor 4A), a component of the eIF4F complex [96,97].

Lysosomal biogenesis is critical process inhibited by mTORC1 signaling via suppression of TFEB. TFEB, together with TFE3, TFEC, and MITF, belongs to the microphthalmia/transcription factor E (MiT/TFE) family of basic helix–loop–helix leucine zipper (bHLH-Zip) transcription factors, and acts as a master regulator of lysosomal biogenesis by regulating transcription of lysosomal membrane proteins and lysosomal hydrolases. TFEB was recently shown to be regulated in a non-canonical manner, being recruited by the Rag GTPases to the lysosomal surface instead of by RAPTOR-mediated substrate recruitment, which is explained by the lack of a TOS-motif [98]. Further, its phosphorylation was shown to be independent of RHEB (and growth factors), but crucially required RagC in its active conformation for recruitment to occur. A recent structural paper showed the presence of an mTORC1-TFEB-Rag-Ragulator megacomplex that contained non-canonical Rag-Ragulator complexes that presented TFEB to the kinase [99]. In the absence of mTORC1-mediated phosphorylation, or due to any dysregulation that prevented RagC from its GDP-bound state, TFEB could no longer be sequestered in the cytosol and translocated to the nucleus to carry out its transcriptional program[100-102].

Concomitant with suppression of lysosomal biogenesis, mTORC1 also suppresses autophagy by inhibiting substrates such as unc-51-like autophagy-activating kinase 1 (ULK1) and autophagy-related protein 13 (ATG13), thus suppressing initiation of autophagy when nutrients are sufficient [103].

A comprehensive list of substrates under regulation of mTORC1 as well as the processes

they are involved in is portrayed in Figure 2.

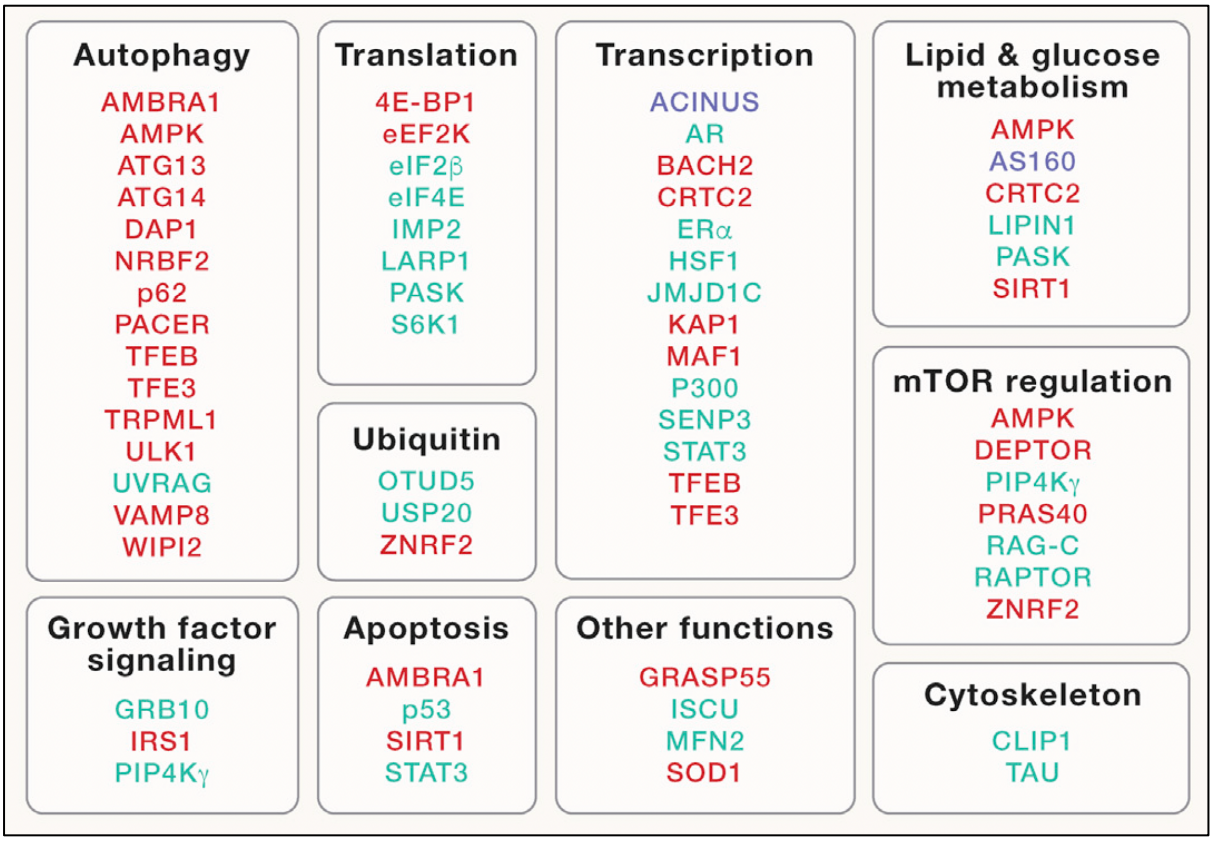

Figure 2: List of mTORC1 substrates, adapted from Battaglioni et al., 2022 [19]. Substrates shown in green or red are activated or inhibited, respectively, upon mTORC1-mediated phosphorylation. For substrates shown in blue, the effect of phosphorylation is unknown.

1.5 Aims of the thesis

mTORC1 occupies a pivotal position in nutrient sensing and signaling, underscored by the elaborate crosstalk that it maintains with a multitude of other pathways, both upstream and downstream, within the cell. Entrusted with the complex task of continually surveilling cellular resources and synchronizing the downstream program (anabolism or catabolism) undertaken by the cell, it comes as no surprise that an intricate upstream machinery exists for its regulation and for keeping its activity in check. Indeed, dysregulation of even one component within this delicate network can lead to loss of homeostasis and have deleterious effects, as signified by the different pathological conditions in which mTORC1 dysregulation has been implicated.

In the hierarchy of mTORC1 regulation, its subcellular localization occupies a prominent position, with the lysosomal landscape serving as a stage where a significant portion of mTORC1 regulation and signaling is orchestrated. Therefore, a comprehensive understanding of the central principles that govern the localization and function of mTORC1 is of prime importance. In this regard, the work in this thesis has attempted to further our knowledge with the following specific research aims:

Aim 1: To explore the relation between the localization and activity of mTORC1

A complex network of regulatory factors upstream of mTORC1 serve to bring about its lysosomal localization, which is a key site for its activation. Thus far, the connection between localization and activity has been considered as unidirectional. However, given the regulatory loops that exist within the mTORC1 signaling pathway to fine-tune its activity, and the fact that localization is a key determinant of its activity, I aimed to investigate whether activity of mTORC1 reciprocally regulates its subcellular location.

Aim 2: To elucidate the contribution of the TSC-RHEB signaling axis to mTORC1 localization

As per the described model, the TSC-RHEB axis upstream of mTORC1 works in tandem with the Rag GTPase axis to stimulate signaling— the latter recruits mTORC1 to the lysosomal surface where the former induces its activity. Although for the most part these two upstream axes were considered to function independently of each other, more

recent work illuminated the functional overlap that actually exists between them in terms of nutrient sensing, a recurring feature of the mTORC1 signaling pathway. Thus, I aimed to uncover the potential role of the TSC-Rheb axis in influencing mTORC1 localization, in addition to its activity.

-

2 Results

2.1 mTORC1 activity licenses its own release from the lysosomal surface

This chapter of the Results addresses Aim 1.

It contains a published article:

Acharya A, Demetriades C. mTORC1 activity licenses its own release from the lysosomal surface. Mol Cell. 2024 Nov 21;84(22):4385-4400.e7. doi: 10.1016/j.molcel.2024.10.008. Epub 2024 Oct 31. PMID: 39486418.

In addition to results, the methods, discussion and references associated with these results are included within the chapter. A more expanded discussion can be found in Section 3.

Article

Molecular Cell

mTORC1 activity licenses its own release from the lysosomal surface

Graphical abstract

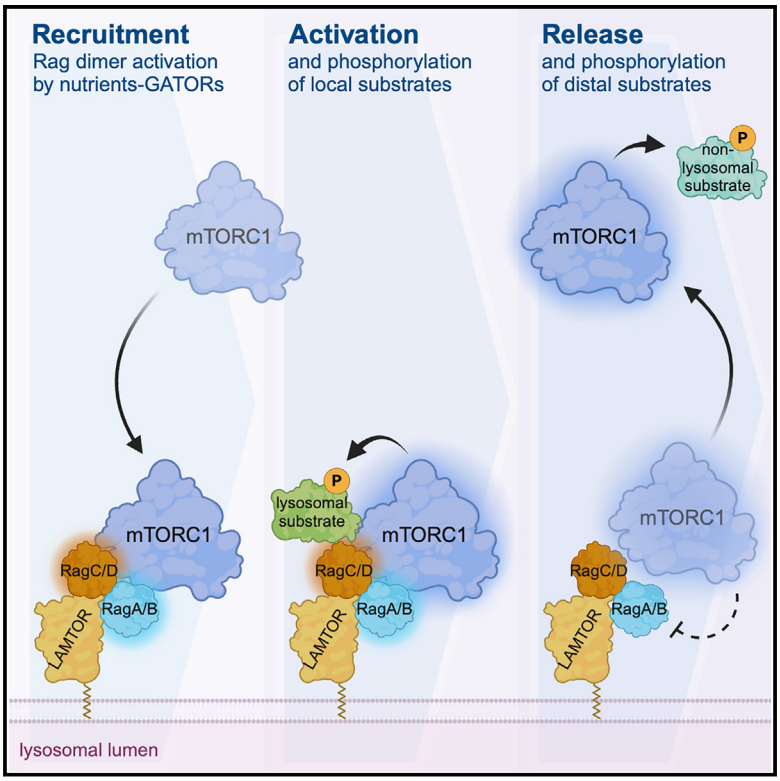

Highlights

- Inhibition of mTORC1 augments its lysosomal presence due to impaired release
- Inactive mTORC1 is strongly lysosomal even upon starvation or lysosome dysfunction
- Enhanced lysosomal mTORC1 concomitantly impacts TFEB phosphorylation and activation
- mTORC1 autoregulates its cycling on/off lysosomes via changes in RagA activation

Authors

Aishwarya Acharya,
Constantinos Demetriades

Correspondence

demetriades@age.mpg.de

In brief

The activation of mTORC1 is intricately linked to its subcellular localization, with the Rag GTPases controlling its lysosomal recruitment in response to nutrient cues. Acharya and Demetriades uncover another layer of regulation of mTORC1 localization, wherein its intrinsic kinase activity governs its own lysosomal tethering by influencing RagA nucleotide loading.

Acharya & Demetriades, 2024, Molecular Cell *84*, 4385–4400
November 21, 2024
https://doi.org/10.1016/j.molcel.2024.10.008

CellPress

Molecular Cell

CellPress
OPEN ACCESS

Article

mTORC1 activity licenses its own release from the lysosomal surface

Aishwarya Acharya[1,2] and Constantinos Demetriades[1,2,3,4,*]
[1]Max Planck Institute for Biology of Ageing (MPI-AGE), 50931 Cologne, Germany
[2]Cologne Graduate School of Ageing Research (CGA), 50931 Cologne, Germany
[3]Cologne Excellence Cluster on Cellular Stress Responses in Aging-Associated Diseases (CECAD), University of Cologne, 50931 Cologne, Germany
[4]Lead contact
*Correspondence: demetriades@age.mpg.de
https://doi.org/10.1016/j.molcel.2024.10.008

SUMMARY

Nutrient signaling converges on mTORC1, which, in turn, orchestrates a physiological cellular response. A key determinant of mTORC1 activity is its shuttling between the lysosomal surface and the cytoplasm, with nutrients promoting its recruitment to lysosomes by the Rag GTPases. Active mTORC1 regulates various cellular functions by phosphorylating distinct substrates at different subcellular locations. Importantly, how mTORC1 that is activated on lysosomes is released to meet its non-lysosomal targets and whether mTORC1 activity itself impacts its localization remain unclear. Here, we show that, in human cells, mTORC1 inhibition prevents its release from lysosomes, even under starvation conditions, which is accompanied by elevated and sustained phosphorylation of its lysosomal substrate TFEB. Mechanistically, "inactive" mTORC1 causes persistent Rag activation, underlining its release as another process actively mediated via the Rags. In sum, we describe a mechanism by which mTORC1 controls its own localization, likely to prevent futile cycling on and off lysosomes.

INTRODUCTION

Biological systems commonly respond to diverse intra- and extracellular stimuli via dynamic changes in the localization of key signaling molecules between different subcellular compartments. Thus, protein relocalization facilitates compartmentalized and location-specific cellular responses.[1–3] Characteristic examples are the nuclear translocation of steroid receptors upon hormonal stimulation[4,5] and the relocalization of STING protein from the ER to the Golgi upon infection to activate immune signaling.[6,7]

The mammalian/mechanistic target of rapamycin (mTORC1) functions both as a molecular nutrient sensor and a central coordinator of cellular physiology via controlling virtually all cellular biosynthetic and recycling processes.[8–12] The lysosomal surface is a major site of mTORC1 activation by nutrients like amino acids (AAs) and glucose, which also control its dynamic shuttling between lysosomes and the cytoplasm.[13] Under nutrient starvation conditions, mTORC1 is cytoplasmic and inactive, whereas nutrient sufficiency causes the recruitment and activation of a fraction of mTORC1 on lysosomes.[14–16] While the regulation of mTORC1 activity by means of its subcellular relocalization has been studied extensively, how and whether its activation status affects its localization is not clear to date.

The recruitment and tethering of mTORC1 on the lysosomal surface is mediated by the Rag GTPases that function as an obligate heterodimer composed of RagA or RagB bound to RagC or RagD.[14,17,18] Information about nutrient availability is conveyed through a complex signaling network to the Rags and determines their activity via changes in their guanosine triphosphate (GTP)/guanosine diphosphate (GDP) loading status: in the presence of nutrients, the Rag dimer adopts an active conformation (GTP-bound RagA/B and GDP-bound RagC/D), which presents high affinity for mTORC1 and brings it in the vicinity of its direct activator Rheb.[14,19] By contrast, nutrient starvation causes the inactivation of the Rags (GDP-bound RagA/B and GTP-bound RagC/D) that allows the release of mTORC1 from the lysosomal surface to the cytoplasm and the subsequent downregulation of its activity.[14]

We recently showed that, in cells grown in nutrient-replete media, active mTORC1 is present both on lysosomes and in the cytoplasm, phosphorylating distinct substrates and regulating different cellular functions at each subcellular location. For instance, while cytoplasmic mTORC1 phosphorylates S6K and 4E-BP1 to control *de novo* protein synthesis, lysosomal mTORC1 controls lysosome biogenesis via the phosphorylation of the TFEB/TFE3 transcription factors.[20] Because several of its effectors are non-lysosomal proteins[20–25] and because of the dynamic and transient nature of its lysosomal localization,[13] it

CellPress OPEN ACCESS

Molecular Cell
Article

is conceivable that mTORC1 that is activated on lysosomes needs to be set free to phosphorylate its non-lysosomal targets elsewhere. However, whether its release from the lysosomal surface is a regulated process is currently not known.

Previous studies have reported stronger lysosomal accumulation of mTOR in cells treated with pharmacological mTOR inhibitors; however, the underlying mechanisms and the functional outcomes of this relocalization have not been investigated so far.[26–29] Here, by using pharmacological or genetic means to inhibit mTORC1, we show that its activity is tightly linked to its release from the lysosomal surface, with inactive complexes localizing more strongly to lysosomes via a mechanism that involves the mTORC1-induced locking of the Rag GTPase complex, particularly RagA, in its active state. Furthermore, this enhanced lysosomal mTORC1 localization leads to stronger phosphorylation of its non-canonical lysosomal substrates, like TFEB/TFE3, with these phenomena persisting even under nutrient starvation or lysosomal dysfunction conditions. Overall, our findings reveal an important mechanistic aspect of mTORC1 regulation and highlight the dynamic nature of its shuttling between lysosomes and the cytoplasm, as well as the role of its intrinsic activity in this process.

RESULTS

Pharmacological or genetic downregulation of mTORC1 activity enhances its lysosomal localization and TFEB phosphorylation

In cells grown under basal culture conditions in nutrient-replete media, mTOR presents a mixed localization pattern in immunofluorescence and confocal microscopy experiments, with part of the signal showing diffuse cytoplasmic localization and another part accumulating in puncta that colocalize with lysosomal markers like LAMP2 (Figures 1A and 1B), in agreement with previous studies that described its dynamic shuttling between the lysosomal surface and the cytoplasm.[13,15,30] To investigate whether acute changes in mTORC1 activity influence its localization, we treated human embryonic kidney HEK293FT cells grown in full culture media with rapamycin, a specific allosteric mTORC1 inhibitor,[31] or Torin1, an ATP-competitive catalytic mTOR inhibitor[32] (Figure 1A). Treatment with either compound for 1 h strongly enhanced the lysosomal accumulation of mTOR (Figure 1B) and its colocalization with LAMP2 (Figure 1C). Similar data were obtained using WI-26 human lung fibroblasts or non-transformed human foreskin fibroblasts (HFFs), showing that this effect is not cell-type specific (Figures S1A–S1E). The confocal microscopy data were independently confirmed by biochemical lysosomal enrichment (Lyso-IP) experiments,[33] with increased levels of Raptor and mTOR proteins co-purifying with intact lysosomes isolated from rapamycin- or Torin1-treated cells (Figure 1D). Previous studies showed that RagC is loosely associated with lysosomes[18] and also shuttles between the lysosomal surface and the cytoplasm.[13] However, we did not observe rapamycin or Torin1 strengthening the lysosomal localization of RagC (Figures S1F and S1G), indicating that this effect is specific for mTORC1.

While catalytic mTOR inhibitors like Torin1 block its activity toward all of its substrates, rapamycin only affects the phosphorylation of some mTORC1 targets.[32] For instance, while phosphorylation of S6K on Thr^{389} is rapamycin-sensitive, that of TFEB on Ser^{211} is resistant to rapamycin treatment.[28] As expected, Torin1 diminished the phosphorylation of all mTORC1 substrates tested (i.e., TFEB, S6K, and 4E-BP1) (Figures 1E–1G). Interestingly, however, treatment with rapamycin caused increased phosphorylation of the lysosomal mTORC1 substrate TFEB (Figures 1E, 1F, and S1E), in line with the enhanced localization of mTOR on lysosomes in these cells (Figures 1B–1D). Similar data were obtained by leveraging the reversible nature of Torin1: we pre-treated cells with a low Torin1 concentration (50 nM) for 15 min to promote the lysosomal localization of mTORC1 and then washed out the drug for 1 h to allow for its reactivation. Indeed, the re-phosphorylation of the lysosomal mTORC1 substrates TFEB and TFE3 was stronger upon Torin1 pre-treatment and wash-out (Figure S1H).

To test if the rapamycin effects are due to downregulation of mTORC1 activity itself or stem from potential mTOR-independent effects, we used a cell line that expresses a rapamycin-resistant mTOR point mutant ($mTOR^{RR}$) that we recently described.[31] Indeed, while Torin1 caused substantially stronger lysosomal mTOR localization in both wild-type ($mTOR^{WT}$) and $mTOR^{RR}$ cells, rapamycin enhanced the accumulation of mTOR on lysosomes and the phosphorylation of TFEB only in $mTOR^{WT}$ cells (Figures S2A–S2C). S6K is a downstream target and key effector of mTORC1-dependent processes like protein synthesis.[34] Unlike rapamycin, treatment with two independent S6K inhibitors that abolished phosphorylation of its direct target S6 (Figure S2D) did not influence mTOR localization in cells (Figures S2E and S2F), further suggesting that changes in the activity of mTORC1 itself are responsible for its enhanced lysosomal presence.

To investigate if the observed effects are specific for pharmacological inhibition of mTORC1, we also expanded our analyses to a genetic model of low mTORC1 activity, namely Rheb knockout (KO) cells (Figure 1A). While phosphorylation of the canonical mTORC1 substrates like S6K and 4E-BP1 strongly depends on Rheb, its non-canonical substrates like TFEB and TFE3 are regulated in a Rheb-independent manner.[35] Indeed, Rheb KOs demonstrated blunted mTORC1 activity toward its canonical substrates S6K and 4E-BP1, as expected (Figure 1H). Interestingly, however, loss of Rheb caused strongly enhanced lysosomal mTOR localization accompanied by elevated phosphorylation of TFEB and TFE3 (Figures 1H–1J and S3A), similar to our findings from rapamycin treatments. As the downregulation of mTORC1 activity in Rheb KO cells (as seen by S6K phosphorylation, for instance) is strong but not complete (Figures 1H and S3A), we next combined Rheb loss with pharmacological mTOR inhibition. As expected, Torin1 treatment further decreased S6K phosphorylation in Rheb KO cells (Figure S3A). Moreover, rapamycin or Torin1 further enhanced mTOR localization to lysosomes also in Rheb KO cells (Figures S3B and S3C), again indicating this is not due to the absence of Rheb expression but rather due to decreased mTORC1 activity.

Inactive mTORC1 shows persistent lysosomal localization and TFEB/TFE3 phosphorylation even under starvation or lysosomal dysfunction

The subcellular localization of mTOR is regulated by AA availability, with AA starvation causing its delocalization away from

Molecular Cell
Article

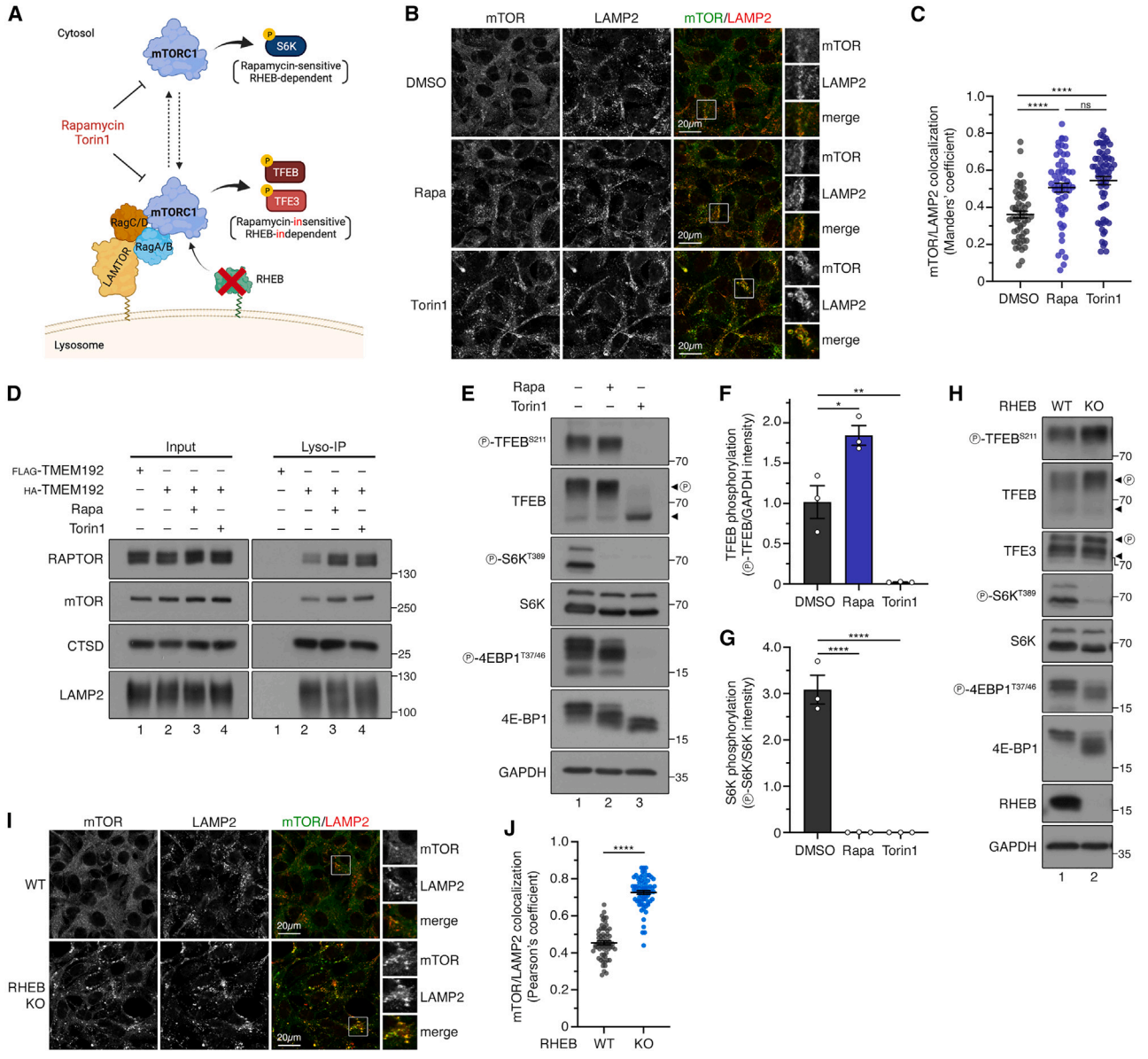

Figure 1. mTORC1 downregulation enhances its lysosomal localization and TFEB phosphorylation

(A) Schematic representation of the experimental setup and relevant readouts to assay mTOR localization and activity upon pharmacological or genetic inhibition. See text for details.

(B and C) Colocalization analysis of mTOR with LAMP2 (lysosomal marker) in WT HEK293FT cells, treated with DMSO (vehicle), rapamycin (20 nM), or Torin1 (250 nM) for 1 h as indicated, using confocal microscopy. Magnified insets shown to the right (B). Quantification of colocalization in (C). n = 55–60 individual cells from 3 independent fields per condition.

(D) Lyso-IP experiments with WT HEK293FT cells stably expressing HA-tagged TMEM192 (or FLAG-TMEM192 as negative control), treated with DMSO (vehicle), rapamycin (20 nM), or Torin1 (250 nM) for 1 h as indicated. Intact lysosomes were immunopurified by anti-HA IPs under native conditions, and the presence of LAMP2, cathepsin D (CTSD), mTOR, and RAPTOR proteins in the lysosomal fractions and in whole-cell lysates was analyzed by immunoblotting.

(E–G) Immunoblots with lysates from WT HEK293FT cells, treated with DMSO (vehicle), rapamycin (20 nM), or Torin1 (250 nM) for 1 h, and probed with the indicated antibodies (E). Quantification of TFEB phosphorylation (p-TFEB/GAPDH ratio normalized to DMSO controls) in (F). Quantification of S6K phosphorylation (p-S6K/S6K ratio normalized to DMSO controls) in (G). n = 3 independent experiments.

(H) Immunoblots with lysates from WT and RHEB KO HEK293FT cells, grown under basal conditions, probed with the indicated antibodies.

(I and J) Colocalization analysis of mTOR with LAMP2 (lysosomal marker) in WT and RHEB KO HEK293FT cells, using confocal microscopy. Magnified insets shown to the right (I). Quantification of colocalization in (J). n = 64–68 individual cells from 4 independent fields per condition.

Scale bars, 20 μm. Arrowheads indicate bands corresponding to different protein forms when multiple bands are present. P, phosphorylated form. Data in graphs shown as mean ± SEM. * $p < 0.05$, ** $p < 0.01$, **** $p < 0.0001$, ns: non-significant.

See also Figures S1–S3.

CellPress OPEN ACCESS

Molecular Cell
Article

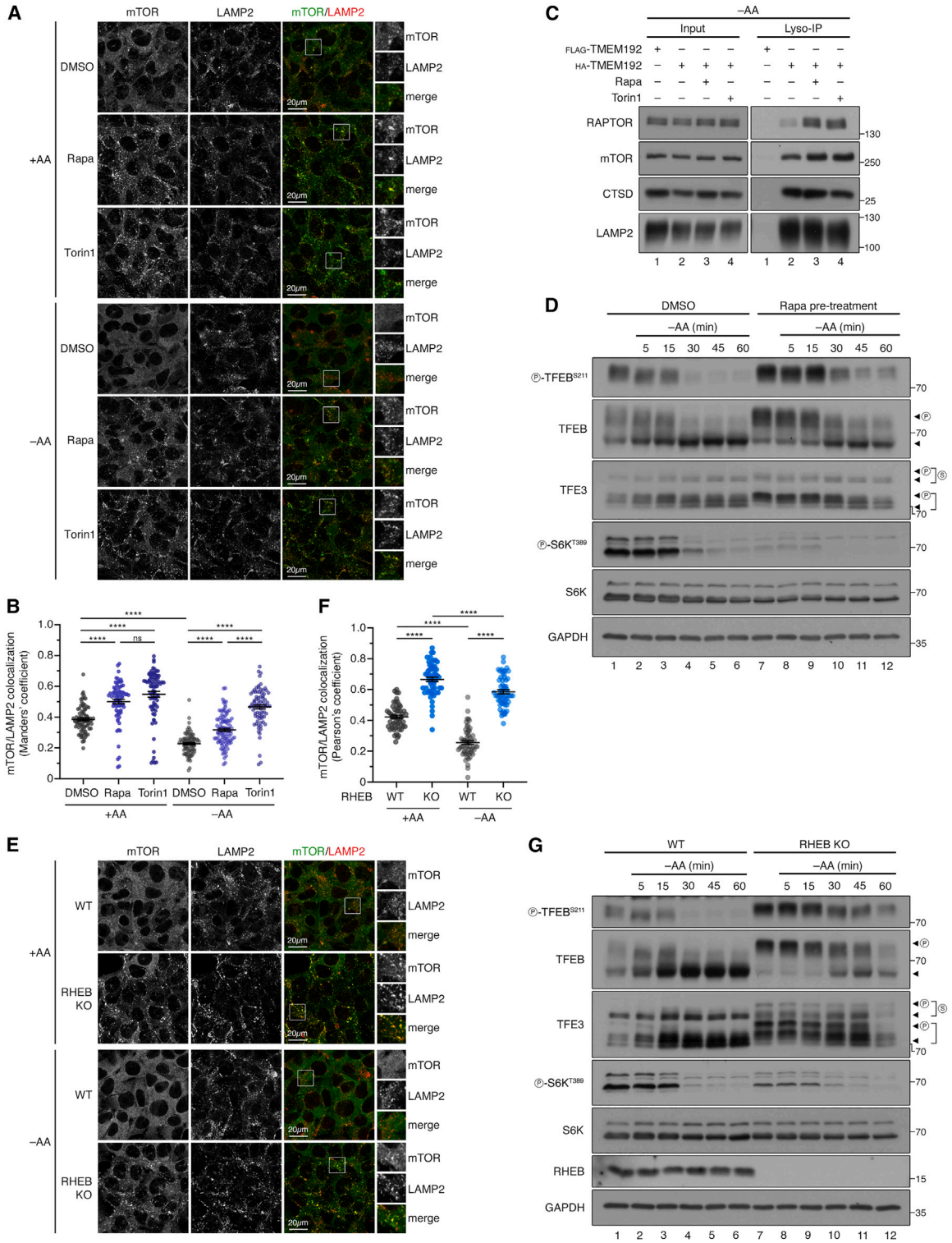

Figure 2. Inactive mTORC1 shows persistent lysosomal localization and TFEB/TFE3 phosphorylation even under AA starvation

(A and B) Colocalization analysis of mTOR with LAMP2 (lysosomal marker) in WT HEK293FT cells, pre-treated with DMSO (vehicle), rapamycin (20 nM), or Torin1 (250 nM) for 1 h, followed by treatment with media containing (+AA) or lacking AAs (−AA) without inhibitors for an additional hour, using confocal microscopy. Magnified insets shown to the right (A). Quantification of colocalization in (B). *n* = 77–100 individual cells from 5 independent fields per condition.

(legend continued on next page)

Molecular Cell
Article

lysosomes.[15,16,30] Therefore, we next tested how changes in mTORC1 activity influence its dynamic relocalization upon treatment with media specifically lacking AAs. Interestingly, although AA starvation (1 h) caused mTOR to become non-lysosomal in control conditions, cells pre-treated with rapamycin or Torin1 showed persistent lysosomal mTOR localization even upon treatment with starvation media, as shown by confocal microscopy (Figures 2A and 2B) and Lyso-IP experiments (Figure 2C). This effect was recapitulated also when a shorter (15 min, compared with 60 min for other experiments) Torin1 pre-treatment was carried out before AA removal for 1 additional hour, underscoring the rapid nature of this phenotype (Figures S4A and S4B). Of note, the persistent enrichment of mTOR on lysosomes of rapamycin-treated cells was accompanied by delayed and incomplete dephosphorylation of TFEB/TFE3 upon AA starvation (Figure 2D). Similarly, the lysosomal localization of mTOR and the phosphorylation of TFEB/TFE3 were also sustained in AA-starved Rheb KO cells (Figures 2E–2G).

Besides AAs, also glucose availability signals to mTORC1 via the Rag GTPases, with glucose starvation causing delocalization of mTORC1 from the lysosomal surface and downregulation of its activity toward both its cytoplasmic and lysosomal substrates.[36,37] Furthermore, blockage of proper lysosomal function using bafilomycin (BafA1) to inhibit the lysosomal v-ATPase results in cytoplasmic mTOR localization[16,20] and dephosphorylation of its lysosomal substrates like TFEB.[20] Similar to what we observed for AA starvation, we found that downregulation of mTORC1 activity upon loss of Rheb expression caused persistent lysosomal mTOR localization even in cells starved for glucose (Figures 3A and 3B) or treated with BafA1 (Figures 3C and 3D). Strikingly, TFEB phosphorylation was largely unaffected by these treatments in Rheb KO cells even at much later time points (Figures 3E and 3F). Similar data were obtained by pharmacological inhibition of mTORC1 using rapamycin or Torin1, which led to lysosomal mTOR localization and elevated TFEB phosphorylation also in glucose-starved cells (Figures S5A–S5C).

Dephosphorylation of the TFEB/TFE3 transcription factors, for instance, upon inactivation of mTORC1, is responsible for their translocation to the nucleus, where they induce the expression of lysosome-biogenesis- and autophagy-related genes.[28,38–40] By contrast, phosphorylation of these transcription factors by active mTORC1 at the lysosomal surface leads to their sequestration in the cytoplasm and lowers expression of their targets. In agreement with this, Rheb KO cells, in which TFEB/TFE3 are hyperphosphorylated, exhibited decreased expression levels of their target genes *UAP1L1* (Figure S5D), *LAMP2* (Figure S5E), and *ATP6AP1* (Figure S5F). Furthermore, downregulation of mTORC1 activity by glucose starvation promoted lysosome biogenesis (shown as significantly increased LysoTracker signal) in control cells. By contrast, these starvation-induced effects were strongly blunted in Rheb KO cells (Figures 3G and 3H) that show persistent TFEB phosphorylation even upon glucose withdrawal (Figure 3E). Overall, these data indicate that inactivation of mTORC1 by pharmacological or genetic means enhances its enrichment on lysosomes even under conditions that were previously shown to cause its relocalization to the cytoplasm and, concomitantly, maintains TFEB phosphorylation and prevents activation of the lysosome-biogenesis transcriptional program downstream of TFEB.

Enhanced lysosomal tethering of inactive mTORC1 is mediated by the Rag GTPases

The increased lysosomal localization of mTOR could be due to either stronger recruitment of cytoplasmic molecules to lysosomes or weaker release of molecules that are already present there. To interrogate these two potential explanations, we either pre-treated cells with Torin1 before AA starvation or we first starved cells for AAs and then treated them with Torin1 (Figures 4A and 4B). Notably, while Torin1 pre-treatment prevented mTOR delocalization from lysosomes in AA-starved cells, as also described above (Figure 2), mTORC1 inhibition was unable to promote its recruitment to the lysosomal surface when cells were first treated with AA-depleted media and mTOR was already delocalized to the cytoplasm (Figures 4A and 4B). Therefore, we conclude that downregulation of mTORC1 activity prevents its release from the lysosomal surface.

As mTORC1 localizes to lysosomes via binding to the Rag GTPases, we next tested if its enhanced lysosomal tethering upon pharmacological or genetic inhibition requires the presence of a functional Rag dimer. Indeed, unlike in control cells, treatment of quadruple RagA-D KO HEK293FT cells (qKOs; described in Gollwitzer et al.[18]) with rapamycin or Torin1 was unable to promote lysosomal mTOR localization (Figures 5A and 5B). Similarly, transient knockdown of RagA/B blunted the localization of mTOR to lysosomes not only in wild-type (WT) but also in Rheb KO cells (Figures 5C and 5D). These data further support

(C) Lyso-IP experiments with WT HEK293FT cells stably expressing HA-tagged TMEM192 (or FLAG-TMEM192 as negative control), pre-treated with DMSO (vehicle), rapamycin (20 nM), or Torin1 (250 nM) for 1 h, followed by treatment with media lacking AAs (−AA) in the presence of the respective drug for an additional hour. Intact lysosomes were immunopurified by anti-HA IPs under native conditions, and the presence of LAMP2, cathepsin D (CTSD), mTOR, and RAPTOR proteins in the lysosomal fractions and in whole-cell lysates was analyzed by immunoblotting.

(D) Immunoblots with lysates from WT HEK293FT cells, pre-treated with DMSO (vehicle) or rapamycin (Rapa, 20 nM) for 1 h, followed by treatment with media containing (+AA) or lacking AAs (−AA) for different times and probed with different antibodies, as indicated.

(E and F) Colocalization analysis of mTOR with LAMP2 (lysosomal marker) in WT and RHEB KO HEK293FT cells, treated with media containing (+AA) or lacking AAs (−AA) for 1 h, using confocal microscopy. Magnified insets shown to the right (E). Quantification of colocalization in (F). n = 54–59 individual cells from 3 independent fields per condition.

(G) Immunoblots with lysates from WT and RHEB KO HEK293FT cells, treated with media containing (+AA) or lacking AAs (−AA) for different times and probed with different antibodies, as indicated.

Scale bars, 20 μm. Arrowheads indicate bands corresponding to different protein forms when multiple bands are present. P, phosphorylated form; S, SUMOylated form. Data in graphs shown as mean ± SEM. **** $p < 0.0001$, ns: non-significant.

See also Figure S4.

CellPress OPEN ACCESS

Molecular Cell
Article

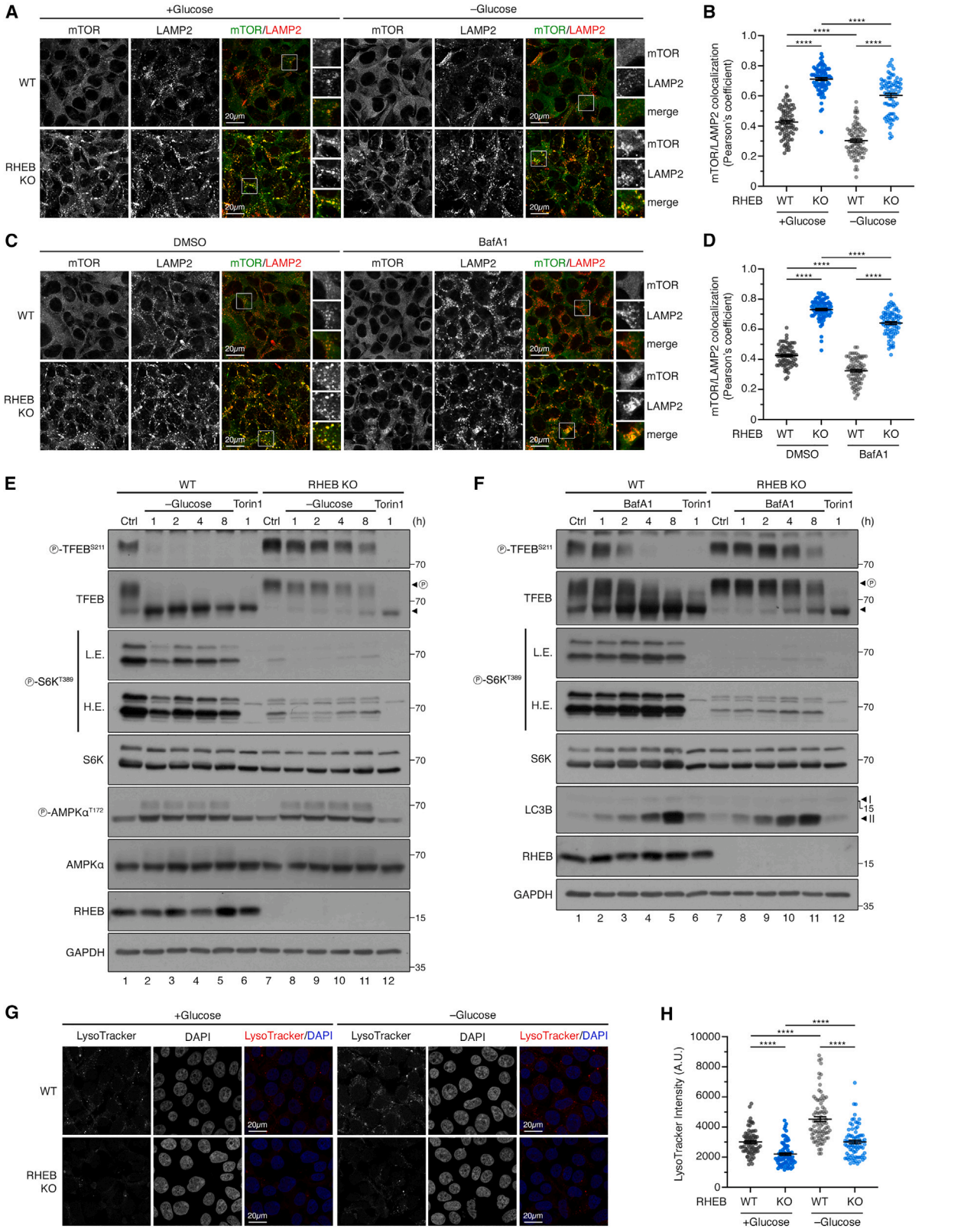

(legend on next page)

Molecular Cell
Article

CellPress
OPEN ACCESS

a model whereby mTORC1 downregulation causes stronger lysosomal tethering of this complex via interactions with the Rags.

mTORC1 inactivation causes locking of the Rag dimer in its active state

The Rag-mediated localization of mTORC1 to the lysosomal surface depends on the nucleotide-binding status of the Rag GTPase heterodimer, which responds to AA availability. More specifically, active $RagA^{GTP}$/$RagC^{GDP}$ dimers recruit mTORC1 to lysosomes when AAs are sufficient, whereas AA starvation results in inactive $RagA^{GDP}$/$RagC^{GTP}$ dimers that exhibit low affinity to mTORC1 and allow its release to the cytoplasm.[14] Therefore, we speculated that the persistent lysosomal localization of inhibited mTORC1 in AA-starved cells may be mechanistically explained by changes in the Rag dimer activation status. To test this hypothesis, we stably reconstituted Rag qKO cells with WT RagA/C or with active- or inactive-locked point mutants ($RagA^{QL}$/C^{SN} or $RagA^{TN}$/C^{QL}, respectively; described in Sancak et al.[14] and Demetriades et al.[30]) and probed the effects of Torin1 or rapamycin on mTOR localization on lysosomes. Indeed, Rag qKO reconstitution with WT or active RagA/C, but not the inactive Rag dimer, rescued mTOR localization (Figures 6A, 6B, S6A, and S6B) and TFEB phosphorylation (Figure S6C). In line with our data from experiments using parental cells (e.g., see Figures 1B, 1C, 2A, and 2B), lysosomal mTOR localization increased further upon mTORC1 inhibition with Torin1 or rapamycin in qKO cells stably expressing WT Rags (Figures 6A, 6B, S6A, and S6B). Moreover, rapamycin partially rescued the AA-starvation-induced dephosphorylation of TFEB in these cells (Figure S6C, compare lanes 2 and 3). Interestingly, however, neither Torin1 nor rapamycin had any effect on mTOR localization in qKOs expressing an active-locked Rag dimer (Figures 6A, 6B, S6A, and S6B), suggesting that the enhanced lysosomal tethering of mTORC1 upon its inhibition may work through Rag dimer activation.

To test this notion, we used binding of RagA/C to FLCN (the RagC/D GAP enzyme) as a readout for Rag activation and nucleotide loading status, since it preferentially interacts with inactive Rag dimers, which mediate its lysosomal recruitment upon AA starvation. As also shown previously by others,[41–43] FLCN interacted more strongly with inactive Rag dimers compared with WT Rags, whereas FLCN-Rag binding was undetectable in cells expressing active-locked RagA/C mutants (Figure 6C). Moreover, in agreement with our mTOR localization data (Figures S6A and S6B), rapamycin treatment did not influence the interaction of inactive-locked RagA/C mutants with FLCN, while it weakened its binding to WT Rags, suggesting their activation upon mTOR inhibition (Figure S6D). Further confirming that this assay can function as a reliable proxy for Rag activation, co-immunoprecipitation of FLCN with WT RagA/C was strengthened by AA starvation (Figure 6D). Notably, pre-treatment of qKO cells expressing WT RagA/C with rapamycin or Torin1 displayed decreased binding between FLCN and the Rags also in AA-starved cells (Figure 6D), indicating that mTORC1 inhibition prevents the starvation-induced inactivation of Rag dimers. Similar data were obtained by immunoprecipitation of endogenous RagC from parental HEK293FT cells, with rapamycin treatment (Figure S6E) or Rheb KO (Figure S6F) weakening the specific interaction of the Rags with FLCN. We complemented the co-immunoprecipitation experiments with Lyso-IPs that showed strongly decreased FLCN levels in the lysosomal fraction of rapamycin- or Torin1-pretreated cells, in line with its weaker binding to the Rags (Figure 6E). Collectively, these data confirm that mTORC1 downregulation (e.g., by pharmacological inhibition) promotes its stronger association with lysosomes by sustaining activation of the Rag heterodimer, both under nutrient-replete and under starvation conditions.

The GATOR1-RagA axis controls the release of active mTORC1 from lysosomes

The Rag GTPases are unique among the small GTPase superfamily proteins as they function as obligate heterodimers. Although the Rag dimer is often seen as a functional unit that conveys signals about AA availability to mTORC1 on the lysosomal surface, the nucleotide-binding state of its two subunits (e.g., RagA and RagC) can be regulated independently, downstream of distinct protein complexes: while the trimeric GATOR1 complex—comprised of the NPRL2, NPRL3, and DEPDC5 proteins—exerts its GAP activity toward RagA/B to regulate its GTP/GDP loading,[44] that of RagC/D is controlled by the GAP activity of the FLCN-FNIP1/2 complex.[41,45] Besides their distinct regulation, the two Rag dimer components also demonstrate functional diversification, with the RagA/B

Figure 3. Inactive mTORC1 shows persistent lysosomal localization and TFEB/TFE3 phosphorylation even under glucose starvation or lysosomal blockage

(A and B) Colocalization analysis of mTOR with LAMP2 (lysosomal marker) in WT and RHEB KO HEK293FT cells, treated with media containing (+glucose) or lacking glucose (−glucose) for 1 h, using confocal microscopy. Magnified insets shown to the right (A). Quantification of colocalization in (B). n = 78–85 individual cells from 5 independent fields per condition.

(C and D) As in (A), but with BafA1 treatment to block lysosomal function (100 nM, 6 h). Magnified insets shown to the right (C). Quantification of colocalization in (D). n = 79–81 individual cells from 5 independent fields per condition.

(E) Immunoblots with lysates from WT or RHEB KO HEK293FT cells, treated with media containing or lacking glucose for different times (1–8 h) and probed with different antibodies, as indicated. Torin1 treatment (250 nM, 1 h) was used as a control.

(F) As in (E), but with BafA1 treatment to block lysosomal function (100 nM, 1–8 h).

(G and H) LysoTracker staining in WT and Rheb KO HEK293FT cells, treated with media containing (+glucose) or lacking glucose (−glucose) for 8 h, using confocal microscopy. Nuclei stained with DAPI (G). Quantification of LysoTracker signal intensity (arbitrary units, A.U.) in (H). n = 74–85 individual cells from 5 independent fields per condition.

Scale bars, 20 μm. Arrowheads indicate bands corresponding to different protein forms when multiple bands are present. P, phosphorylated form. L.E., low exposure; H.E., high exposure. Data in graphs shown as mean ± SEM. **** $p < 0.0001$.

See also Figure S5.

CellPress OPEN ACCESS

Molecular Cell
Article

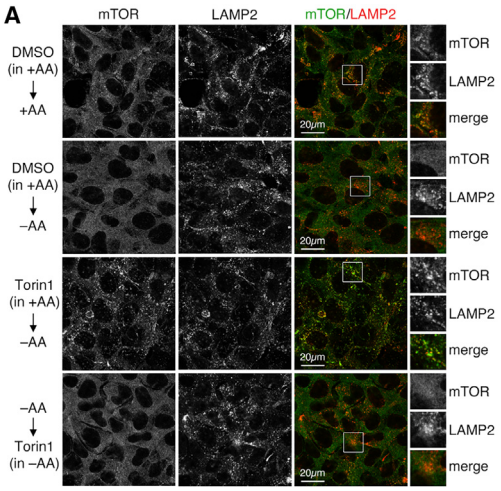

Figure 4. mTORC1 inhibition prevents its release from lysosomes rather than promoting its recruitment

(A and B) Colocalization analysis of mTOR with LAMP2 (lysosomal marker) in WT HEK293FT cells, treated with combinations of media containing (+AA) or lacking AAs (−AA) and Torin1 (250 nM) or DMSO as control, as indicated in the panel, using confocal microscopy. Pre-treatments and follow-up treatments were performed for 1 h each. Scale bars, 20 μm. Magnified insets shown to the right (A). Quantification of colocalization in (B). n = 55–62 individual cells from 3 independent fields per condition. Data shown as mean ± SEM. **** $p < 0.0001$, ns: non-significant.

counterpart being responsible primarily for the lysosomal recruitment of mTORC1, and the RagC/D counterpart controlling primarily the recruitment of the TFEB/TFE3 substrates to the lysosomal surface.[35,46–49] To test whether mTORC1 inactivation controls its own localization via regulating the nucleotide loading of the RagA or the RagC component of the Rag dimer, we first stably reconstituted the Rag qKO cells with WT Rags ($RagA^{WT}/RagC^{WT}$) or with one WT and one active-locked Rag mutant ($RagA^{WT}/RagC^{SN}$, or $RagA^{QL}/RagC^{WT}$). We reasoned that, if the enhanced lysosomal localization of mTOR was primarily driven by one Rag over the other, locking of the required Rag in a particular conformation would eliminate any effect of mTOR inhibition on its nucleotide loading and, thereby, mTOR enrichment on lysosomes. As also described above, Torin1 treatment caused enhanced lysosomal mTOR localization in cells expressing WT Rags (Figures 7A and 7B). Virtually the same effect was observed in cells expressing WT RagA with active-locked RagC (Figures 7A and 7B). However, while cells expressing active-locked RagA with WT RagC showed basally elevated mTOR localization to lysosomes, treatment with Torin1 did not further enhance the lysosomal presence of mTOR (Figures 7A and 7B). To further test this using the above-mentioned FLCN binding as a biochemical readout, we then stably reconstituted the Rag qKO cells with WT Rags ($RagA^{WT}/RagC^{WT}$) or with one WT and one inactive-locked Rag mutant ($RagA^{WT}/RagC^{QL}$, or $RagA^{TN}/RagC^{WT}$). In line with the microscopy results (Figures 7A and 7B), while rapamycin treatment decreased the interaction of FLCN with WT RagA/C or $RagA^{WT}/RagC^{QL}$ dimers, it did not influence FLCN binding to $RagA^{TN}/RagC^{WT}$ dimers (Figure 7C). In sum, these data indicate that the activation status of RagA, but not RagC, is responsible for the enhanced lysosomal localization of mTORC1 upon its inactivation.

To independently confirm this hypothesis, we generated genetic models of RagA or RagC activation or inactivation, respectively, namely GATOR1 or FLCN loss-of-function cell lines. The NPRL3 protein is necessary for the GAP activity of the GATOR1 complex toward RagA.[50] Indeed, in agreement with previous studies,[51] depletion of NPRL3 made mTORC1 signaling insensitive to AA starvation (Figure S7A) and enhanced the lysosomal localization of mTOR (Figures 7D and 7E). Interestingly, mTORC1 inhibition by rapamycin did not cause a further increase of lysosomal mTOR localization in NPRL3 KOs (Figures 7D and 7E), likely because RagA is already maximally activated in these cells, further supporting the predominant role of RagA in mediating the enrichment of mTOR to lysosomes. By contrast, while knocking out FLCN fully ablated lysosomal mTORC1 signaling (Figure S7B), mTOR localization was only mildly affected in control-treated cells (Figures S7C and S7D), but remained sensitive to mTORC1 inhibition by rapamycin (Figures S7C and S7D). Taken together, our findings indicate that the lysosomal localization of mTORC1 is primarily controlled downstream of the GATOR1-RagA signaling axis, in agreement with previous studies,[35,48] and also suggest that the activation state of mTORC1 regulates its own release via changes in the nucleotide loading of RagA (Figure 7F). Finally, we find that the FLCN-RagC axis plays a minor role in this process, which places FLCN downstream—and not upstream—of lysosomal mTORC1-RagA signaling.

DISCUSSION

The dynamic relocalization of mTORC1 between lysosomes and the cytoplasm is controlled by its intrinsic activity and the Rag GTPases

Previous work showed that the association of mTOR with lysosomes is transient and that it dynamically cycles between the lysosomal surface and the cytoplasm.[13] Nutrient availability controls the balance between lysosomal and non-lysosomal mTOR localization via a mechanism that involves the Rag GTPase heterodimers and changes in their activation status, with active Rags recruiting mTOR on lysosomes and facilitating its activation under conditions of AA sufficiency.[14–16] Here, we show that the inverse mode of regulation is also true, as changes in the activity of mTORC1 itself determine its cycling on and off lysosomes. Using pharmacological mTOR inhibitors or loss of Rheb as tools to downregulate mTORC1 activity, we capture a snapshot of a continuously occurring phenomenon at the lysosomal surface: while activation of mTORC1 licenses its own release from lysosomes, inactive mTORC1 causes locking of the Rag dimer (primarily RagA) in its active conformation, thus promoting enhanced lysosomal tethering of mTORC1 likely via its stronger association with the Rags. Therefore, it is the blunted

Molecular Cell
Article

CellPress
OPEN ACCESS

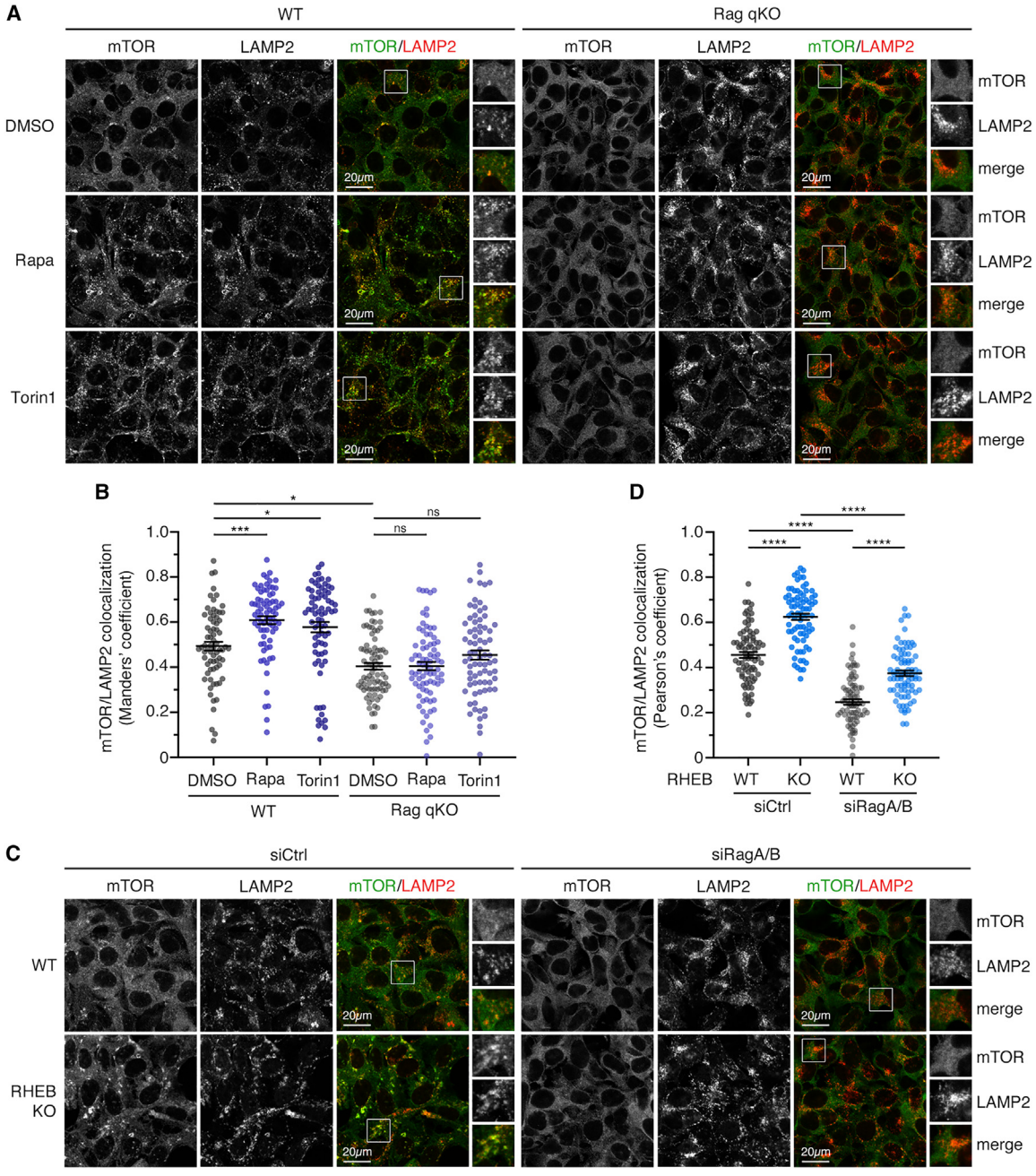

Figure 5. Enhanced lysosomal tethering of inactive mTORC1 is mediated by the Rag GTPases

(A and B) Colocalization analysis of mTOR with LAMP2 (lysosomal marker) in WT or quadruple Rag KO (qKO) HEK293FT cells, treated with DMSO (vehicle), rapamycin (20 nM), or Torin1 (250 nM) for 1 h as indicated, using confocal microscopy. Magnified insets shown to the right (A). Quantification of colocalization in (B). n = 71–83 individual cells from 5 independent fields per condition.

(C and D) Colocalization analysis of mTOR with LAMP2 (lysosomal marker) in WT or RHEB KO HEK293FT cells, with or without transient RagA/B knockdown, using confocal microscopy. Magnified insets shown to the right (C). Quantification of colocalization in (D). n = 79–84 individual cells from 5 independent fields per condition.

Scale bars, 20 μm. Data in graphs shown as mean ± SEM. * $p < 0.05$, *** $p < 0.001$, **** $p < 0.0001$, ns: non-significant.

release and not the enhanced recruitment of inactive mTORC1 that is responsible for its lysosomal accumulation. Furthermore, inactive mTORC1 shows persistent lysosomal localization even under AA starvation, glucose starvation, or BafA1 treatment conditions. This localization pattern is accompanied by delayed dephosphorylation of lysosomal, non-canonical mTORC1 substrates like TFEB/TFE3, whose phosphorylation is known to be resistant to rapamycin and to not require Rheb.[28,35]

CellPress OPEN ACCESS

Molecular Cell
Article

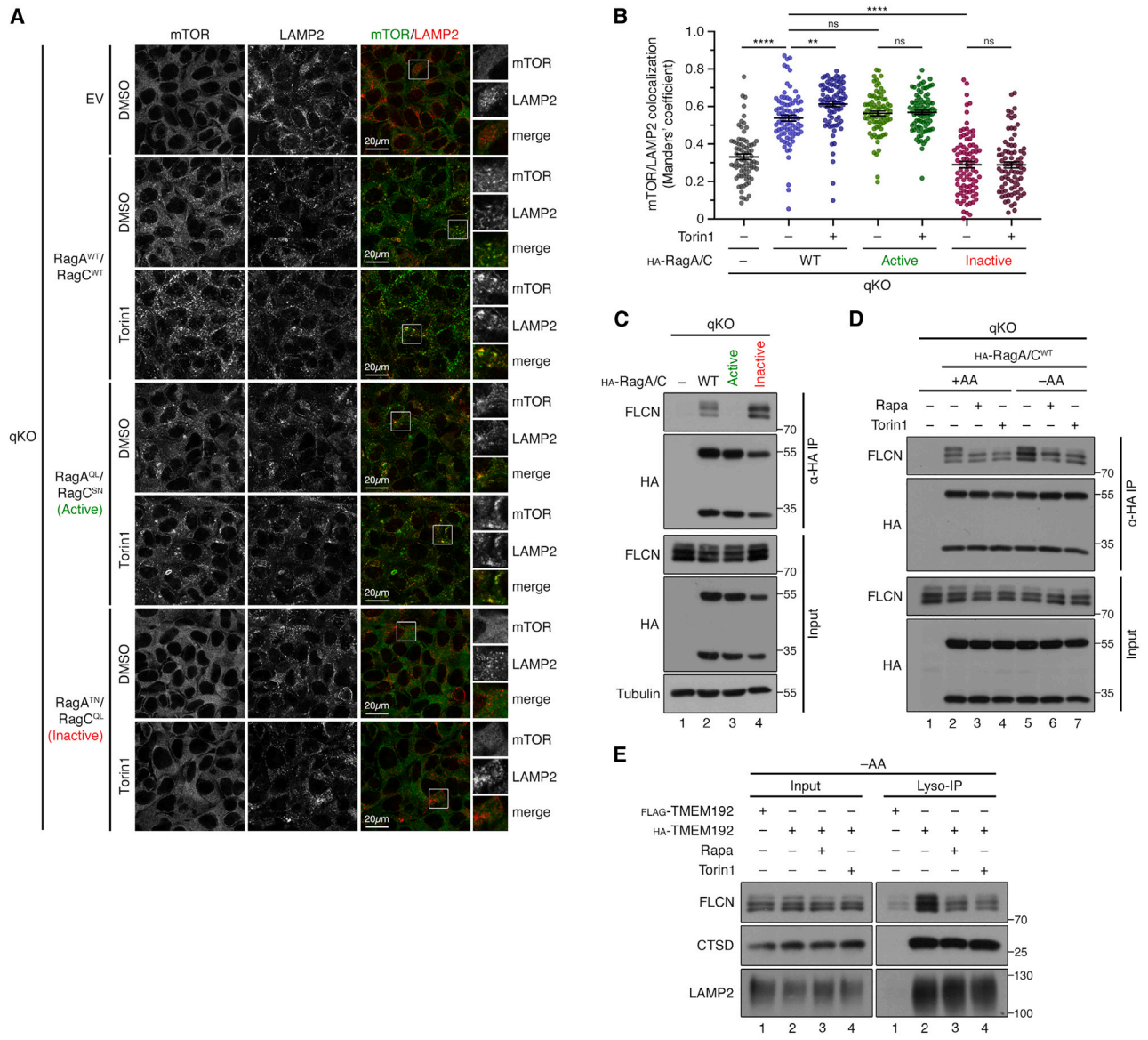

Figure 6. mTORC1 inactivation causes locking of the Rag dimer in its active state

(A and B) Colocalization analysis of mTOR with LAMP2 (lysosomal marker) in Rag qKO HEK293FT cells stably expressing HA-tagged WT, active (RagA^{QL}/RagC^{SN}), or inactive (RagA^{TN}/RagC^{QL}) Rag dimers, treated with DMSO (vehicle) or Torin1 (250 nM) for 1 h as indicated, using confocal microscopy. Cells transfected with an empty vector (EV) used as control. Magnified insets shown to the right. Scale bars, 20 μm (A). Quantification of colocalization in (B). $n = 77–87$ individual cells from 5 independent fields per condition. Data shown as mean ± SEM. ** $p < 0.01$, **** $p < 0.0001$, ns, non-significant.

(C) Binding of endogenous FLCN to Rags functions as a proxy for the activation state of the Rag dimer. Co-immunoprecipitation of HA-tagged RagA/RagC dimers from HEK293FT Rag qKO cells stably expressing WT, active, or inactive Rags. The input and IP samples were analyzed by immunoblotting using antibodies against the indicated proteins.

(D) As in (C), but with Rag qKO HEK293FT cells stably expressing HA-tagged WT RagA/C dimers. Cells were pre-treated with DMSO, rapamycin (20 nM), or Torin1 (250 nM) for 1 h followed by treatment with media containing (+AA) or lacking AAs (−AA) and the respective inhibitor for an additional hour. The input and IP fractions were analyzed by immunoblotting using antibodies against the indicated proteins.

(E) Lyso-IP experiments with WT HEK293FT cells stably expressing HA-tagged TMEM192 (or FLAG-TMEM192 as negative control), pre-treated with DMSO (vehicle), rapamycin (20 nM), or Torin1 (250 nM) for 1 h, followed by treatment with AA starvation media (−AA) for an additional hour in the presence of the inhibitors as indicated. Intact lysosomes were immunopurified by anti-HA IPs under native conditions, and the presence of LAMP2, cathepsin D (CTSD), and FLCN proteins in the lysosomal fractions and in whole-cell lysates was analyzed by immunoblotting.

See also Figure S6.

Molecular Cell
Article

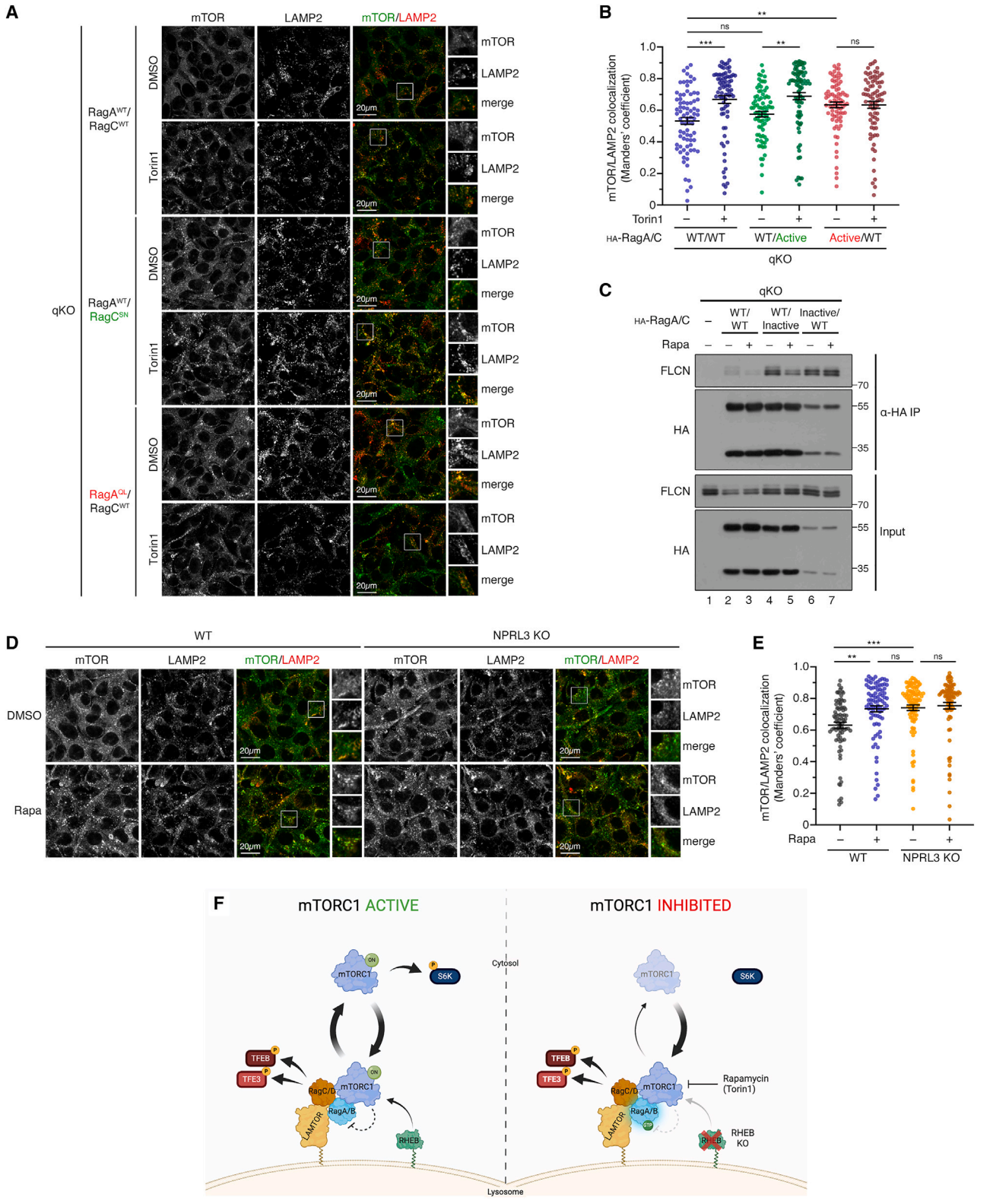

Figure 7. The GATOR1-RagA axis controls the release of active mTORC1 from lysosomes

(A and B) Colocalization analysis of mTOR with LAMP2 (lysosomal marker) in Rag qKO HEK293FT cells stably expressing HA-tagged WT Rags (RagA^{WT}/RagC^{WT}), active-locked RagC (RagA^{WT}/RagC^{SN}), or active-locked RagA (RagA^{QL}/RagC^{WT}), treated with DMSO (vehicle) or Torin1 (250 nM) for 1 h as indicated, using

(legend continued on next page)

CellPress OPEN ACCESS

Molecular Cell
Article

The enhanced lysosomal accumulation of mTOR upon treatment with its pharmacological inhibitors has also been observed previously[26–29]; however, this phenomenon was not investigated further in any of these studies. In fact, in certain cases, the visual effect of more punctate mTOR signal was interpreted as increased total mTOR protein levels, however, without accompanying data (e.g., immunoblots) to support such an explanation.[52] Our data from confocal microscopy and biochemical lysosome-enrichment experiments show that even acute inhibition of mTORC1 activity is sufficient to induce its stronger lysosomal association without influencing total mTOR protein levels and rather indicate a local signaling event occurring at lysosomes.

Another example of substrate specificity downstream of mTORC1

Based on our data from multiple pharmacological and genetic models of mTORC1 inhibition, we describe here an apparently counter-intuitive phenomenon: lowering mTORC1 activity leads to stronger phosphorylation of its non-canonical, lysosomal substrates, like TFEB/TFE3. By contrast, as expected, inactivation of mTORC1 causes decreased phosphorylation of its canonical, non-lysosomal targets, like S6K and 4E-BP1. Although this differential regulation of distinct downstream mTORC1 targets appears peculiar at first sight, we believe it is readily explained by the fact that (1) unlike with S6K/4E-BP1 phosphorylation by mTORC1, that of TFEB/TFE3 is insensitive to rapamycin[28] and does not require Rheb,[35] and (2) mTORC1 inhibition promotes its stronger presence on the lysosomal surface, where phosphorylation of TFEB/TFE3 takes place. Therefore, we propose that it is not accurate to define mTORC1 as '"active" or "inactive," but one would need to specify whether a particular genetic or pharmacological perturbation of mTORC1 activity makes mTORC1 more or less active toward specific subsets of its direct targets.[20]

This phenomenon is reminiscent of the findings described in recent studies by the Henske and Lotan labs, in which TSC loss of function is found to upregulate mTORC1 toward its canonical substrates (e.g., S6K), but causes hypo-phosphorylation of the TFEB/TFE3 transcription factors, their relocalization to the nucleus, and activation of their downstream transcriptional program.[46,49,53] Moreover, we have previously demonstrated that mTORC1 is more strongly lysosomal in TSC2 KO cells via enhanced interactions with hyperactive Rheb.[30] Therefore, one would expect that hyperactive and more lysosome-associated mTORC1 would result in higher TFEB/TFE3 phosphorylation, which is the opposite of what has been described in these studies. This seemingly paradoxical phenomenon is explained by lack of spatial coincidence between the kinase and its substrates. In brief, the authors reveal that loss of TSC expression or activity results in decreased lysosomal recruitment of TFEB/TFE3 via a mechanism that centers around an mTORC1-FLCN-RagC-related machinery.[53] Hence, although the kinase (i.e., mTORC1) is hyperactive in TSC KO cells, its substrates (i.e., TFEB/TFE3) cannot be properly phosphorylated because they are not presented to the kinase at the lysosomal surface, where their phosphorylation normally takes place.

Although our findings present some similarities to the phenomena of substrate specificity described previously by others, our data suggest these are mechanistically different. In contrast to these previous studies, we find that neither RagC nor its upstream regulator FLCN are involved in the enhanced lysosomal localization of inactive mTORC1 (Figures 7A, 7B, and S7B–S7D). Instead, this is dependent primarily on the nucleotide loading state of RagA and hence is influenced by the RagA negative regulator, the GATOR1 complex (Figure 7). More specifically, we find that mTORC1 inactivation causes locking of RagA in its active state, which in turn is responsible for the enhanced lysosomal tethering of mTORC1 (Figure 7C). As also discussed below in more detail, we do not know yet if the regulation of RagA by mTORC1 is direct or indirect, but we speculate that it may involve the mTORC1-dependent phosphorylation of multiple proteins of the lysosomal AA sensing machinery. Finally, the TSC-independent nature of the mechanism that governs the lysosomal localization of mTORC1 in response to its intrinsic activity is also supported by an accompanying study from the Zwartkruis lab showing that (1) rapamycin can enhance lysosomal mTOR localization also in TSC2 KO cells and (2) TSC2 KO (that causes mTORC1 hyperactivation) does not phenocopy cells with activating mTOR mutations, as mTOR localization to lysosomes is higher in the former but lower in the latter, while both genetic models demonstrate enhanced nuclear localization of TFE3.[54]

Insights into the mechanistic aspects of Rag inactivation by active lysosomal mTORC1

How does active mTORC1 inactivate RagA to facilitate its own release from the lysosomal surface? A plausible scenario is that

confocal microscopy. Magnified insets shown to the right (A). Quantification of colocalization in (B). n = 77–81 individual cells from 5 independent fields per condition.

(C) The Rag-FLCN interaction is weakened by rapamycin treatment in cells expressing WT RagA but not RagC, indicating RagA activation by mTORC1 inhibition. Co-immunoprecipitation of HA-tagged RagA/RagC dimers from HEK293FT Rag qKO cells stably expressing WT Rags, inactive-locked RagC (with WT RagA), or inactive-locked RagA (with WT RagC), treated with DMSO (vehicle) or rapamycin (Rapa, 20 nM) for 1 h as indicated. The input and IP samples were analyzed by immunoblotting using antibodies against the indicated proteins.

(D and E) Removal of GATOR1, which locks RagA in its active state, blunts the mTOR inhibition effect on mTOR localization. Colocalization analysis of mTOR with LAMP2 (lysosomal marker) in WT and NPRL3 KO HEK293FT cells, treated with DMSO (vehicle) or rapamycin (20 nM) for 1 h, using confocal microscopy. Magnified insets shown to the right (D). Quantification of colocalization in (E). n = 82–94 individual cells from 5 independent fields per condition.

(F) Proposed model of the interplay between mTORC1 activity and lysosomal localization. Active mTORC1 dynamically cycles between the lysosomal surface and the cytoplasm, phosphorylating the respective substrates at each subcellular location. The activation of mTORC1 on the lysosomal surface licenses its release to the cytoplasm (left). Downregulation of mTORC1 activity (e.g., upon its pharmacological inhibition or genetic ablation of RHEB) causes locking of the RagA component of the Rag dimer in its active conformation, which in turn promotes stronger lysosomal tethering of mTORC1.

Scale bars, 20 μm. Data in graphs shown as mean ± SEM. ** $p < 0.01$, *** $p < 0.001$, ns: non-significant.

See also Figure S7.

Molecular Cell
Article

mTORC1-dependent phosphorylation may play an important role in this process. For instance, the tethering of mTORC1 on the lysosomal surface is mediated by interactions between the Rag dimer and Raptor.[14] Interestingly, multiple residues on both RagC and Raptor have been previously identified as direct mTORC1 targets[55–57]; hence, these phosphorylations may create negatively charged surfaces that weaken the Raptor-Rag interaction. Furthermore, the GTP/GDP loading of the RagA/B and RagC/D proteins is regulated by the GATOR1 and FLCN-FNIP1/2 complexes, respectively.[41,45,51] Intriguingly, FLCN phosphorylation on multiple residues is induced downstream of a TSC2-Rheb signaling axis,[58] while Lst4, the yeast FNIP1/2 ortholog, is phosphorylated directly by TORC1.[59] Indeed, we too observed mTORC1-activity-dependent changes in the migration pattern of Rag-bound or lysosome-localized FLCN in immunoblots (e.g., see Figures 6D, 6E, and S6D–S6F), suggesting that FLCN phosphorylation may be affected—directly or indirectly—downstream of mTORC1. However, our data argue against FLCN playing a major role in mTOR localization on lysosomes upon inactivation of the latter (Figures S7B–S7D), suggesting the existence of an independent and parallel mTOR-FLCN signaling pathway that warrants further investigation. Finally, it is noteworthy that the accompanying study by Zwakenberg et al. identified DEPDC5, a component of the GATOR1 complex, as a putative target of mTORC1.[54] As our data indicate that the GATOR1-RagA signaling axis holds a key role for the release of activated mTORC1 from the lysosomal surface, a plausible hypothesis is that mTORC1 may be regulating its own localization by phosphorylating DEPDC5. In any case, the mild quantitative differences between rapamycin and Torin1 treatment in the strength of lysosomal mTORC1 tethering suggest that both rapamycin-sensitive and rapamycin-resistant sites and substrates may participate in this mechanism, which remain to be identified in the future. In sum, our data combined with previous reports in the literature raise the intriguing hypothesis that the release of active mTORC1 from lysosomes is a rapid, multifactorial event that presumably involves the phosphorylation of several key molecular players to bring about a concerted response upon its activation on the lysosomal surface.

Taken together, the work by us and others suggests the existence of a two-branch mechanism that controls the spatial coincidence of mTORC1 and TFEB/TFE3 on lysosomes and involves—on the one hand—the GATOR1-RagA-dependent recruitment of the kinase (i.e., mTORC1) and—on the other hand—the FLCN-RagC-dependent recruitment of the substrate (i.e., TFEB/TFE3) on the lysosomal surface and its presentation to the kinase. Only when both of these conditions are met and both branches are active will TFEB/TFE3 be phosphorylated by mTORC1. By contrast, the inactivation or dysregulation of either of these AA sensing branches (e.g., under depletion of specific nutrients or in diseases like tuberous sclerosis) will ensure that TFEB/TFE3 signaling will be activated to promote survival and recycling-related cellular functions like lysosome- and autophagosome-biogenesis.

A signaling checkpoint to prevent futile cycling of mTORC1 between lysosomes and the cytoplasm

mTORC1 is activated on the lysosomal surface via a mechanism that involves the local production of AAs inside lysosomes by proteolysis and their efflux from the lysosomal lumen.[16,20] We recently showed that mTORC1 can be active also away from lysosomes and phosphorylates its non-lysosomal substrates like S6K in the cytoplasm to regulate *de novo* protein synthesis.[20] Conceivably, this means that mTORC1 that is activated on lysosomes needs to be released from these organelles to meet its targets elsewhere. Here we unravel a mechanism by which active mTORC1 licenses its own release from lysosomes and acts as a signaling checkpoint to ensure that, when nutrient cues are sufficient, recruitment of mTORC1 to the lysosomes for reactivation is not futile and to prevent its anomalous lysosomal retention. This checkpoint may also act as a point of regulation in the cycling of mTORC1, where the balance between cytosolic and lysosomal activities of mTORC1 is established and maintained according to cellular needs.[13,20] Finally, this mechanism warrants that inactive mTORC1 complexes stay associated with lysosomes, presumably to be primed for reactivation once fresh nutrients are produced locally. In sum, our work reveals that not only the recruitment but also the release of mTORC1 from the lysosomal surface is an active process mediated by the Rag GTPases.

Limitations of the study

Our findings presented here indicate that the stronger lysosomal tethering that is observed upon downregulation of mTORC1 activity is mediated by the Rag GTPases. Moreover, we show that inactivation of mTORC1 causes persistent activation of the Rag dimer, even under conditions that normally promote its inactive conformation, like AA starvation. Inversely, this means that activation of mTORC1 on the lysosomal surface is necessary to allow the inactivation of the Rag dimer and, subsequently, license the release of active mTOR to the cytoplasm. Whether mTORC1 directly or indirectly regulates Rag dimer activation via the phosphorylation of one or more participating proteins is not clear yet, and future studies will be necessary to identify the complete mechanism. Finally, as also discussed above in more detail, it is reasonable to speculate that the lysosome-based molecular machinery that regulates the localization of mTORC1 in response to its activation state (described in our study) may be directly or indirectly associated to the one that is responsible for the diminished lysosomal recruitment and phosphorylation of TFEB in TSC KO cells.[53] Again, future work will be necessary to fully understand the potential interplay between the recruitment of mTORC1 and TFEB/TFE3 on the lysosomal surface, as well as how these two processes are coordinated to ensure the finely tuned regulation of lysosomal mTORC1 signaling.

RESOURCE AVAILABILITY

Lead contact

Further information and reasonable requests for resources and reagents should be directed to and will be fulfilled by the lead contact, Dr. Constantinos Demetriades (Demetriades@age.mpg.de).

Materials availability

All unique plasmids and cell lines generated in this study are available from the lead contact with a completed material transfer agreement.

CellPress OPEN ACCESS

Molecular Cell
Article

Data and code availability

- Original western blot images and microscopy data reported in this paper will be shared by the lead contact upon request.
- This paper does not report original code.
- Any additional information required to reanalyze the data reported in this paper is available from the lead contact upon request.

ACKNOWLEDGMENTS

We thank all members of the Demetriades lab for critical discussions; Andreas Lamprakis, Julian Nüchel, Peter Gollwitzer, and Marija Kovacevic-Sarmiento for support with cloning; and the MPI-AGE FACS & Imaging Core Facility for support with confocal microscopy. A.A. received support by the Cologne Graduate School of Ageing Research. C.D. is funded by the European Research Council (ERC) under the European Union's Horizon 2020 research and innovation program (grant agreement no 757729) and by the Max Planck Society. Parts of this work were supported by the Deutsche Forschungsgemeinschaft (DFG, German Research Foundation) through the Research Unit Grant FOR2722 (DE 3170/1-1; project no 384170921) to C.D. Models in figures created with BioRender.com.

AUTHOR CONTRIBUTIONS

Experimental work: A.A.; data analysis: A.A.; project design and conceptualization: A.A. and C.D.; supervision: C.D.; funding acquisition: C.D.; figure preparation: A.A. and C.D.; manuscript draft: C.D. with contributions from A.A. Both authors approved the final version of the manuscript and agree on the content and conclusions.

DECLARATION OF INTERESTS

The authors declare no competing interests.

STAR★METHODS

Detailed methods are provided in the online version of this paper and include the following:

- KEY RESOURCES TABLE
- EXPERIMENTAL MODEL AND STUDY PARTICIPANT DETAILS
  - Cell culture
  - Plasmid DNA transfections
  - Generation of knockout cell lines
  - Generation of stable cell lines
  - Gene silencing experiments
- METHOD DETAILS
  - Cell culture treatments
  - Antibodies
  - Plasmids and Molecular Cloning
  - Cell lysis and immunoblotting
  - Co-immunoprecipitation (co-IP)
  - Lysosome purification (Lyso-IP) assays
  - Immunofluorescence and confocal microscopy
  - mRNA isolation, cDNA synthesis and quantitative real-time PCR
  - LysoTracker staining
- QUANTIFICATION AND STATISTICAL ANALYSIS
  - Statistical analysis
  - Quantification of colocalization
  - Quantification of LysoTracker intensity

SUPPLEMENTAL INFORMATION

Supplemental information can be found online at https://doi.org/10.1016/j.molcel.2024.10.008.

Received: October 12, 2023
Revised: August 17, 2024
Accepted: October 7, 2024
Published: October 31, 2024

REFERENCES

1. Dönnes, P., and Höglund, A. (2004). Predicting protein subcellular localization: past, present, and future. Genomics Proteomics Bioinformatics *2*, 209–215. https://doi.org/10.1016/s1672-0229(04)02027-3.
2. Shaffer, K.L., Sharma, A., Snapp, E.L., and Hegde, R.S. (2005). Regulation of protein compartmentalization expands the diversity of protein function. Dev. Cell *9*, 545–554. https://doi.org/10.1016/j.devcel.2005.09.001.
3. Lee, M.J., and Yaffe, M.B. (2016). Protein Regulation in Signal Transduction. Cold Spring Harb. Perspect. Biol. *8*, a005918. https://doi.org/10.1101/cshperspect.a005918.
4. Guiochon-Mantel, A., and Milgrom, E. (1993). Cytoplasmic-nuclear trafficking of steroid hormone receptors. Trends Endocrinol. Metab. *4*, 322–328. https://doi.org/10.1016/1043-2760(93)90074-o.
5. Levin, E.R., and Hammes, S.R. (2016). Nuclear receptors outside the nucleus: extranuclear signalling by steroid receptors. Nat. Rev. Mol. Cell Biol. *17*, 783–797. https://doi.org/10.1038/nrm.2016.122.
6. Dobbs, N., Burnaevskiy, N., Chen, D., Gonugunta, V.K., Alto, N.M., and Yan, N. (2015). STING Activation by Translocation from the ER Is Associated with Infection and Autoinflammatory Disease. Cell Host Microbe *18*, 157–168. https://doi.org/10.1016/j.chom.2015.07.001.
7. Mukai, K., Ogawa, E., Uematsu, R., Kuchitsu, Y., Kiku, F., Uemura, T., Waguri, S., Suzuki, T., Dohmae, N., Arai, H., et al. (2021). Homeostatic regulation of STING by retrograde membrane traffic to the ER. Nat. Commun. *12*, 61. https://doi.org/10.1038/s41467-020-20234-9.
8. Fernandes, S.A., and Demetriades, C. (2021). The Multifaceted Role of Nutrient Sensing and mTORC1 Signaling in Physiology and Aging. Front. Aging *2*, 707372. https://doi.org/10.3389/fragi.2021.707372.
9. Kennedy, B.K., and Lamming, D.W. (2016). The Mechanistic Target of Rapamycin: The Grand ConducTOR of Metabolism and Aging. Cell Metab. *23*, 990–1003. https://doi.org/10.1016/j.cmet.2016.05.009.
10. González, A., and Hall, M.N. (2017). Nutrient sensing and TOR signaling in yeast and mammals. EMBO J. *36*, 397–408. https://doi.org/10.15252/embj.201696010.
11. Liu, G.Y., and Sabatini, D.M. (2020). mTOR at the nexus of nutrition, growth, ageing and disease. Nat. Rev. Mol. Cell Biol. *21*, 183–203. https://doi.org/10.1038/s41580-019-0199-y.
12. Rabanal-Ruiz, Y., and Korolchuk, V.I. (2018). mTORC1 and Nutrient Homeostasis: The Central Role of the Lysosome. Int. J. Mol. Sci. *19*, 818. https://doi.org/10.3390/ijms19030818.
13. Lawrence, R.E., Cho, K.F., Rappold, R., Thrun, A., Tofaute, M., Kim, D.J., Moldavski, O., Hurley, J.H., and Zoncu, R. (2018). A nutrient-induced affinity switch controls mTORC1 activation by its Rag GTPase-Ragulator lysosomal scaffold. Nat. Cell Biol. *20*, 1052–1063. https://doi.org/10.1038/s41556-018-0148-6.
14. Sancak, Y., Peterson, T.R., Shaul, Y.D., Lindquist, R.A., Thoreen, C.C., Bar-Peled, L., and Sabatini, D.M. (2008). The Rag GTPases bind raptor and mediate amino acid signaling to mTORC1. Science *320*, 1496–1501. https://doi.org/10.1126/science.1157535.
15. Sancak, Y., Bar-Peled, L., Zoncu, R., Markhard, A.L., Nada, S., and Sabatini, D.M. (2010). Ragulator-Rag complex targets mTORC1 to the lysosomal surface and is necessary for its activation by amino acids. Cell *141*, 290–303. https://doi.org/10.1016/j.cell.2010.02.024.
16. Zoncu, R., Bar-Peled, L., Efeyan, A., Wang, S., Sancak, Y., and Sabatini, D.M. (2011). mTORC1 senses lysosomal amino acids through an inside-out mechanism that requires the vacuolar H(+)-ATPase. Science *334*, 678–683. https://doi.org/10.1126/science.1207056.

Molecular Cell
Article

17. Kim, E., Goraksha-Hicks, P., Li, L., Neufeld, T.P., and Guan, K.L. (2008). Regulation of TORC1 by Rag GTPases in nutrient response. Nat. Cell Biol. *10*, 935–945. https://doi.org/10.1038/ncb1753.

18. Gollwitzer, P., Grützmacher, N., Wilhelm, S., Kümmel, D., and Demetriades, C. (2022). A Rag GTPase dimer code defines the regulation of mTORC1 by amino acids. Nat. Cell Biol. *24*, 1394–1406. https://doi.org/10.1038/s41556-022-00976-y.

19. Long, X., Lin, Y., Ortiz-Vega, S., Yonezawa, K., and Avruch, J. (2005). Rheb binds and regulates the mTOR kinase. Curr. Biol. *15*, 702–713. https://doi.org/10.1016/j.cub.2005.02.053.

20. Fernandes, S.A.A., Angelidaki, D.-D., Nüchel, J., Pan, J., Gollwitzer, P., Elkis, Y., Artoni, F., Wilhelm, S., Kovacevic-Sarmiento, M., and Demetriades, C. (2024). Spatial and functional separation of mTORC1 signalling in response to different amino acid sources. Nat. Cell Biol. https://doi.org/10.1038/s41556-024-01523-7.

21. Manifava, M., Smith, M., Rotondo, S., Walker, S., Niewczas, I., Zoncu, R., Clark, J., and Ktistakis, N.T. (2016). Dynamics of mTORC1 activation in response to amino acids. eLife *5*, e19960. https://doi.org/10.7554/eLife.19960.

22. Laqtom, N.N., Dong, W., Medoh, U.N., Cangelosi, A.L., Dharamdasani, V., Chan, S.H., Kunchok, T., Lewis, C.A., Heinze, I., Tang, R., et al. (2022). CLN3 is required for the clearance of glycerophosphodiesters from lysosomes. Nature *609*, 1005–1011. https://doi.org/10.1038/s41586-022-05221-y.

23. Pavan, I.C.B., Yokoo, S., Granato, D.C., Meneguello, L., Carnielli, C.M., Tavares, M.R., do Amaral, C.L., de Freitas, L.B., Paes Leme, A.F., Luchessi, A.D., and Simabuco, F.M. (2016). Different interactomes for p70-S6K1 and p54-S6K2 revealed by proteomic analysis. Proteomics *16*, 2650–2666. https://doi.org/10.1002/pmic.201500249.

24. Nüchel, J., Tauber, M., Nolte, J.L., Mörgelin, M., Türk, C., Eckes, B., Demetriades, C., and Plomann, M. (2021). An mTORC1-GRASP55 signaling axis controls unconventional secretion to reshape the extracellular proteome upon stress. Mol. Cell *81*, 3275–3293.e12. https://doi.org/10.1016/j.molcel.2021.06.017.

25. Demetriades, C., Nüchel, J., and Plomann, M. (2021). GRASPing the unconventional secretory machinery to bridge cellular stress signaling to the extracellular proteome. Cell Stress *5*, 173–175. https://doi.org/10.15698/cst2021.11.259.

26. Ohsaki, Y., Suzuki, M., Shinohara, Y., and Fujimoto, T. (2010). Lysosomal accumulation of mTOR is enhanced by rapamycin. Histochem. Cell Biol. *134*, 537–544. https://doi.org/10.1007/s00418-010-0759-x.

27. Korolchuk, V.I., Saiki, S., Lichtenberg, M., Siddiqi, F.H., Roberts, E.A., Imarisio, S., Jahreiss, L., Sarkar, S., Futter, M., Menzies, F.M., et al. (2011). Lysosomal positioning coordinates cellular nutrient responses. Nat. Cell Biol. *13*, 453–460. https://doi.org/10.1038/ncb2204.

28. Settembre, C., Zoncu, R., Medina, D.L., Vetrini, F., Erdin, S., Erdin, S., Huynh, T., Ferron, M., Karsenty, G., Vellard, M.C., et al. (2012). A lysosome-to-nucleus signalling mechanism senses and regulates the lysosome via mTOR and TFEB. EMBO J. *31*, 1095–1108. https://doi.org/10.1038/emboj.2012.32.

29. Zhou, J., Tan, S.H., Nicolas, V., Bauvy, C., Yang, N.D., Zhang, J., Xue, Y., Codogno, P., and Shen, H.M. (2013). Activation of lysosomal function in the course of autophagy via mTORC1 suppression and autophagosome-lysosome fusion. Cell Res. *23*, 508–523. https://doi.org/10.1038/cr.2013.11.

30. Demetriades, C., Doumpas, N., and Teleman, A.A. (2014). Regulation of TORC1 in response to amino acid starvation via lysosomal recruitment of TSC2. Cell *156*, 786–799. https://doi.org/10.1016/j.cell.2014.01.024.

31. Artoni, F., Grützmacher, N., and Demetriades, C. (2023). Unbiased evaluation of rapamycin's specificity as an mTOR inhibitor. Aging Cell *22*, e13888. https://doi.org/10.1111/acel.13888.

32. Thoreen, C.C., Kang, S.A., Chang, J.W., Liu, Q., Zhang, J., Gao, Y., Reichling, L.J., Sim, T., Sabatini, D.M., and Gray, N.S. (2009). An ATP-competitive mammalian target of rapamycin inhibitor reveals rapamycin-resistant functions of mTORC1. J. Biol. Chem. *284*, 8023–8032. https://doi.org/10.1074/jbc.M900301200.

33. Abu-Remaileh, M., Wyant, G.A., Kim, C., Laqtom, N.N., Abbasi, M., Chan, S.H., Freinkman, E., and Sabatini, D.M. (2017). Lysosomal metabolomics reveals V-ATPase- and mTOR-dependent regulation of amino acid efflux from lysosomes. Science *358*, 807–813. https://doi.org/10.1126/science.aan6298.

34. Holz, M.K., Ballif, B.A., Gygi, S.P., and Blenis, J. (2005). mTOR and S6K1 mediate assembly of the translation preinitiation complex through dynamic protein interchange and ordered phosphorylation events. Cell *123*, 569–580. https://doi.org/10.1016/j.cell.2005.10.024.

35. Napolitano, G., Di Malta, C., Esposito, A., de Araujo, M.E.G., Pece, S., Bertalot, G., Matarese, M., Benedetti, V., Zampelli, A., Stasyk, T., et al. (2020). A substrate-specific mTORC1 pathway underlies Birt-Hogg-Dube syndrome. Nature *585*, 597–602. https://doi.org/10.1038/s41586-020-2444-0.

36. Efeyan, A., Zoncu, R., Chang, S., Gumper, I., Snitkin, H., Wolfson, R.L., Kirak, O., Sabatini, D.D., and Sabatini, D.M. (2013). Regulation of mTORC1 by the Rag GTPases is necessary for neonatal autophagy and survival. Nature *493*, 679–683. https://doi.org/10.1038/nature11745.

37. Efeyan, A., Schweitzer, L.D., Bilate, A.M., Chang, S., Kirak, O., Lamming, D.W., and Sabatini, D.M. (2014). RagA, but not RagB, is essential for embryonic development and adult mice. Dev. Cell *29*, 321–329. https://doi.org/10.1016/j.devcel.2014.03.017.

38. Sardiello, M., Palmieri, M., di Ronza, A., Medina, D.L., Valenza, M., Gennarino, V.A., Di Malta, C., Donaudy, F., Embrione, V., Polishchuk, R.S., et al. (2009). A gene network regulating lysosomal biogenesis and function. Science *325*, 473–477. https://doi.org/10.1126/science.1174447.

39. Settembre, C., Di Malta, C., Polito, V.A., Garcia Arencibia, M., Vetrini, F., Erdin, S., Erdin, S.U., Huynh, T., Medina, D., Colella, P., et al. (2011). TFEB links autophagy to lysosomal biogenesis. Science *332*, 1429–1433. https://doi.org/10.1126/science.1204592.

40. Puertollano, R., Ferguson, S.M., Brugarolas, J., and Ballabio, A. (2018). The complex relationship between TFEB transcription factor phosphorylation and subcellular localization. EMBO J. *37*, e98804. https://doi.org/10.15252/embj.201798804.

41. Tsun, Z.Y., Bar-Peled, L., Chantranupong, L., Zoncu, R., Wang, T., Kim, C., Spooner, E., and Sabatini, D.M. (2013). The folliculin tumor suppressor is a GAP for the RagC/D GTPases that signal amino acid levels to mTORC1. Mol. Cell *52*, 495–505. https://doi.org/10.1016/j.molcel.2013.09.016.

42. Meng, J., and Ferguson, S.M. (2018). GATOR1-dependent recruitment of FLCN-FNIP to lysosomes coordinates Rag GTPase heterodimer nucleotide status in response to amino acids. J. Cell Biol. *217*, 2765–2776. https://doi.org/10.1083/jcb.201712177.

43. Lawrence, R.E., Fromm, S.A., Fu, Y., Yokom, A.L., Kim, D.J., Thelen, A.M., Young, L.N., Lim, C.Y., Samelson, A.J., Hurley, J.H., and Zoncu, R. (2019). Structural mechanism of a Rag GTPase activation checkpoint by the lysosomal folliculin complex. Science *366*, 971–977. https://doi.org/10.1126/science.aax0364.

44. Egri, S.B., Ouch, C., Chou, H.T., Yu, Z., Song, K., Xu, C., and Shen, K. (2022). Cryo-EM structures of the human GATOR1-Rag-Ragulator complex reveal a spatial-constraint regulated GAP mechanism. Mol. Cell *82*, 1836–1849.e5. https://doi.org/10.1016/j.molcel.2022.03.002.

45. Shen, K., Rogala, K.B., Chou, H.T., Huang, R.K., Yu, Z., and Sabatini, D.M. (2019). Cryo-EM Structure of the Human FLCN-FNIP2-Rag-Ragulator Complex. Cell *179*, 1319–1329.e8. https://doi.org/10.1016/j.cell.2019.10.036.

46. Alesi, N., Akl, E.W., Khabibullin, D., Liu, H.J., Nidhiry, A.S., Garner, E.R., Filippakis, H., Lam, H.C., Shi, W., Viswanathan, S.R., et al. (2021). TSC2 regulates lysosome biogenesis via a non-canonical RAGC and

CellPress OPEN ACCESS

Molecular Cell
Article

TFEB-dependent mechanism. Nat. Commun. *12*, 4245. https://doi.org/10.1038/s41467-021-24499-6.

47. Li, K., Wada, S., Gosis, B.S., Thorsheim, C., Loose, P., and Arany, Z. (2022). Folliculin promotes substrate-selective mTORC1 activity by activating RagC to recruit TFE3. PLoS Biol. *20*, e3001594. https://doi.org/10.1371/journal.pbio.3001594.
48. Cui, Z., Napolitano, G., de Araujo, M.E.G., Esposito, A., Monfregola, J., Huber, L.A., Ballabio, A., and Hurley, J.H. (2023). Structure of the lysosomal mTORC1-TFEB-Rag-Ragulator megacomplex. Nature *614*, 572–579. https://doi.org/10.1038/s41586-022-05652-7.
49. Alesi, N., Khabibullin, D., Rosenthal, D.M., Akl, E.W., Cory, P.M., Alchoueiry, M., Salem, S., Daou, M., Gibbons, W.F., Chen, J.A., et al. (2024). TFEB drives mTORC1 hyperactivation and kidney disease in Tuberous Sclerosis Complex. Nat. Commun. *15*, 406. https://doi.org/10.1038/s41467-023-44229-4.
50. Shen, K., Huang, R.K., Brignole, E.J., Condon, K.J., Valenstein, M.L., Chantranupong, L., Bomaliyamu, A., Choe, A., Hong, C., Yu, Z., and Sabatini, D.M. (2018). Architecture of the human GATOR1 and GATOR1-Rag GTPases complexes. Nature *556*, 64–69. https://doi.org/10.1038/nature26158.
51. Bar-Peled, L., Chantranupong, L., Cherniack, A.D., Chen, W.W., Ottina, K.A., Grabiner, B.C., Spear, E.D., Carter, S.L., Meyerson, M., and Sabatini, D.M. (2013). A Tumor suppressor complex with GAP activity for the Rag GTPases that signal amino acid sufficiency to mTORC1. Science *340*, 1100–1106. https://doi.org/10.1126/science.1232044.
52. Zhitomirsky, B., Yunaev, A., Kreiserman, R., Kaplan, A., Stark, M., and Assaraf, Y.G. (2018). Lysosomotropic drugs activate TFEB via lysosomal membrane fluidization and consequent inhibition of mTORC1 activity. Cell Death Dis. *9*, 1191. https://doi.org/10.1038/s41419-018-1227-0.
53. Asrani, K., Woo, J., Mendes, A.A., Schaffer, E., Vidotto, T., Villanueva, C.R., Feng, K., Oliveira, L., Murali, S., Liu, H.B., et al. (2022). An mTORC1-mediated negative feedback loop constrains amino acid-induced FLCN-Rag activation in renal cells with TSC2 loss. Nat. Commun. *13*, 6808. https://doi.org/10.1038/s41467-022-34617-7.
54. Zwakenberg, S., Westland, D., van Es, R.M., Rehmann, H., Anink, J., Ciapaite, J., Bosma, M., Stelloo, E., Liv, N., Sobrevals Alcaraz, P., et al. (2024). mTORC1 restricts TFE3 activity by auto-regulating its presence on lysosomes. Mol. Cell *84*. https://doi.org/10.1016/j.molcel.2024.10.009.
55. Wang, L., Lawrence, J.C., Jr., Sturgill, T.W., and Harris, T.E. (2009). Mammalian target of rapamycin complex 1 (mTORC1) activity is associated with phosphorylation of raptor by mTOR. J. Biol. Chem. *284*, 14693–14697. https://doi.org/10.1074/jbc.C109.002907.
56. Foster, K.G., Acosta-Jaquez, H.A., Romeo, Y., Ekim, B., Soliman, G.A., Carriere, A., Roux, P.P., Ballif, B.A., and Fingar, D.C. (2010). Regulation of mTOR complex 1 (mTORC1) by raptor Ser863 and multisite phosphorylation. J. Biol. Chem. *285*, 80–94. https://doi.org/10.1074/jbc.M109.029637.
57. Yang, G., Humphrey, S.J., Murashige, D.S., Francis, D., Wang, Q.P., Cooke, K.C., Neely, G.G., and James, D.E. (2019). RagC phosphorylation autoregulates mTOR complex 1. EMBO J. *38*, e99548. https://doi.org/10.15252/embj.201899548.
58. Piao, X., Kobayashi, T., Wang, L., Shiono, M., Takagi, Y., Sun, G., Abe, M., Hagiwara, Y., Zhang, D., Okimoto, K., et al. (2009). Regulation of folliculin (the BHD gene product) phosphorylation by Tsc2-mTOR pathway. Biochem. Biophys. Res. Commun. *389*, 16–21. https://doi.org/10.1016/j.bbrc.2009.08.070.
59. Péli-Gulli, M.P., Raucci, S., Hu, Z., Dengjel, J., and De Virgilio, C. (2017). Feedback Inhibition of the Rag GTPase GAP Complex Lst4-Lst7 Safeguards TORC1 from Hyperactivation by Amino Acid Signals. Cell Rep. *20*, 281–288. https://doi.org/10.1016/j.celrep.2017.06.058.
60. Ran, F.A., Hsu, P.D., Wright, J., Agarwala, V., Scott, D.A., and Zhang, F. (2013). Genome engineering using the CRISPR-Cas9 system. Nat. Protoc. *8*, 2281–2308. https://doi.org/10.1038/nprot.2013.143.
61. Kowarz, E., Löscher, D., and Marschalek, R. (2015). Optimized Sleeping Beauty transposons rapidly generate stable transgenic cell lines. Biotechnol. J. *10*, 647–653. https://doi.org/10.1002/biot.201400821.
62. Schindelin, J., Arganda-Carreras, I., Frise, E., Kaynig, V., Longair, M., Pietzsch, T., Preibisch, S., Rueden, C., Saalfeld, S., Schmid, B., et al. (2012). Fiji: an open-source platform for biological-image analysis. Nat. Methods *9*, 676–682. https://doi.org/10.1038/nmeth.2019.
63. Demetriades, C., Plescher, M., and Teleman, A.A. (2016). Lysosomal recruitment of TSC2 is a universal response to cellular stress. Nat. Commun. *7*, 10662. https://doi.org/10.1038/ncomms10662.
64. Mane, S.M., Marzella, L., Bainton, D.F., Holt, V.K., Cha, Y., Hildreth, J.E., and August, J.T. (1989). Purification and characterization of human lysosomal membrane glycoproteins. Arch. Biochem. Biophys. *268*, 360–378. https://doi.org/10.1016/0003-9861(89)90597-3.
65. Bryk, B., Hahn, K., Cohen, S.M., and Teleman, A.A. (2010). MAP4K3 regulates body size and metabolism in Drosophila. Dev. Biol. *344*, 150–157. https://doi.org/10.1016/j.ydbio.2010.04.027.
66. Fitzian, K., Brückner, A., Brohée, L., Zech, R., Antoni, C., Kiontke, S., Gasper, R., Linard Matos, A.L., Beel, S., Wilhelm, S., et al. (2021). TSC1 binding to lysosomal PIPs is required for TSC complex translocation and mTORC1 regulation. Mol. Cell *81*, 2705–2721.e8. https://doi.org/10.1016/j.molcel.2021.04.019.
67. Manders, E.M.M., Verbeek, F.J., and Aten, J.A. (1993). Measurement of co-localization of objects in dual-colour confocal images. J. Microsc. *169*, 375–382. https://doi.org/10.1111/j.1365-2818.1993.tb03313.x.
68. Costes, S.V., Daelemans, D., Cho, E.H., Dobbin, Z., Pavlakis, G., and Lockett, S. (2004). Automatic and quantitative measurement of protein-protein colocalization in live cells. Biophys. J. *86*, 3993–4003. https://doi.org/10.1529/biophysj.103.038422.
69. Dunn, K.W., Kamocka, M.M., and McDonald, J.H. (2011). A practical guide to evaluating colocalization in biological microscopy. Am. J. Physiol. Cell Physiol. *300*, C723–C742. https://doi.org/10.1152/ajpcell.00462.2010.

Molecular Cell
Article

STAR★METHODS

KEY RESOURCES TABLE

REAGENT or RESOURCE	SOURCE	IDENTIFIER
Antibodies		
Rabbit monoclonal anti-mTOR (7C10)	Cell Signaling Technology	Cat#2983S; RRID: AB_2105622
Mouse monoclonal anti-LAMP2 (H4B4)	Developmental Studies Hybridoma Bank	Cat#H4B4; RRID: AB_2134755
Rabbit monoclonal anti-phospho-TFEB (Ser211) (E9S8N)	Cell Signaling Technology	Cat#37681; RRID: AB_2799117
Rabbit polyclonal anti-TFEB	Cell Signaling Technology	Cat#4240; RRID: AB_11220225
Rabbit polyclonal anti-TFE3	Cell Signaling Technology	Cat#14779; RRID: AB_2687582
Rabbit monoclonal anti-phospho-p70 S6 Kinase (Thr389) (D5U1O)	Cell Signaling Technology	Cat#97596; RRID: AB_2800283
Rabbit polyclonal anti-S6 Kinase	Cell Signaling Technology	Cat#9202; RRID: AB_331676
Rabbit polyclonal anti-phospho-4E-BP1 (Thr37/46)	Cell Signaling Technology	Cat#9459; RRID: AB_330985
Rabbit polyclonal anti-4E-BP1	Cell Signaling Technology	Cat#9452; RRID: AB_331692
Mouse monoclonal anti-RHEB (M01) (clone 2C11)	Abnova	Cat#H00006009-M01; RRID: AB_1146837
Rabbit monoclonal anti-GAPDH (14C10)	Cell Signaling Technology	Cat#2118; RRID: AB_561053
Rabbit polyclonal anti-RAPTOR	Proteintech	Cat#20984-1-AP; RRID: AB_11182390
Rabbit polyclonal anti-CathepsinD	Cell Signaling Technology	Cat#2284; RRID: AB_10694258
Rabbit monoclonal anti-phospho-AMPKα (Thr172) (40H9)	Cell Signaling Technology	Cat#2535; RRID: AB_331250
Rabbit polyclonal anti-AMPKα	Cell Signaling Technology	Cat#2532; RRID: AB_330331
Rabbit polyclonal anti-LC3B	Sigma-Aldrich	Cat#L7543; RRID: AB_796155
Rabbit monoclonal anti-FLCN (D14G9)	Cell Signaling Technology	Cat#3697; RRID: AB_2231646
Rabbit polyclonal anti-NPRL3	Sigma-Aldrich	Cat#HPA011741; RRID: AB_1845577
Rat monoclonal anti-HA (3F10)	Roche	Cat#11867423001; RRID: AB_390918
Mouse monoclonal anti-α-Tubulin	Sigma-Aldrich	Cat#T9026; RRID: AB_477593
Rabbit monoclonal anti-phospho-S6 ribosomal protein (Ser235/236) (D57.2.2E)	Cell Signaling Technology	Cat#4858; RRID: AB_916156
Rabbit monoclonal anti-phospho-S6 ribosomal protein (Ser240/244) (D68F8)	Cell Signaling Technology	Cat#5364; RRID: AB_10694233
Mouse monoclonal anti-S6 ribosomal protein (52D2)	Cell Signaling Technology	Cat#2317; RRID: AB_2238583

(*Continued on next page*)

CellPress OPEN ACCESS

Molecular Cell
Article

Continued

REAGENT or RESOURCE	SOURCE	IDENTIFIER
Rabbit monoclonal anti-RagA (D8B5)	Cell Signaling Technology	Cat#4357; RRID: AB_10545136
Rabbit monoclonal anti-RagC (D8H5) (for IPs and IFs)	Cell Signaling Technology	Cat#9480; RRID: AB_10614716
Rabbit polyclonal anti-RagC (for WBs)	Cell Signaling Technology	Cat#3360; RRID: AB_2180068
Alexa Fluor 488 AffiniPure Donkey Anti-Rabbit IgG (H+L)	Jackson ImmunoResearch	Cat#711-545-152; RRID: AB_2313584
Alexa Fluor 594 AffiniPure Donkey Anti-Mouse IgG (H+L)	Jackson ImmunoResearch	Cat#715-585-151; RRID: AB_2340855
Peroxidase-AffiniPure Donkey Anti-Rabbit IgG (H+L)	Jackson ImmunoResearch	Cat#711-035-152; RRID: AB_10015282
Peroxidase-AffiniPure Donkey Anti-Mouse IgG (H+L)	Jackson ImmunoResearch	Cat#715-035-151; RRID: AB_2340771
Peroxidase AffiniPure Donkey Anti-Rat IgG (H+L)	Jackson ImmunoResearch	Cat#712-035-153; RRID: AB_2340639
Peroxidase IgG Fraction Monoclonal Mouse Anti-Rabbit IgG, light chain specific	Jackson ImmunoResearch	Cat#211-032-171; RRID: AB_2339149
Bacterial and virus strains		
E. coli DH5-alpha	New England Biolabs	N/A
Chemicals, peptides, and recombinant proteins		
anti-HA-Agarose beads	Sigma-Aldrich	Cat#A2095
Bafilomycin A1	Enzo Life Sciences	Cat#BML-CM110-0100 CAS: 88899-55-2
Blasticidin	Gibco	Cat#A1113903 CAS: 3513-03-9
Bovine Serum Albumin	Roche	Cat#10735086001
Bovine Serum Albumin	Carl Roth	Cat#8076
CHAPS	Carl Roth	Cat#1479 CAS: 75621-03-3
cOmplete protease inhibitors	Roche	Cat#11697498001
DAPI (4',6-diamidino-2-phenylindole)	VWR	Cat#A1001
DMEM (Dulbecco's Modified Eagle Medium)	Gibco	Cat#41965039
DMEM/F12 GlutaMAX	Gibco	Cat#31331093
DMEM GlutaMAX	Gibco	Cat#61965026
DMEM AA-free	Demetriades et al.[30]	N/A
DMEM Glucose-free	Gibco	Cat#11966025
DMSO (Dimethyl sulfoxide)	Carl Roth	Cat#4720.1
Doxycycline	Sigma-Aldrich	Cat#9891 CAS: 24390-14-5
ECL Western Blotting Substrate	Promega	Cat#W1015
Effectene Transfection Reagent	QIAGEN	Cat#301425
Fetal Bovine Serum (FBS)	Sigma	Cat#S7524
Fetal Bovine Serum (FBS)	PAN-Biotech	Cat#P30-3306
Fetal Bovine Serum (FBS)	Bio&SELL	Cat#FBS.HP.0500
Fluoromount-G	Invitrogen	Cat#00-4958-02
Gelatin	Sigma-Aldrich	Cat#G1393
Lipofectamine RNAiMAX	Invitrogen	Cat#13778075
LY2584702 (S6Ki)	Cayman Chemical	Cat#15320 CAS: 1082949-68-5
LysoTracker Red DND-99	Invitrogen	Cat#L7528

(*Continued on next page*)

Molecular Cell
Article

Continued

REAGENT or RESOURCE	SOURCE	IDENTIFIER
Paraformaldehyde	Thermo Scientific	Cat#28908
Penicillin-Streptomycin	Gibco	Cat#15140122
Penicillin-Streptomycin	Sigma-Aldrich	Cat#P4333-100ML
PF-4708671 (S6Ki)	Sigma-Aldrich	Cat#PZ0143 CAS: 1255517-76-0
PhosSTOP phosphatase inhibitors	Roche	Cat#04906837001
Pierce anti-HA magnetic beads	Thermo Scientific	Cat#88837
Protein Assay Dye Reagent	Biorad	Cat#5000006
Protein A Agarose	Roche	Cat#11134515001
Puromycin	Gibco	Cat#A1113803 CAS: 58-58-2
Rapamycin (mTORi)	Selleckchem	Cat#S1039 CAS: 53123-88-9
Sodium Pyruvate	Gibco	Cat#11360039
SuperSignal West Femto Substrate	Thermo Scientific	Cat#34095
Torin1 (mTORi)	Tocris Bioscience	Cat#4247 CAS: 1222998-36-8
TRIzol reagent	Invitrogen	Cat#15596018
Critical commercial assays		
RevertAid H Minus Reverse Transcriptase kit	Invitrogen	Cat#EP0451
Maxima SYBR Green/ROX qPCR master mix	Thermo Scientific	Cat#K0223
Deposited data		
N/A	N/A	N/A
Experimental models: Cell lines		
Human: HEK293FT cells	Invitrogen	Cat#R70007; RRID: CVCL_6911
Human: HFF-1 cells	ATCC	Cat#SCRC-1041; RRID: CVCL_3285
Human: WI26 SV40 cells	ATCC	Cat#CCL-95.1; RRID: CVCL_2758
Experimental models: Organisms/strains		
N/A	N/A	N/A
Oligonucleotides		
See Table S2	This study	Table S2
Recombinant DNA		
Plasmid: pSpCas9(BB)-2A-Puro 2.0 (pX459)	Ran et al.[60]	Addgene Plasmid #62988
Plasmid: pX459-hRHEB-5CDS	This manuscript	N/A
Plasmid: pX459-hRHEB-3UTR	This manuscript	N/A
Plasmid: pX459-hNPRL3-exon8	This manuscript	N/A
Plasmid: pX459-hFLCN-exon4	This manuscript	N/A
Plasmid: pX459-hFLCN-exon5	This manuscript	N/A
Plasmid: pITR-TTP-puro	Nüchel et al.[24]; Kowarz et al.[61]	N/A
Plasmid: pITR-TTP-bsd	This manuscript	N/A
Plasmid: pITR-HA-hRagA^{WT}-puro	This manuscript	N/A
Plasmid: pITR-HA-hRagA^{QL} (Q66L)-puro	This manuscript	N/A
Plasmid: pITR-HA-hRagA^{TN} (T21N) -puro	This manuscript	N/A
Plasmid: pITR-HA-hRagC^{WT}-bsd	This manuscript	N/A
Plasmid: pITR-HA-hRagC^{SN} (S75N) -bsd	This manuscript	N/A
Plasmid: pITR-HA-hRagC^{QL} (Q120L) -bsd	This manuscript	N/A

(*Continued on next page*)

CellPress OPEN ACCESS

Molecular Cell
Article

Continued

REAGENT or RESOURCE	SOURCE	IDENTIFIER
Software and algorithms		
Fiji	Schindelin et al.[62]	https://imagej.net/software/fiji/
GelAnalyzer 19.1	www.gelanalyzer.com	www.gelanalyzer.com
GraphPad Prism 10.2.3	GraphPad Software	www.graphpad.com
Other		
N/A	N/A	N/A

EXPERIMENTAL MODEL AND STUDY PARTICIPANT DETAILS

Cell culture

All cell lines were grown at 37°C, 5% CO_2. Human female embryonic kidney HEK293FT cells (#R70007, Invitrogen; RRID: CVCL_6911) were cultured in high-glucose Dulbecco's Modified Eagle Medium (DMEM) (#41965039, Gibco), supplemented with 10% fetal bovine serum (FBS) (#F7524, Sigma; #P30-3306, PAN-Biotech; #FBS.HP.0500, Bio&SELL). Human male diploid lung WI-26 SV40 fibroblasts (WI-26 cells; #CCL-95.1, ATCC; RRID: CVCL_2758) were cultured in DMEM/F12 GlutaMAX medium (#31331093, Gibco) containing 10% FBS. Normal (non-transformed) human male foreskin fibroblasts HFF-1 (HFFs; #SCRC-1041, ATCC; RRID: CVCL_3285) were cultured in high-glucose DMEM GlutaMAX (#61965026, Gibco), containing 10% FBS and 1 mM sodium pyruvate (#11360039, Gibco). All media were supplemented with 1x Penicillin-Streptomycin (#15140122, Gibco; #P4333-100ML, Sigma).

HEK293FT cells were purchased from Invitrogen and HFFs were purchased from ATCC at the initiation of the project. The identity of the HEK293FT cells was validated by the Multiplex human Cell Line Authentication test (Multiplexion GmbH), which uses a single nucleotide polymorphism (SNP) typing approach, and was performed as described at www.multiplexion.de. The identity of the WI-26 cells was validated using the Short Tandem Repeat (STR) profiling service, provided by Multiplexion GmbH. No commonly misidentified cell lines were used in this study. All cell lines were regularly tested for *Mycoplasma* contamination, using a PCR-based approach and were confirmed to be *Mycoplasma*-free.

Plasmid DNA transfections

Plasmid DNA transfections in HEK293FT cells were performed using Effectene transfection reagent (#301425, QIAGEN), according to the manufacturer's instructions.

Generation of knockout cell lines

The HEK293FT Rag quadruple knockout cell line (qKO)[18] and the base-edited, rapamycin-resistant mTOR cell line ($mTOR^{RR}$) have been described previously.[31] The HEK293FT RHEB, NPRL3, and FLCN knockout cell lines were generated using the pX459-based CRISPR/Cas9 method, as described elsewhere.[60] The sgRNA expression vectors were generated by cloning appropriate DNA oligonucleotides (Table S2) into the BbsI restriction sites of the pX459 vector (#62988, Addgene). An empty pX459 vector was used to generate matching control cell lines. In brief, transfected cells were selected with 3 μg/ml puromycin (#A1113803, Gibco) 36-40 hours post transfection. Single-cell clones were generated by FACS-sorting into 96-well plates and knockout clones were validated by immunoblotting and functional assays.

Generation of stable cell lines

The stable HEK293FT cell lines expressing HA-tagged TMEM192 (Lyso-IP lines) or FLAG-tagged TMEM192 (negative control lines for anti-HA Lyso-IPs) were described previously.[20] The polyclonal reconstituted Rag qKO cell lines stably expressing the various combinations of RagA and RagC dimers were generated using a doxycycline-inducible sleeping-beauty-based transposon system.[24,61] In brief, Rag qKO cells were transfected with equal amounts of the desired pITR-HA-RagA-puro and pITR-HA-RagC-bsd expression constructs (see 'Plasmid' section below) in a 10:1 ratio together with the transposase-expressing pCMV-Trp vector. Thirty-six to 40 hours post transfection, cells were selected with 3 μg/ml puromycin (#A1113803, Gibco) and 10 μg/mL blasticidin (#A1113903, Gibco). The polyclonal cell lines were subsequently maintained in media containing the selection agents. Doxycycline-induced expression from the integrated transposon was checked by treating the cells overnight with 2 μg/mL doxycycline (#D9891, Sigma). For experiments, all cell lines (except for the $RagA^{TN}$/$RagC^{QL}$-expressing cells; see below) were used without doxycycline induction as similarly low expression levels were obtained due to leaky expression. An exception was the $RagA^{TN}$/$RagC^{QL}$ expressing cell line that was plated for experiments in the presence of 10 ng/mL doxycycline in order to bring the expression levels of the inactive Rag dimer proteins closer to that of the wild-type and active Rag mutant proteins that are expressed in the respective reconstituted cell lines.

Molecular Cell
Article

Gene silencing experiments

Transient knockdown of *RRAGA* and *RRAGB* was performed using siGENOME (pool of 4) gene-specific siRNAs (Horizon Discoveries). An siRNA duplex targeting the *R. reniformis* luciferase gene (RLuc) (#P-002070-01-50, Horizon Discoveries) was used as a control. Transfections were performed using 20 nM siRNA and the Lipofectamine RNAiMAX transfection reagent (#13778075, Invitrogen), according to the manufacturer's instructions. Cells were fixed 72 hours post-transfection and knockdown efficiency was verified by immunoblotting.

METHOD DETAILS

Cell culture treatments

Amino acid (AA) starvation experiments were performed as described previously.[30,63] In brief, custom-made starvation media were formulated according to the Gibco recipe for high-glucose DMEM, specifically omitting all amino acids. The media were filtered through a 0.22-μm filter device and tested for proper pH and osmolality before use. For the respective AA-replete (+AA) treatment media, commercially available high-glucose DMEM was used (#41965039, Gibco). All treatment media were supplemented with 10% dialyzed FBS (dFBS) and 1x Penicillin-Streptomycin (#15140122, Gibco; #P4333-100ML, Sigma). For this purpose, FBS was dialyzed against 1x PBS through 3,500 MWCO dialysis tubing. For basal (+AA) conditions, the culture media were replaced with +AA treatment media 1 hour before lysis or fixation. For amino-acid starvation (-AA), culture media were replaced with starvation media for 1 hour, unless otherwise indicated in the figure legends. For glucose starvation experiments, cells were cultured in glucose-free DMEM (#11966025, Gibco) supplemented with 10% dFBS and 1x Penicillin-Streptomycin. For the respective control wells, the culture media were replaced with high-glucose DMEM containing 10% dFBS and 1x Penicillin-Streptomycin at the beginning of the experiment. Treatment times are indicated in the respective figures and figure legends.

To inhibit mTOR kinase activity, Torin1 (#4247, Tocris Bioscience) was added in the culture media to a final concentration of 250 nM for 1 hour unless otherwise indicated in the figure legends. Specific mTORC1 inhibition was performed by adding rapamycin (#S1039; Selleckchem) to the culture media to a final concentration of 20nM for 1 hour unless otherwise indicated. For S6K inhibition, LY2584702 (#15320, Cayman Chemical) or PF-4708671 (#PZ0143, Sigma) were added to the media at a final concentration of 20μM for 4 hours. For Bafilomycin A1 (#BML-CM110-0100, Enzo Life Sciences) treatment, the drug was added to a final concentration of 100 nM in the media for 6 hours before lysis or fixation, unless otherwise indicated in the figure legends. For all drug treatments, DMSO (#4720.1, Roth) was used as vehicle control. For experiments involving pre-treatments, the drugs were added directly to the culture media for the indicated times, and cells were then treated with media containing or lacking the respective inhibitors as specified in the figure legends. In general, co-IP and Lyso-IP experiments were performed with the inhibitors present also in the treatment media, and all other experiments were performed in the absence of inhibitors from the treatment media.

Antibodies

A list of all primary antibodies used in this study is found in Table S1 and in the respective section of the key resources table. The H4B4 antibody against LAMP2 was obtained from the Developmental Studies Hybridoma Bank, created by the NICHD of the NIH and maintained at The University of Iowa, Department of Biology. H4B4 was deposited to the DSHB by August, J.T. / Hildreth, J.E.K. (DSHB Hybridoma Product H4B4).[64]

Plasmids and Molecular Cloning

To be able to select for the expression of both RagA and RagC in reconstituted Rag knockout cells, we have generated a version of the pITR-TTP-puro vector (described in Nüchel et al.[24] and Kowarz et al.[61]) conferring blasticidin, instead of puromycin, resistance (namely pITR-TTP-bsd). All RagA and RagC expression vectors were generated using the pITR-TTP-puro and pITR-TTP-bsd vectors, respectively. In brief, we first generated an MluI restriction site upstream of the puromycin selection cassette via site-directed mutagenesis; and then replaced the puromycin cassette with the respective blasticidin cassette using the MluI and SfaAI restriction sites. The pITR-HA-hRagA^{WT}, pITR-HA-hRagC^{WT}, pITR-HA-hRagA^{QL} (Q66L), pITR-HA-hRagC^{SN} (S75N), pITR-HA-hRagA^{TN} (T21N), and pITR-HA-hRagC^{QL} (Q120L) plasmids expressing the respective Rag proteins were cloned by PCR amplification of the Rag CDS (described in Gollwitzer et al.[18] and Bryk et al.[65]) into the SfiI and NotI restriction sites of the pITR-TTP vectors using appropriate primers. The respective empty pITR vectors (pITR-EV) were used in control transfections. The pSpCas9(BB)-2A-Puro (PX459) V2.0 plasmid was purchased from Addgene (plasmid #62988; deposited by Feng Zhang and described in Ran et al.[60]). All restriction enzymes were purchased from Fermentas/Thermo Scientific. The integrity of all constructs was verified by sequencing. All DNA oligonucleotides used in this study are listed in Table S2.

Cell lysis and immunoblotting

For standard SDS-PAGE and immunoblotting experiments, cells from one well of a 6-well plate were treated as indicated in the figures and lysed in 300 μl of ice-cold Triton lysis buffer (50 mM Tris pH 7.5, 1% Triton X-100, 150 mM NaCl, 50 mM NaF, 2 mM Na-vanadate, 0.011 gr/ml beta-glycerophosphate), supplemented with 1x PhosSTOP phosphatase inhibitors (#04906837001, Roche) and 1x cOmplete protease inhibitors (#11697498001, Roche), for 10 minutes on ice. Lysates were clarified by centrifugation (15000 rpm, 10 min, 4 °C) and supernatants transferred to a new tube. Protein concentration was determined using a Protein Assay

CellPress OPEN ACCESS

Molecular Cell
Article

Dye Reagent (#5000006, Bio-Rad). Normalized samples were boiled in 1x SDS sample buffer for 5 min at 95 °C (6x SDS sample buffer: 350 mM Tris-HCl pH 6.8, 30% glycerol, 600 mM DTT, 12.8% SDS, 0.12% bromophenol blue).

Protein samples were subjected to electrophoretic separation on SDS-PAGE and analysed by standard Western blotting techniques. In brief, proteins were transferred to nitrocellulose membranes (#10600002 or #10600001, Amersham) and stained with 0.2% Ponceau solution (#33427-01, Serva) to confirm equal loading. Membranes were blocked with 5% skim milk powder (#42590, Serva) in TBS-T [1x TBS, 0.1% Tween-20 (#A1389, AppliChem)] for 1 hour at room temperature, washed three times for 5 min with TBS-T and then incubated with primary antibodies [1:1000 in TBS-T, 5% bovine serum albumin (BSA; #10735086001, Roche; #8076, Carl Roth)] overnight at 4°C. The next day, membranes were washed three times for 5 min with TBS-T and incubated with the appropriate HRP-conjugated secondary antibodies (1:10000 in 5% milk in TBS-T) for 1 hour at room temperature. Signals were detected by enhanced chemiluminescence (ECL), using ECL Western Blotting Substrate (#W1015, Promega); or SuperSignal West Femto Substrate (#34095, Thermo Scientific) for weaker signals. Immunoblot images were captured on films (#28906835, GE Healthcare; #4741019289, Fujifilm). Blots were scanned and then quantified using GelAnalyzer 19.1. A list of all primary and secondary antibodies used in this study is provided in Table S1 and in the respective section of the key resources table.

Co-immunoprecipitation (co-IP)

For co-immunoprecipitation experiments, cells of a near-confluent 10 cm dish were lysed in 1 ml CHAPS IP buffer (50 mM Tris pH 7.5, 0.3% CHAPS, 150 mM NaCl, 50 mM NaF, 2 mM Na-vanadate, 0.011 gr/ml beta-glycerophosphate) supplemented with 1x PhosSTOP phosphatase inhibitors (#04906837001, Roche) and 1x cOmplete protease inhibitors (#11697498001, Roche) for 10 minutes on ice. Samples were clarified by centrifugation (15000 rpm, 10 min, 4°C) and a portion of the samples was taken as input. For anti-HA IPs, 30 μl of pre-washed anti-HA-Agarose beads (#A2095, Sigma) were added to the remaining volume of the supernatants and the IP samples were incubated at 4°C on a rotating mixer for 2 h. For anti-RagC IPs, the remaining volume of the supernatants was incubated with 1-2 μl anti-RagC antibody (#9480, Cell Signaling Technology) at 4°C on a rotating mixer for 3 h, followed by incubation with 30 μl pre-washed Protein A Agarose bead slurry (#11134515001, Roche) for an additional hour at 4 °C on a rotating mixer. For all IPs, beads were then washed four times with CHAPS IP wash buffer (50 mM Tris pH 7.5, 0.3% CHAPS, 150 mM NaCl, 50 mM NaF) and boiled in 2x SDS loading buffer. Samples were analysed by SDS-PAGE and the presence of co-immunoprecipitated proteins was detected by immunoblotting with appropriate specific antibodies.

Lysosome purification (Lyso-IP) assays

To biochemically isolate intact lysosomes and associated proteins, the Lyso-IP method was performed as described previously,[33] with minor modifications. In brief, cells were seeded on a 15 cm dish until they reached 80-90% confluency, washed 2x with ice-cold PBS and scraped in 1 mL ice-cold PBS containing 1x PhosSTOP phosphatase inhibitors (#04906837001, Roche) and 1x cOmplete protease inhibitors (#11697498001, Roche). Cells were then pelleted by centrifugation (1000 x g, 2 min, 4°C) and resuspended in 1 mL ice-cold PBS containing phosphatase and protease inhibitors. For input samples, 25 μl of the cell suspension were transferred to a new tube and lysed by the addition of 125 μl of Triton lysis buffer (50 mM Tris pH 7.5, 1% Triton X-100, 150 mM NaCl, 50 mM NaF, 2mM Na-vanadate, 0.011 gr/ml beta-glycerophosphate), supplemented with 1x PhosSTOP phosphatase inhibitors (#04906837001, Roche) and 1x cOmplete protease inhibitors (#11697498001, Roche) on ice for 10 min. Lysed input samples were then cleared by centrifugation (15000 x g, 10 min, 4°C) and the supernatants were transferred to new tubes containing 37.5 μl of 6x SDS sample buffer and boiled for 5 min at 95°C. For obtaining the intact lysosomal fractions, the remaining cell suspension was homogenized with 20 strokes in pre-chilled 2 mL hand dounce homogenizers kept on ice. The homogenate was cleared by centrifugation to remove unbroken cells (1000 x g, 2 min, 4°C) and the supernatant was incubated with 100 μl pre-washed Pierce anti-HA magnetic beads (#88837, Thermo Scientific) on a nutating mixer for 3 min at room temperature. After the incubation, beads were washed three times with ice-cold PBS containing phosphatase and protease inhibitors using a DynaMag spin magnet (#12320D, Invitrogen). After the last wash, lysosomes were eluted from the beads and lysed by addition of 50 μl Triton lysis buffer and incubation for 10 min on ice. Isolated lysosomes were then transferred to a new tube containing 12.5 μl 6x SDS sample buffer, and then boiled for 5 min at 95°C.

Immunofluorescence and confocal microscopy

Immunofluorescence/confocal microscopy experiments were performed as described previously.[30,66] In brief, cells were seeded on glass coverslips coated with 0.1% Gelatin (#G1393, Sigma), treated as described in the figure legends, and fixed with 4% paraformaldehyde (PFA) (#28908, Thermo Scientific) in 1x PBS (10 min, room temperature), followed by a permeabilization step with PBT (1x PBS, 0.1 % Tween-20) for 20 min. Cells were blocked in BBT (1x PBS, 0.1% Tween-20, 1% BSA) for 45 minutes. Staining with anti-mTOR (#2983, Cell Signaling Technology), anti-RagC (#9480, Cell Signaling Technology), and anti-LAMP2 (#H4B4, Developmental Studies Hybridoma Bank) primary antibodies diluted 1:200 in BBT solution was performed for 2h at room temperature. After staining with primary antibodies, coverslips were washed three times with PBT and then stained with highly cross-adsorbed fluorescent secondary antibodies (Donkey anti-Rabbit Alexa Fluor 488, Donkey anti-Mouse Alexa Fluor 594; both from Jackson ImmunoResearch) diluted 1:400 in BBT for 1 hour. Nuclei were stained with DAPI (#A1001, VWR) (1:2000 in PBT) for 10 min and coverslips were washed two times for 10 min with PBT solution before mounting on glass slides with Fluoromount-G (#00-4958-02, Invitrogen). All images were acquired on an SP8 Leica confocal microscope (TCS SP8 X or TCS SP8 DLS, Leica Microsystems) using a 40x oil objective lens. Image acquisition was performed using the LAS X software (Leica Microsystems). Images from single channels

Molecular Cell
Article

are shown in grayscale, whereas in merged images, Alexa Fluor 488 is shown in green and Alexa Fluor 594 in red. Brightness and contrast were adjusted for visualization purposes using Fiji (https://imagej.net/software/fiji/downloads).[62] Alterations were applied to the entire image, keeping the parameters identical between all images of the same channel in each panel.

mRNA isolation, cDNA synthesis and quantitative real-time PCR

Total mRNA was isolated from cells using a standard TRIzol/chloroform-based method (#15596018, Invitrogen), according to manufacturer's instructions. For cDNA synthesis, mRNA was transcribed to cDNA using the RevertAid H Minus Reverse Transcriptase kit (#EP0451, Thermo Scientific) according to manufacturer's instructions. The cDNAs were diluted 1:100 in nuclease-free water and 4 μl of diluted cDNA (approximately 10 ng) were used per reaction, together with 5 μl 2x Maxima SYBR Green/ROX qPCR master mix (#K0223, Thermo Scientific) and 1 μl primer mix (2.5 μM of forward and reverse primers). Reactions were set in technical triplicates in a StepOnePlus Real-Time PCR system (Applied Biosystems). Relative gene expression was calculated with the $2^{-\Delta\Delta Ct}$ method, with *RPL13a* as an internal control, and normalized to the expression of the gene in the respective WT sample. All qPCR primers used in this study are listed in Table S2.

LysoTracker staining

For LysoTracker staining experiments, cells were seeded on gelatin-coated coverslips and grown until they reached 80-90% confluency. Lysosomes were stained by the addition of 100 nM LysoTracker Red DND-99 (#L7528, Invitrogen) in the treatment media for 1 hour. Cells were then fixed with 4% PFA in PBS for 10 min at room temperature, washed and permeabilized with PBT solution (1x PBS, 0.1% Tween-20), and nuclei stained with DAPI (1:2000 in PBT) for 10 min. Coverslips were mounted on slides using Fluoromount-G (#00-4958-02, Invitrogen). All images were captured on an SP8 Leica confocal microscope (TCS SP8 X or TCS SP8 DLS, Leica Microsystems) using a 40x oil objective lens. Image acquisition was performed using the LAS X software (Leica Microsystems). Brightness and contrast were adjusted for visualization purposes using Fiji (https://imagej.net/software/fiji/downloads).[62] Alterations were applied to the entire image, keeping the parameters identical between all images of the same channel.

QUANTIFICATION AND STATISTICAL ANALYSIS

Statistical analysis

Statistical analysis and presentation of quantification data was performed using GraphPad Prism (versions 9 and 10). All relevant information on the statistical details of experiments is provided in the figure legends. Information on quantifications for each method is also provided in the respective STAR Methods section. Data in all graphs are shown as mean ± SEM. For graphs with only two conditions shown (Figures 1J and S5D–S5F), significance was calculated using Student's t-test (unpaired, two-tailed). For all other graphs, significance for the indicated pairwise comparisons was calculated using one-way ANOVA with *post hoc* Tukey's multiple comparisons test. Sample sizes (n) and significance values are indicated in figure legends (* $p < 0.05$, ** $p < 0.01$, *** $p < 0.001$, **** $p < 0.0001$, ns: non-significant).

All findings were reproducible over multiple independent experiments, within a reasonable degree of variability between replicates. For most experiments, at least three independent replicates were performed. The sample size for microscopy experiments (number of individual cells used in quantifications) is provided in the respective figure legends. No statistical method was used to predetermine sample size, which was determined in accordance with standard practices in the field. No data were excluded from the analyses. The experiments were not randomized, and the investigators were not blinded to allocation during experiments and outcome assessment.

Quantification of colocalization

Colocalization analysis in confocal microscopy experiments was performed as in Demetriades et al.,[63] and Fitzian et al.[66] using the Coloc2 plugin of the Fiji software.[62] On average, 50-100 individual cells from 3-5 independent representative images per condition acquired from one representative experiment (out of 3 independent replicate experiments as indicated in the figure legends) were used to calculate Manders' colocalization coefficient (MCC) with automatic Costes thresholding.[67–69] For experiments in which lysosomal morphology or distribution are affected (for instance, in Rheb KO cells), thus also influencing signal distribution or intensity, Pearson's correlation coefficient (PCC) was used instead.[69] Outlines of individual cells were traced, excluding the area corresponding to the cell nucleus, to generate the region of interest (ROI) used for calculating the MCC to prevent false-positive colocalization due to automatic signal adjustments. MCC and PCC are defined as a part of the signal of interest (mTOR or RagC), which overlaps with a second signal (LAMP2).

Quantification of LysoTracker intensity

Signal intensity was calculated using the Fiji software.[62] Regions-of-interest (ROIs) were determined for approximately 75 cells over 5 independent representative images per condition and integrated density was calculated, representing the sum of the values of all pixels in the given ROI. Exact numbers of individual cells analysed per experiment are indicated in the figure legends.

Molecular Cell, Volume *84*

Supplemental information

mTORC1 activity licenses its own release from the lysosomal surface

Aishwarya Acharya and Constantinos Demetriades

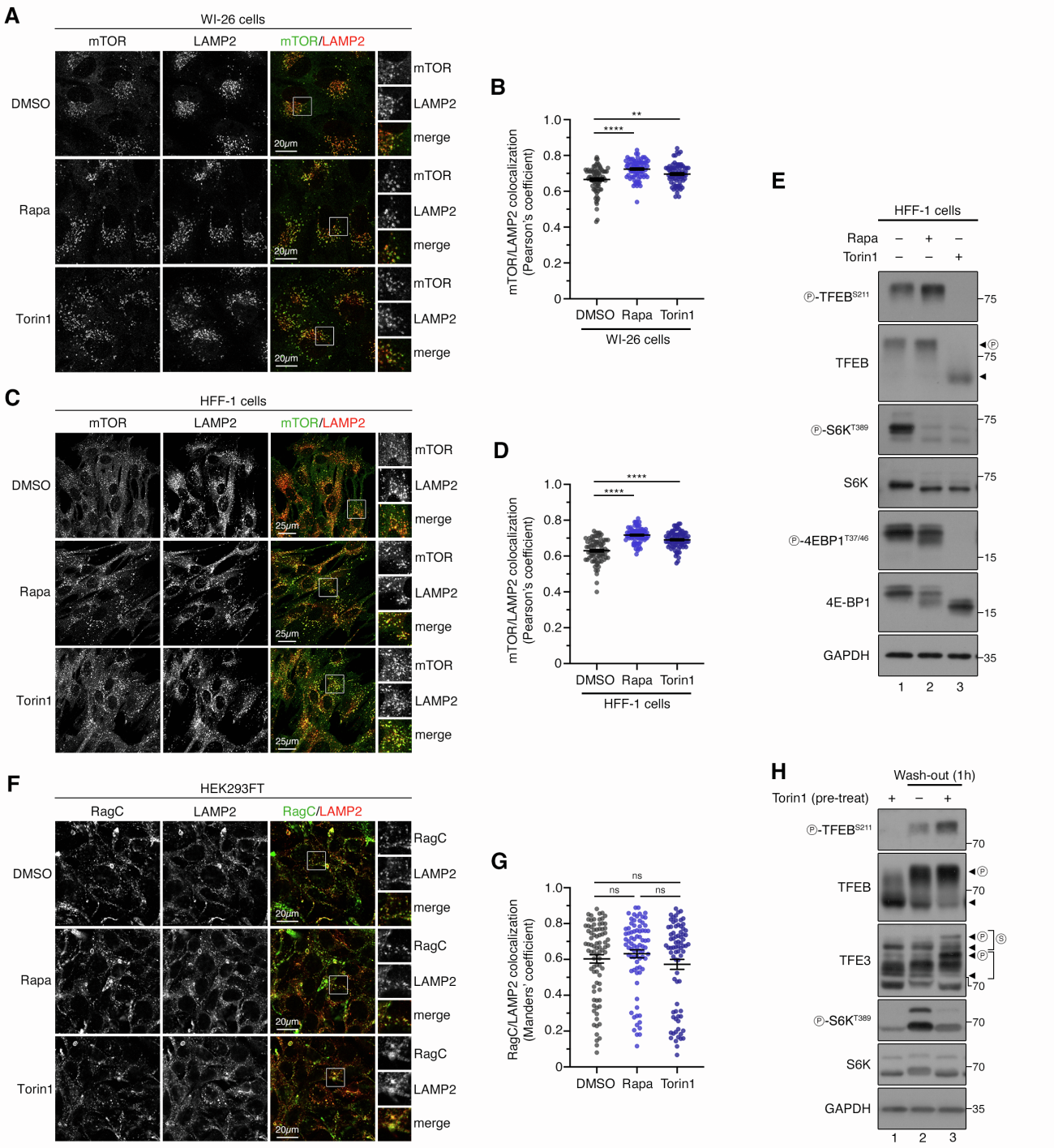

Figure S1. The effect of mTORC1 inhibition on its localization is independent of cell type or changes in RagC localization. Related to Figure 1.

(A-B) Stronger lysosomal accumulation of mTOR upon its inhibition is not cell-type-specific. Colocalization analysis of mTOR with LAMP2 (lysosomal marker) in WI-26 human lung fibroblast cells, treated with DMSO (vehicle), rapamycin (20 nM) or Torin1 (250 nM) for 1 hour as indicated, using confocal microscopy. Magnified insets shown to the right. Scale bars = 20 μm (A). Quantification of colocalization in (B). n = 73-74 individual cells from 5 independent fields per condition.

(C-D) As in (A-B), but using non-transformed human foreskin fibroblasts (HFF-1 cells). Scale bars = 25 μm (C). Quantification of colocalization in (D). n = 80 individual cells from 5 independent fields per condition.

(E) Stronger TFEB phosphorylation by mTORC1 upon rapamycin treatment. Immunoblots with lysates from HFF-1 cells, treated with DMSO (vehicle), rapamycin (20 nM) or Torin1 (250 nM) for 1 hour, and probed with the indicated antibodies.
(F-G) Localization of RagC is not affected by mTORC1 inhibition. Experiment performed as in (A-B), but for RagC/LAMP2 colocalization. Scale bars = 20 μm (F). Quantification of colocalization in (G). n = 77-82 individual cells from 5 independent fields per condition.
(H) Stronger phosphorylation of lysosomal mTORC1 substrates upon Torin1 pre-treatment and wash-out. Immunoblots with lysates from WT HEK293FT cells, treated with DMSO (–) or Torin1 (50 nM, 15 min) as shown, and probed with the indicated antibodies. For lanes 2-3, the pre-treatment media were then replaced by fresh media without inhibitors for 1h to wash-out Torin1.
Arrowheads indicate bands corresponding to different protein forms, when multiple bands are present. P: phosphorylated form, S: SUMOylated form. Data in graphs shown as mean ± SEM. ** $p < 0.01$, **** $p < 0.0001$, ns: non-significant.

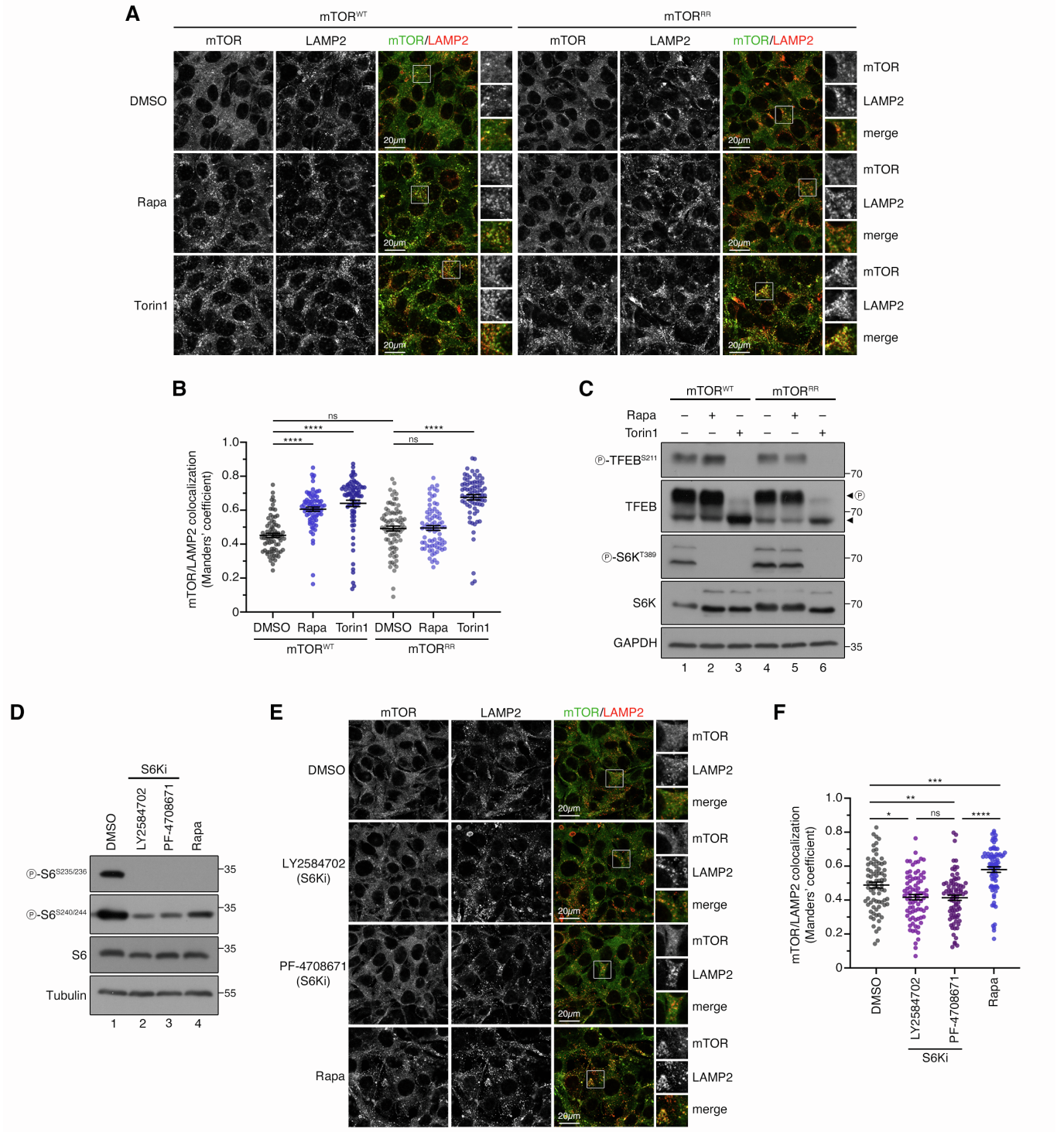

Figure S2. mTORC1 inhibition augments its own lysosomal localization in an mTORC1-dependent, S6K-independent manner. Related to Figure 1.

(A-B) The stronger mTOR accumulation on lysosomes upon rapamycin treatment is not due to mTOR-independent effects. Colocalization analysis of mTOR with LAMP2 (lysosomal marker) in HEK293FT cells expressing wild-type ($mTOR^{WT}$) or rapamycin-resistant mTOR ($mTOR^{RR}$), treated with DMSO (vehicle), rapamycin (20 nM) or Torin1 (250 nM) for 1 hour as indicated, using confocal microscopy. Magnified insets shown to the right (A). Quantification of colocalization in (B). n = 75-82 individual cells from 5 independent fields per condition.

(C) Immunoblots with lysates from HEK293FT cells expressing wild-type ($mTOR^{WT}$) or rapamycin-resistant mTOR ($mTOR^{RR}$), treated with DMSO (vehicle), rapamycin (20 nM) or Torin1 (250 nM) for 1

hour, and probed with the indicated antibodies. Arrowheads indicate bands corresponding to different protein forms, when multiple bands are present. P: phosphorylated form.
(D) Two independent S6K inhibitors robustly downregulate the phosphorylation of its target S6. Immunoblots with lysates from WT HEK293FT cells, treated with DMSO (vehicle), S6K inhibitors LY2584702 (20 μM, 4 h) or PF-4708671 (20 μM, 4 h) or rapamycin (20 nM, 1 h), and probed with the indicated antibodies.
(E-F) The stronger mTOR accumulation on lysosomes upon rapamycin treatment is not mediated by downregulation of S6K activity. Colocalization analysis of mTOR with LAMP2 (lysosomal marker) in WT HEK293FT cells treated as in (D). Magnified insets shown to the right (E). Quantification of colocalization in (F). n = 76-80 individual cells from 5 independent fields per condition.
Scale bars = 20 μm. Data in graphs shown as mean ± SEM. * $p < 0.05$, ** $p < 0.01$, *** $p < 0.001$, **** $p < 0.0001$, ns: non-significant.

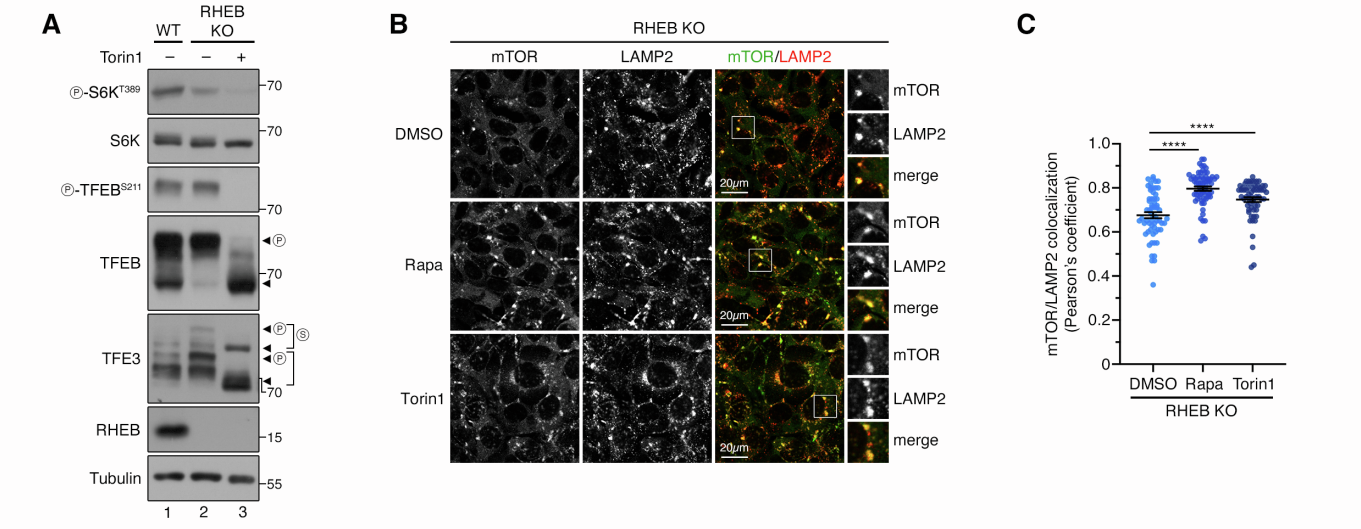

Figure S3. Synergistic effects of RHEB knockout and pharmacological mTOR inhibition. Related to Figure 1.

(A) Removal of RHEB and Torin1 treatment act synergistically to downregulate mTORC1 activity towards S6K. Immunoblots with lysates from WT and RHEB KO HEK293FT cells treated with DMSO (vehicle) or Torin1 (250 nM) for 1 hour, and probed with the indicated antibodies. Arrowheads indicate bands corresponding to different protein forms, when multiple bands are present. P: phosphorylated form, S: SUMOylated form.

(B-C) Removal of RHEB and rapamycin or Torin1 treatment act synergistically to promote stronger lysosomal accumulation of mTOR. Colocalization analysis of mTOR with LAMP2 (lysosomal marker) in RHEB KO HEK293FT cells, treated with DMSO (vehicle), rapamycin (20 nM) or Torin1 (250 nM) for 1 hour as indicated, using confocal microscopy. Scale bars = 20 μm. Magnified insets shown to the right (B). Quantification of colocalization in (C). n = 60-65 individual cells from 4 independent fields per condition. Data shown as mean ± SEM. * $p < 0.05$, ** $p < 0.01$, *** $p < 0.001$, **** $p < 0.0001$, ns: non-significant.

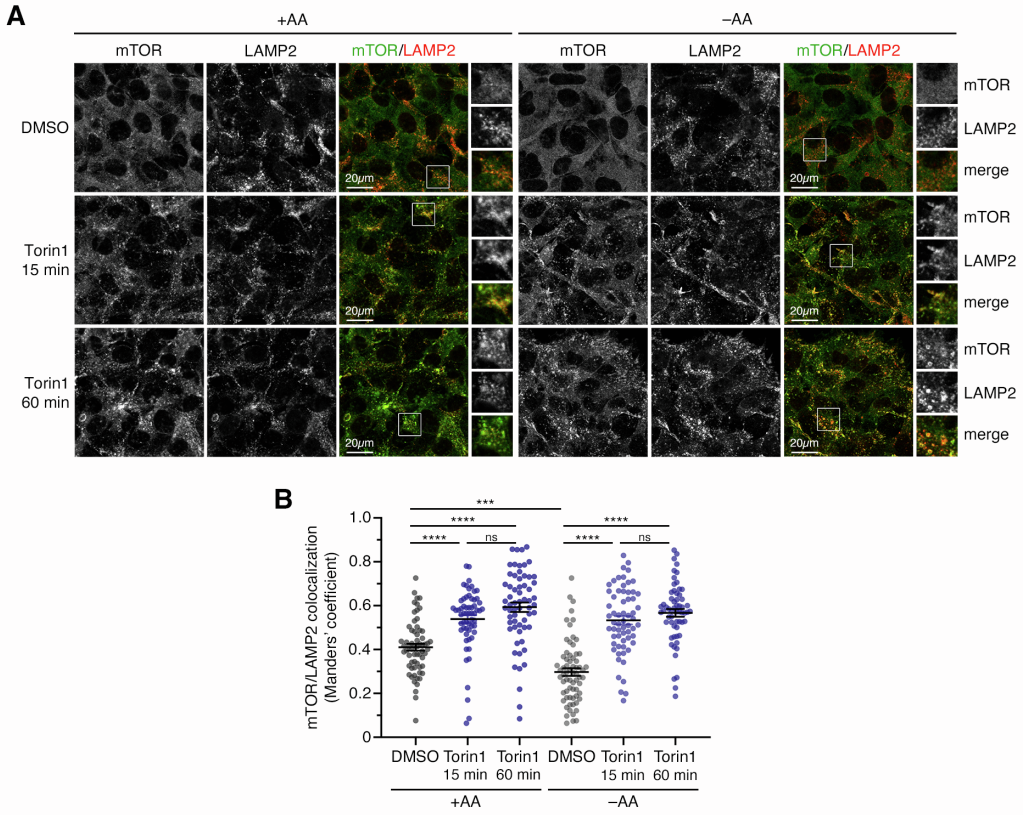

Figure S4. Acute Torin1 treatment is sufficient to promote stronger lysosomal localization of mTOR. Related to Figure 2.

(A-B) Colocalization analysis of mTOR with LAMP2 (lysosomal marker) in HEK293FT cells, pre-treated with DMSO (vehicle) or Torin1 (250 nM) for 15 or 60 min as indicated, followed by treatment with media containing (+AA) or lacking AAs (–AA) without inhibitors for an additional hour, using confocal microscopy. Scale bars = 20 μm. Magnified insets shown to the right (A). Quantification of colocalization in (B). n = 60-67 individual cells from 4 independent fields per condition. Data shown as mean ± SEM. *** $p < 0.001$, **** $p < 0.0001$, ns: non-significant.

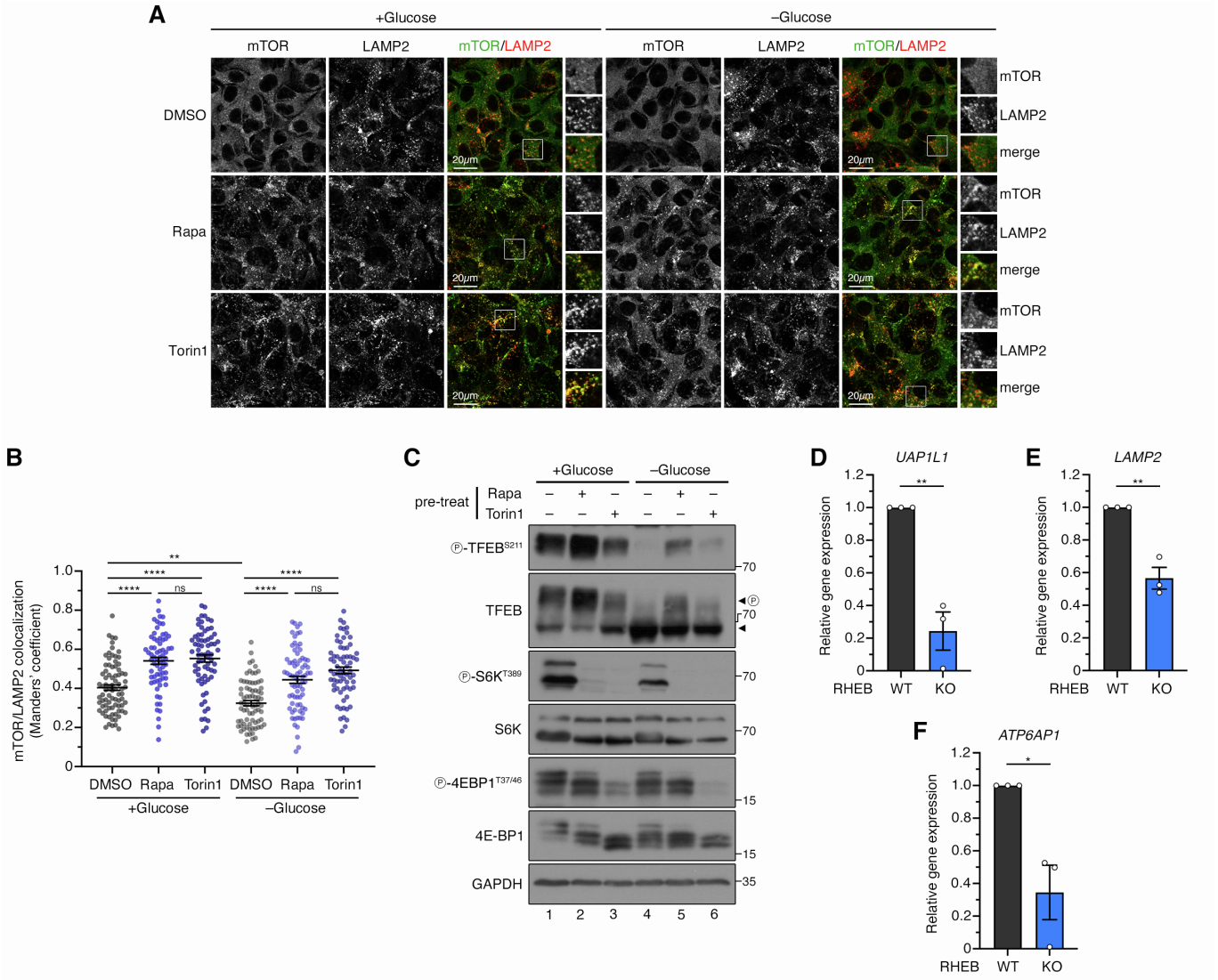

Figure S5. mTORC1 inhibition strengthens lysosomal mTOR localization, enhances TFEB phosphorylation, and downregulates TFEB target gene expression. Related to Figure 3.

(A-B) Inhibited mTOR accumulates to lysosomes even in glucose-starved cells. Colocalization analysis of mTOR with LAMP2 (lysosomal marker) in WT HEK293FT cells, pre-treated with DMSO (vehicle), rapamycin (20 nM) or Torin1 (250 nM) for 1 hour, followed by treatment with media containing (+Glucose) or lacking glucose (–Glucose) without inhibitors for an additional hour, using confocal microscopy. Scale bars = 20 μm. Magnified insets shown to the right (A). Quantification of colocalization in (B). n = 69-84 individual cells from 5 independent fields per condition.

(C) Pre-treatment with mTOR inhibitors causes sustained TFEB phosphorylation in glucose-starved cells. Immunoblots with lysates from WT HEK293FT cells treated as in (A), probed with the indicated antibodies. Arrowheads indicate bands corresponding to different protein forms, when multiple bands are present. P: phosphorylated form.

(D-F) Elevated TFEB phosphorylation in genetic models of downregulated mTORC1 activity correlates with lower transcription of downstream targets. Expression analysis of the TFEB/TFE3 target genes *UAP1L1* (D), *LAMP2* (E), and *ATP6AP1* (F) in HEK293FT WT and Rheb KO cells. n = 3 independent experiments.

Data in graphs shown as mean ± SEM. * $p < 0.05$, ** $p < 0.01$, **** $p < 0.0001$, ns: non-significant.

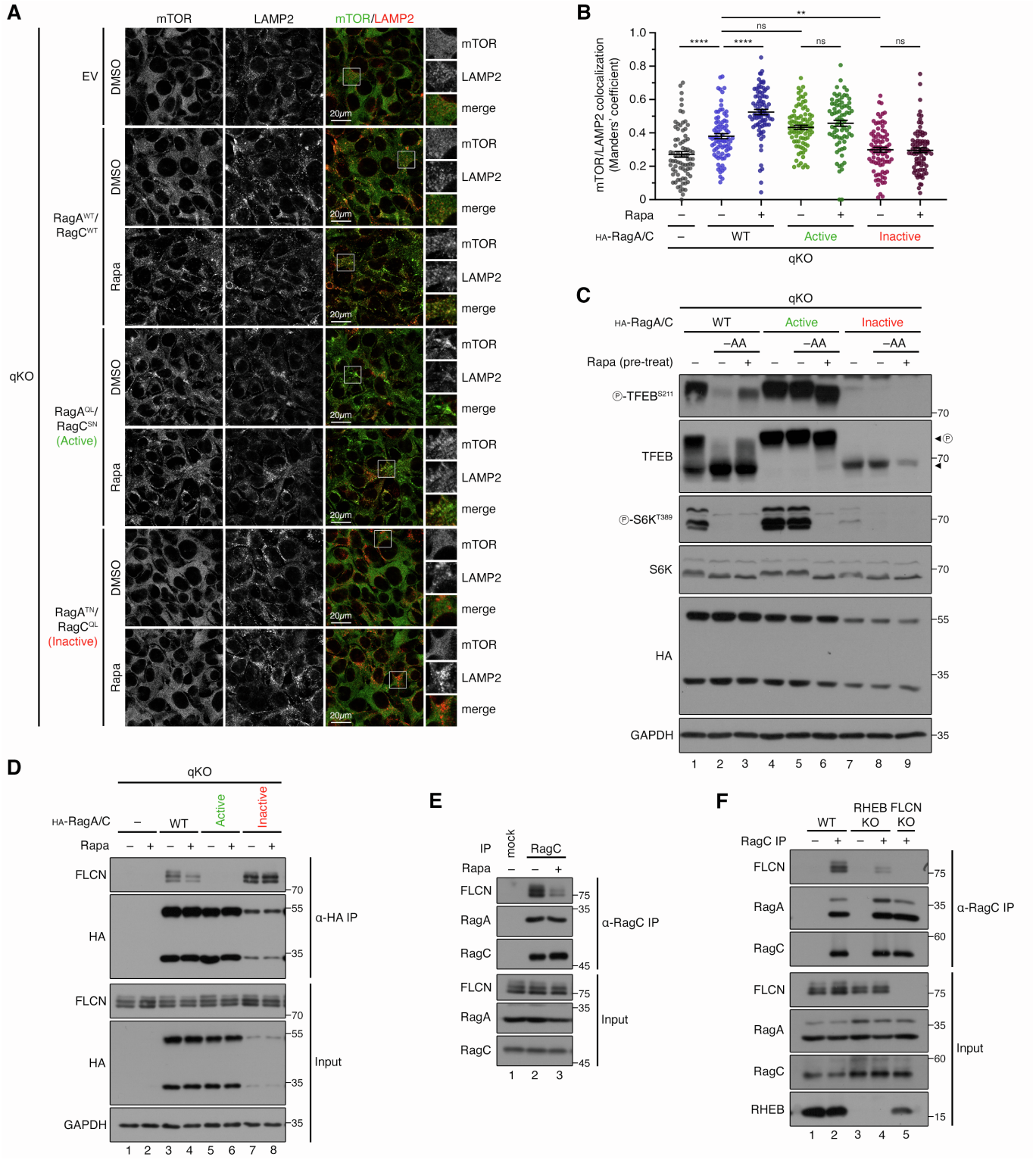

Figure S6. Pharmacological or genetic inhibition of mTORC1 causes locking of the Rag dimer in its active state. Related to Figure 6.

(A-B) Reconstitution of Rag qKO cells with WT or active (but not inactive) RagA/C dimers rescues mTOR localization to lysosomes. Colocalization analysis of mTOR with LAMP2 (lysosomal marker) in Rag qKO HEK293FT cells stably expressing HA-tagged WT, active ($RagA^{QL}$/$RagC^{SN}$), or inactive ($RagA^{TN}$/$RagC^{QL}$) Rag dimers, treated with DMSO (vehicle) or rapamycin (Rapa, 20 nM) for 1 hour as indicated, using confocal microscopy. Cells transfected with an empty vector (EV) used as control. Note that rapamycin further enhances the lysosomal accumulation of mTOR in cells expressing WT RagA/C, but not in active-Rag-expressing cells. Scale bars = 20 μm. Magnified insets shown to the right (A).

Quantification of colocalization in (B). n = 83-89 individual cells from 5 independent fields per condition. Data shown as mean ± SEM. ** p < 0.01, **** p < 0.0001, ns: non-significant.

(C) Reconstitution of Rag qKO cells with WT or active (but not inactive) RagA/C dimers rescues substrate phosphorylation, as expected. Immunoblots with lysates from Rag qKO HEK293FT cells stably expressing HA-tagged WT, active ($RagA^{QL}$/$RagC^{SN}$), or inactive ($RagA^{TN}$/$RagC^{QL}$) Rag dimers, pre-treated with DMSO (vehicle) or rapamycin (20 nM, 1 h), followed by treatment with media containing or lacking AAs (–AA) without inhibitors for an additional hour, and probed with the indicated antibodies. Arrowheads indicate bands corresponding to different protein forms, when multiple bands are present. P: phosphorylated form.

(D) mTORC1 inhibition decreases binding of endogenous FLCN to WT Rags, but not to inactive-locked Rag dimers. Co-immunoprecipitation of HA-tagged RagA/RagC dimers from HEK293FT Rag qKO cells stably expressing WT, active, or inactive Rags, treated with DMSO or rapamycin (Rapa, 20 nM) for 1 h. The input and IP samples were analyzed by immunoblotting using antibodies against the indicated proteins.

(E) The Rag-FLCN interaction is weakened by rapamycin treatment, indicating Rag dimer activation by mTORC1 inhibition. Co-immunoprecipitation of endogenous RagC from HEK293FT WT cells, treated with DMSO (vehicle) or rapamycin (Rapa, 20 nM) for 1 hour. The input and IP samples were analyzed by immunoblotting using antibodies against the indicated proteins.

(F) Genetic downregulation of mTORC1 decreases Rag-FLCN interaction, indicating Rag dimer activation. Co-immunoprecipitation of endogenous RagC from HEK293FT WT or Rheb KO cells. The input and IP samples were analyzed by immunoblotting using antibodies against the indicated proteins. The respective samples from FLCN KO cells were used to confirm signal specificity of the anti-FLCN antibody.

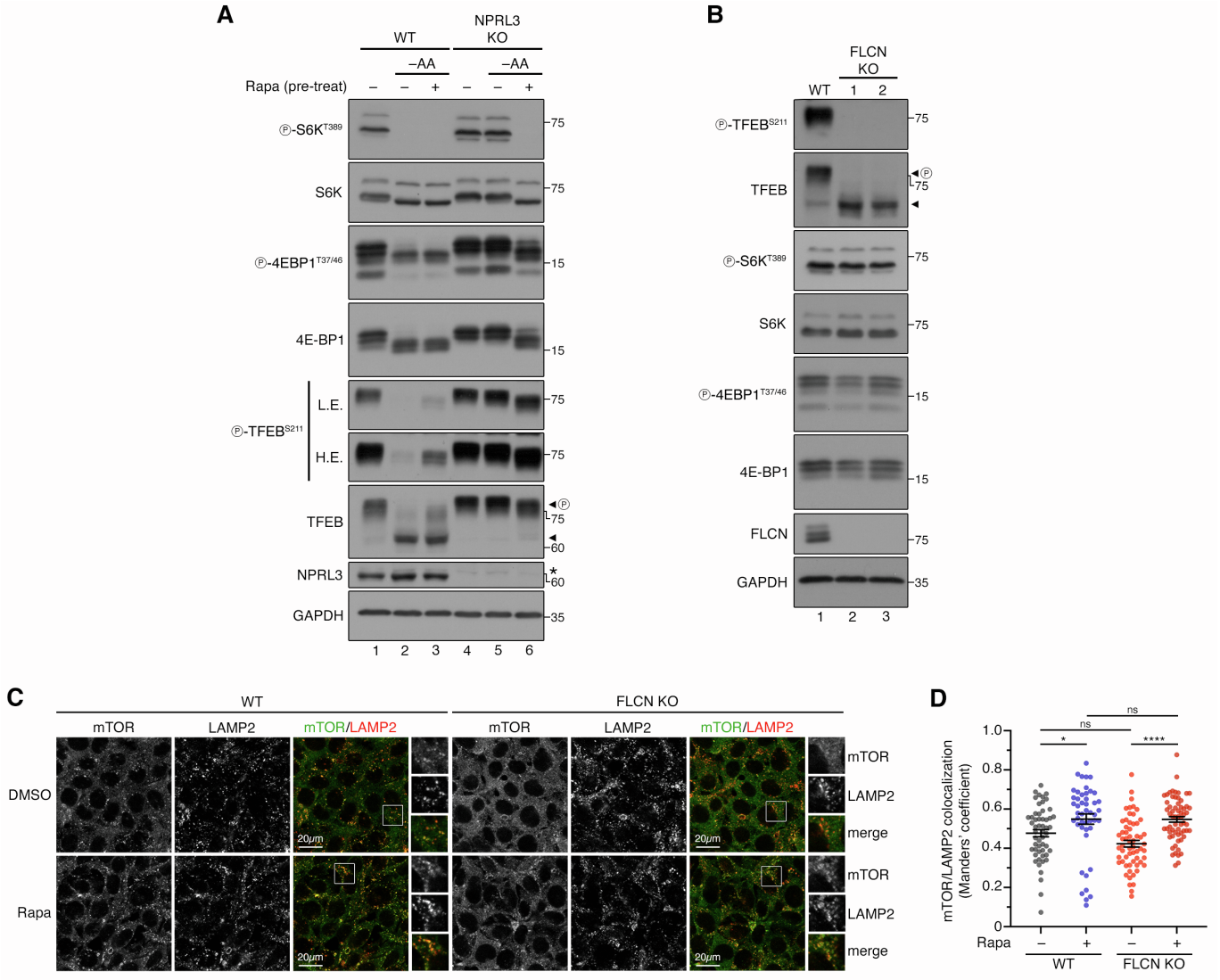

Figure S7. Characterization of GATOR1 and FLCN loss-of-function cellular models. Related to Figure 7.

(A) Validation of GATOR1 loss-of-function cellular models. Immunoblots with lysates from WT and NPRL3 KO HEK293FT cells, pre-treated with DMSO (vehicle) or rapamycin (Rapa, 20 nM) for 1 hour, followed by treatment with media containing (+AA) or lacking AAs (–AA) without DMSO/rapamycin for an additional hour and probed with different antibodies as indicated. Note the resistance of mTORC1 activity to AA starvation in NPRL3 KO cells. L.E.: low exposure; H.E.: high exposure. Asterisk indicates a faint, non-specific band in the NPRL3 blot.

(B) Validation of FLCN loss-of-function cellular models. Immunoblots with lysates from WT and FLCN KO HEK293FT cells, grown under basal culture conditions and probed with different antibodies as indicated. Note the resistance of mTORC1 activity to AA starvation in NPRL3 KO cells.

(C-D) Rapamycin promotes lysosomal mTORC1 localization also in cells with FLCN loss-of-function. Colocalization analysis of mTOR with LAMP2 (lysosomal marker) in WT and FLCN KO HEK293FT cells, treated with DMSO (vehicle) or rapamycin (Rapa, 20 nM) for 1 h, using confocal microscopy. Scale bars = 20 μm. Magnified insets shown to the right (C). Quantification of colocalization in (D). n = 47-63 individual cells from 3 independent fields per condition. Data shown as mean ± SEM. * $p < 0.05$, **** $p < 0.0001$, ns: non-significant.

Arrowheads indicate bands corresponding to different protein forms, when multiple bands are present. P: phosphorylated form.

2.2 Hyperactive Rheb acts as a lysosomal tether for mTORC1

This chapter of the Results addresses Aim 2.

This section contains an unpublished manuscript currently in preparation.

In addition to results, the methods, discussion and references associated with these results are included within the chapter. A more expanded discussion can be found in Section 3.

Hyperactive Rheb acts as a lysosomal tether for mTORC1

Aishwarya Acharya[1,2], Sara Khosraviani[1], and Constantinos Demetriades[1,2,3,4,*]

[1]Max Planck Institute for Biology of Ageing (MPI-AGE), 50931 Cologne, Germany

[2]Cologne Graduate School of Ageing Research (CGA), 50931 Cologne, Germany

[3]University of Cologne, Cologne Excellence Cluster on Cellular Stress Responses in Aging-Associated Diseases (CECAD), 50931 Cologne, Germany

[4]Lead contact

*Correspondence: Demetriades@age.mpg.de (C.D.)

Keywords

mTORC1, Rheb, Lysosomes, Amino acids, TSC, Rag GTPases

Abstract The mammalian/mechanistic Target of Rapamycin complex 1 (mTORC1) is a nodal kinase complex positioned at the center of nutrient signaling, that receives and conveys information about nutrient sufficiency by regulating an array of downstream substrates. To ensure accuracy in receipt of this information, mTORC1 signaling is tightly regulated by two upstream axes that ultimately impact the activity of Rags or Rheb GTPases. The roles of the GTPases were thought to be clearly demarcated from each other, with the Rags involved in localizing mTOR to lysosomes and Rheb activating it there; however, crosstalk between the two axes has become increasingly evident. Thus far, whether Rheb impacts on the localization of mTORC1 and in what capacity remains unclear. Here, we show that in addition to its primary function of activating mTORC1 catalytic activity, Rheb moonlights as a lysosomal tether for mTORC1 when in a state of hyperactivity.

Remodeling the subcellular distribution of proteins is a tactic used by cells to achieve compartmentalized signaling as well as to rapidly respond to upstream stimuli [1]. Anomalous localization of proteins can lead to aberrant signaling which may, in turn, be the underlying cause for the development of several pathophysiological conditions [2].

mTORC1 signaling is a notable example where subcellular localization and downstream activity are intricately linked. mTORC1 (mammalian/mechanistic Target of Rapamycin complex 1) is a central growth-promoting complex that acts by integrating a myriad of upstream factors to bring about a physiological response in accordance with the needs of the cell [3,4]. Among others, amino acids and growth factors are some cues whose availability is conveyed to mTORC1, with amino acids being one of the strongest inputs that regulate its subcellular localization, and as a consequence, its activity [5,6].

According to the conventional model in the field, two upstream branches— amino acid sensing and growth factor signaling— converge on the functioning of two distinct small GTPases, the Rag GTPases and Rheb, respectively. Intracellular amino acid sufficiency is conveyed to the Rag GTPases as an alteration in their nucleotide-binding state, which in turn affects their affinity for mTORC1, resulting in a concomitant increase in recruitment to the lysosomal surface, where it interacts with its direct

activator Rheb [7-9]. Conversely, upon amino acid starvation, this Rag-mediated recruitment to lysosomes is lost, leading to a decline in the lysosomal enrichment of mTORC1 and a consequent loss of mTORC1 activity as it no longer encounters Rheb. Additionally, the growth factor signaling branch of the pathway directly impacts on the nucleotide loading state of RHEB, and hence its activity toward mTORC1, via its negative regulator TSC (Tuberous sclerosis complex) [7,10,11].

Although the initial understanding of the pathway posited that the two upstream branches are discrete, more recently, a growing body of evidence has demonstrated that there is crosstalk between the upstream amino acid sensing and growth factor signaling pathways. For instance, in response to amino acid depletion or growth factor starvation, the TSC complex relocalizes to the lysosomal surface by binding to the inactive Rag GTPases or Rheb, respectively, exemplifying a sophisticated mechanism of signal integration. While the Rag GTPases are currently established to be the sole mode of recruitment for lysosomal mTORC1 under conditions of nutrient sufficiency, given the extensive interplay between Rags and Rheb we wanted to assess the potential role of the TSC-Rheb axis in influencing mTORC1 localization.

Previously we showed that upon amino acid starvation, unlike in wildtype cells where mTOR became diffusely cytosolic in distribution, in *TSC1* or *TSC2* null cells mTOR continued to strongly localize to lysosomes [12]. This phenotype was rescued by siRNA-mediated knockdown of *Rheb*, raising the possibility that Rheb could mediate a second anchoring of mTORC1 to lysosomes in conjunction with the Rag GTPases. To test this hypothesis, we generated human embryonic kidney HEK293FT cell lines stably over-expressing WT Rheb, an active (S16H) or an inactive (I39K) mutant of Rheb and subjected them to media lacking all amino acids for 1 h (Fig. 1A). In control cells, in agreement with previous reports, we observed accumulated puncta of mTOR (Fig. 1A) that colocalized with lysosomal marker LAMP2 (Fig. 1B) in AA-replete media, and a dispersed mTOR localization pattern upon treatment with AA starvation media; in comparison, in cells over-expressing either WT or active Rheb, while there was no significant difference observed in mTOR localization in AA-replete media, mTOR remained at the lysosome despite AA starvation. Over-expression of inactive Rheb did not have a noticeable impact on mTOR localization, underlining the requirement of RHEB to be functionally active to elicit this effect. These data suggest that the mTOR

localization phenotype observed in cells lacking a functional TSC complex could be an outcome of hyperactive Rheb.

Since mTOR localization is a major determinant of its activity [13], we sought to assess mTORC1 signaling toward its downstream targets. Concomitant with its enhanced lysosomal localization, mTORC1 signaling toward its canonical substrates S6K and 4E-BP1 was higher upon overexpression of WT and active Rheb and caused a blunted response to AA starvation, whereas in cells overexpressing inactive Rheb, mTORC1 signaling was largely unaffected (Fig. 1C). Counterintuitively, mTORC1 phosphorylation of its non-canonical substrate TFEB was abolished in WT and active Rheb overexpressing cells; this is in line with previous reports from TSC null cells where a similar paradoxical phenomenon was observed [14,15]. Taken together, these results indicate that over-expression of Rheb causes the forced lysosomal retention of mTORC1 and its persistent activity particularly toward its canonical substrates in an Rheb activity-dependent manner.

To test if the effects observed upon Rheb overexpression were merely transient or persistent in nature, we treated active Rheb overexpressing cells with AA starvation media for up to 8 h and checked both mTORC1 localization and signaling (Fig. S1A-C). Strikingly, even after 8 hours, both mTORC1 lysosomal localization and its canonical substrate phosphorylation displayed resistance to amino acid starvation.

In addition to amino acid sensing, information about glucose sufficiency is also dually communicated via the Rags and Rheb, and in wildtype cells its insufficiency causes loss of both lysosomal localization and signaling of mTORC1[16-20]. Similar to our observations with AA starvation, when cells overexpressing WT or active Rheb were starved for glucose for 1 h, mTOR persisted at lysosomes and phosphorylation of downstream targets (S6K and 4E-BP1) was sustained (Fig. S2A,B). Thus, overexpression of Rheb triggers the forced lysosomal retention of mTORC1, desensitizing it not only to amino acid starvation but also glucose deprivation.

Rheb undergoes post-translational processing to gain a C-terminal farnesylation that endows membrane anchorage [21,22]. This allows it to localize to endomembranes, which has been reported to be a necessary characteristic for its activation of mTORC1 [21,22]. To examine whether endomembrane localization of Rheb is required for the

forced lysosomal tethering of mTORC1, we transiently over-expressed a farnesylation-deficient (C181S) version of the active mutant of Rheb (S16H/C181S) and probed the effect on mTOR localization as well as mTORC1 signaling upon AA starvation (Fig. 2A-C). Notably, the hyperactivity of Rheb was insufficient to overcome the lack of its endomembrane anchorage, in terms of both mTORC1 localization and activity, underscoring the necessity of Rheb farnesylation and appropriate endomembrane localization to cause tethering of mTORC1 to the lysosomal surface.

When nutrients are sufficient, upstream regulatory signals lead to the active conformation of the Rag GTPases, which in turn recruit mTORC1 to lysosomes; conversely, under conditions of nutrient starvation or environmental stress, the Rag GTPases lose their affinity for mTORC1, causing its delocalization[23]. Since the overexpression of Rheb prevented this delocalization from taking place even upon AA or glucose starvation, we reasoned that hyperactive Rheb may be affecting Rag-mTORC1 binding, thus affecting its localization. To test this notion, we assayed for the fraction of mTORC1 bound to RagA/C upon overexpression of WT Rheb (Fig. 3A). Despite an enrichment of mTORC1 at lysosomes, we observed that overexpression of Rheb decreased rather than increased its binding to the Rag dimer, suggesting destabilization of the interaction upon Rheb hyperactivity.

To assess whether mTORC1 binding to the Rag-GTPases is a necessary event for Rheb-mediated mTORC1 enrichment at the lysosome, we employed quadruple RagA-D KO HEK293FT cells (qKOs; described in Gollwitzer et al. [24]) and stably overexpressed WT, active (S16H) or inactive (I39K) Rheb. Similarly to our previous results in WT cells, in qKO cells overexpressing WT or active Rheb, mTORC1-dependent phosphorylation of its canonical substrates was augmented compared to control or inactive Rheb-expressing cells (Fig. 3B). Of note, in active but not WT Rheb-expressing cells, mTORC1 activity was resistant to 1 h of amino acid depletion. We next looked at mTOR localization in this setup (Fig. 3C,D): remarkably, Rag deletion did not interfere with mTOR recruitment to lysosomes in cells expressing WT or active Rheb, suggesting that an intact mTORC1-Rag GTPase interface is dispensable for mTORC1 retention at lysosomes in the presence of hyperactive Rheb.

The effects of Rheb overexpression on the resistance of mTORC1 signaling to amino acid depletion have been reported previously [8,11,25]; however, these effects were

attributed to non-physiological interactions between Rheb and mTORC1 at arbitrary locations within the cell [8]. Here, our data from confocal microscopy show that at least in part, this phenotype is due to the Rheb-mediated retention of mTOR at lysosomes, which in turn affects its signaling to downstream substrates. Furthermore, while we observed similar data from both stable as well as transient overexpression setups, previous studies have claimed that stable overexpression of Rheb fails to desensitize mTORC1 to amino acid starvation [8]. This discrepancy in the findings may be explained by the differences in achieved expression levels, as the tethering activity of Rheb and hence its ability to blunt the starvation response of mTORC1 could be a dose-dependent phenotype and may require net Rheb activity levels to exceed a certain threshold.

By ascertaining similar levels of overexpression of both active and inactive mutants of Rheb in this work, the phenotypes that we have studied are controlled to illuminate the effects of heightened activity of Rheb as opposed to bulk protein expression. Nonetheless, future inquiry using alternative systems, such as transgenic cell lines harboring Rheb point mutants or cells with endogenously higher Rheb protein expression, would be invaluable to verify our findings in the absence of any artifacts associated with overexpression.

In sum, the results of this study describe a new role for Rheb as a lysosomal tether for mTORC1, in addition to its function as its direct activator, and support a model of ‘dual anchoring’ of mTOR at lysosomes — via Rags and Rheb — that has been put forth previously [12] (Fig. 4A). We show that hyperactive Rheb drives the aberrant retention of mTORC1 at lysosomes upon amino acid or glucose depletion, which is the underlying cause for its continued activity toward canonical substrates such as S6K and 4E-BP1, even for prolonged periods of starvation. This tethering activity still relies on the ability of Rheb to localize to endomembranes. Finally, this study suggests that Rheb not only acts as a secondary tether for mTORC1 at the lysosomal surface in coordination with the Rag GTPases but also has the potential to *de novo* recruit mTOR to lysosomes when Rags are missing. Future studies will be important to gain an understanding of the balance between the two tethering activities and their relative contributions in various cellular contexts.

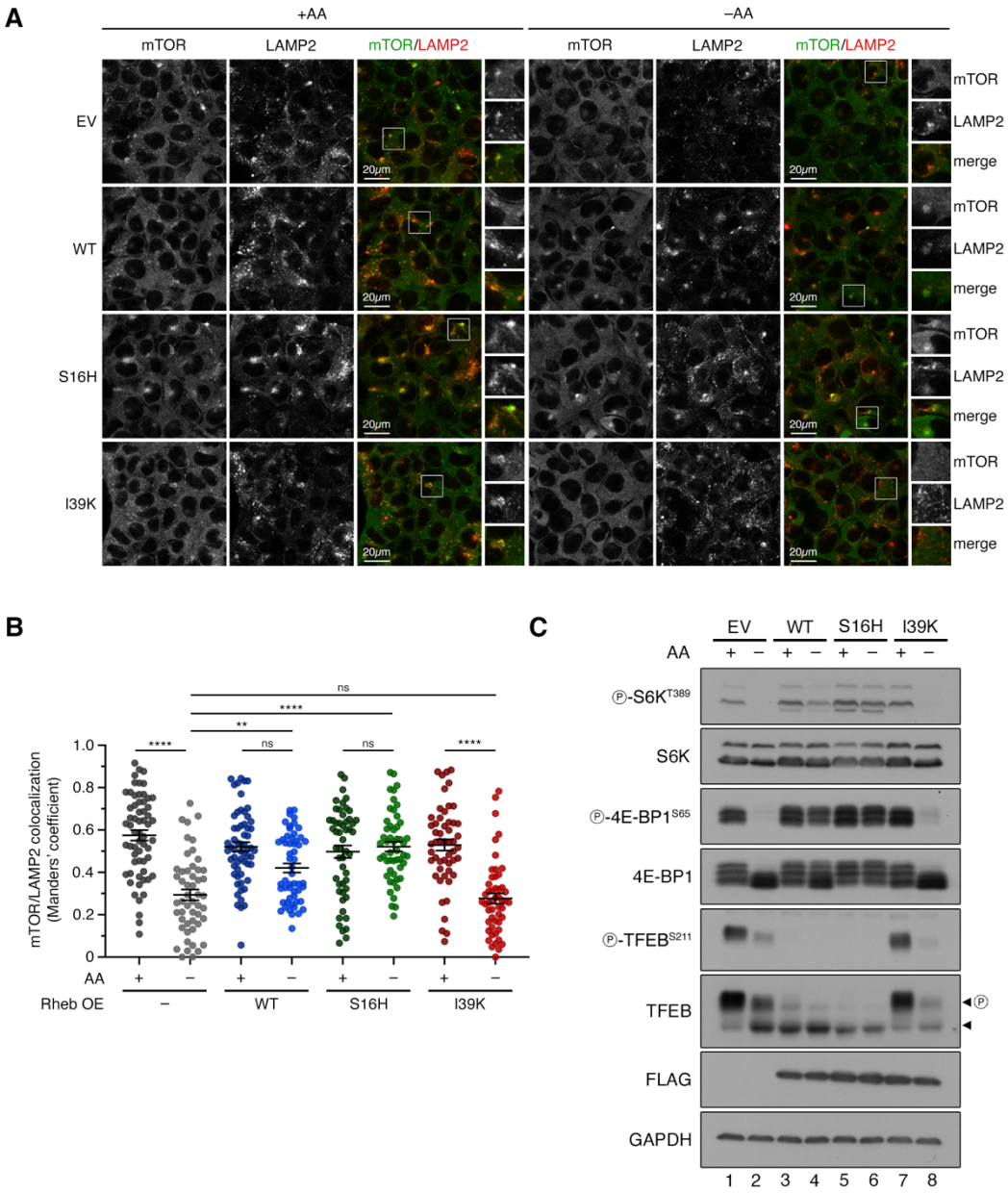

Figure 1. Overexpression of Rheb renders mTORC1 localization and activity insensitive to amino acid starvation.

(A-B) Colocalization analysis of mTOR with LAMP2 (lysosomal marker) in WT HEK293FT cells stably expressing FLAG-tagged WT, active (S16H) or inactive (I39K) Rheb, treated with media containing (+AA) or lacking (-AA) amino acids for 1 hour, using confocal microscopy. Cells transfected with an empty vector (EV) used as control. Magnified insets shown to the right (A). Quantification of colocalization in (B). n = 50-60 individual cells from 3 independent fields per condition.

(C) Immunoblots with lysates from WT HEK293FT cells stably expressing FLAG-tagged WT, active (S16H) or inactive (I39K) Rheb, treated with media containing (+AA)

or lacking (-AA) amino acids for 1 hour, and probed with different antibodies, as indicated.

Scale bars = 20 μm. Arrowheads indicate bands corresponding to different protein forms, when multiple bands are present. P: phosphorylated form. Data in graphs shown as mean ± SEM. ** $p < 0.01$, **** $p < 0.0001$, ns: non-significant.
See also Figure S1 and S2.

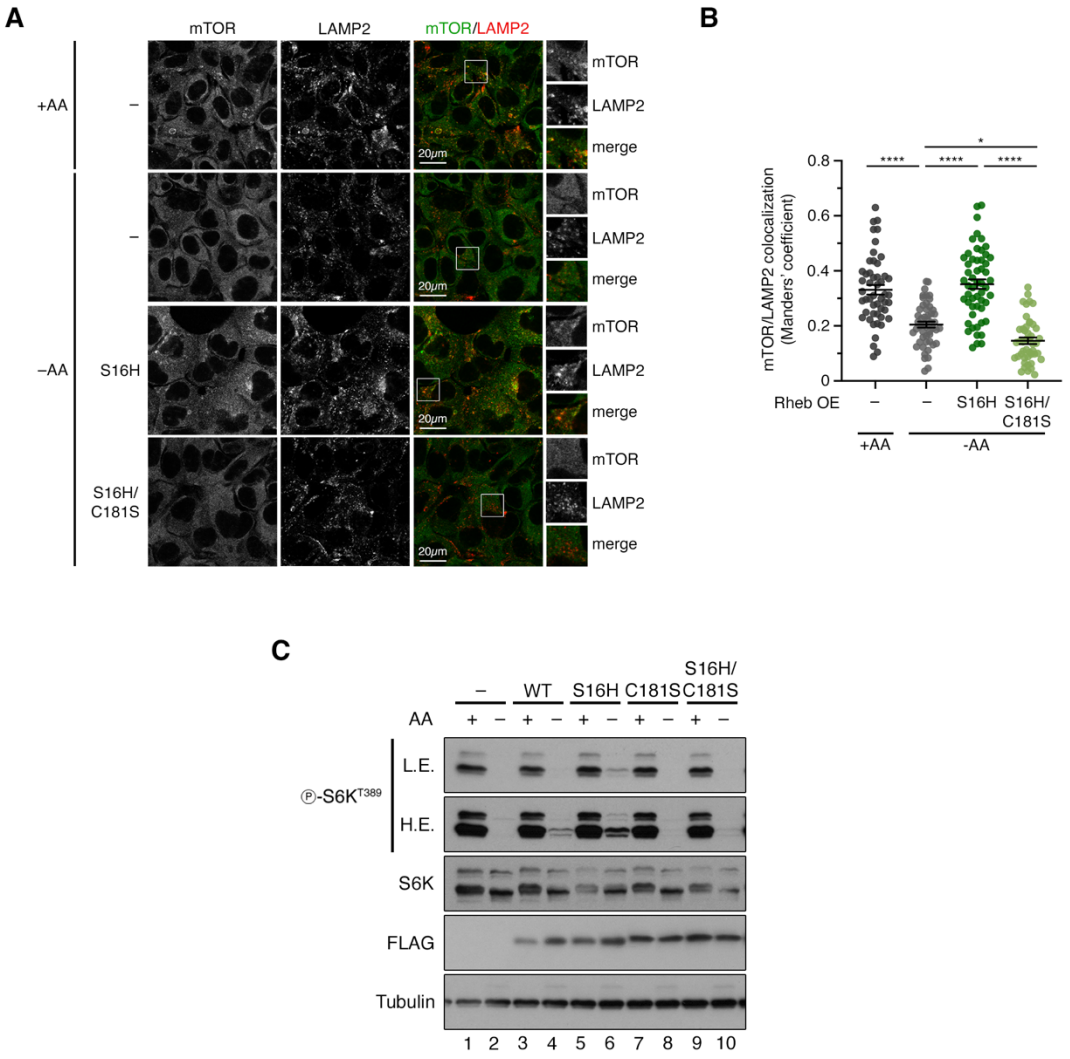

Figure 2. Rheb-mediated lysosomal tethering of mTORC1 requires its endomembrane anchorage.

(A-B) Colocalization analysis of mTOR with LAMP2 (lysosomal marker) in WT HEK293FT cells transiently expressing FLAG-tagged active (S16H) or farnesylation-deficient active (S16H/C181S) mutant of Rheb, treated with media containing (+AA) or lacking (-AA) amino acids for 1 hour, using confocal microscopy. Cells transfected with a FLAG-Luciferase used as control. Magnified insets shown to the right (A). Quantification of colocalization in (B). n = 50-60 individual cells from 3 independent fields per condition.

(C) Immunoblots with lysates from WT HEK293FT cells transiently expressing FLAG-tagged WT, active (S16H), farnesylation-deficient (C181S), or farnesylation-deficient active (S16H/C181S) mutant of Rheb, treated with media containing (+AA) or lacking (-AA) amino acids for 1 hour, probed with different antibodies, as indicated.

Scale bars = 20 μm. P: phosphorylated form. L.E.: low exposure; H.E.: high exposure. Data in graphs shown as mean ± SEM. * $p < 0.05$, **** $p < 0.0001$.

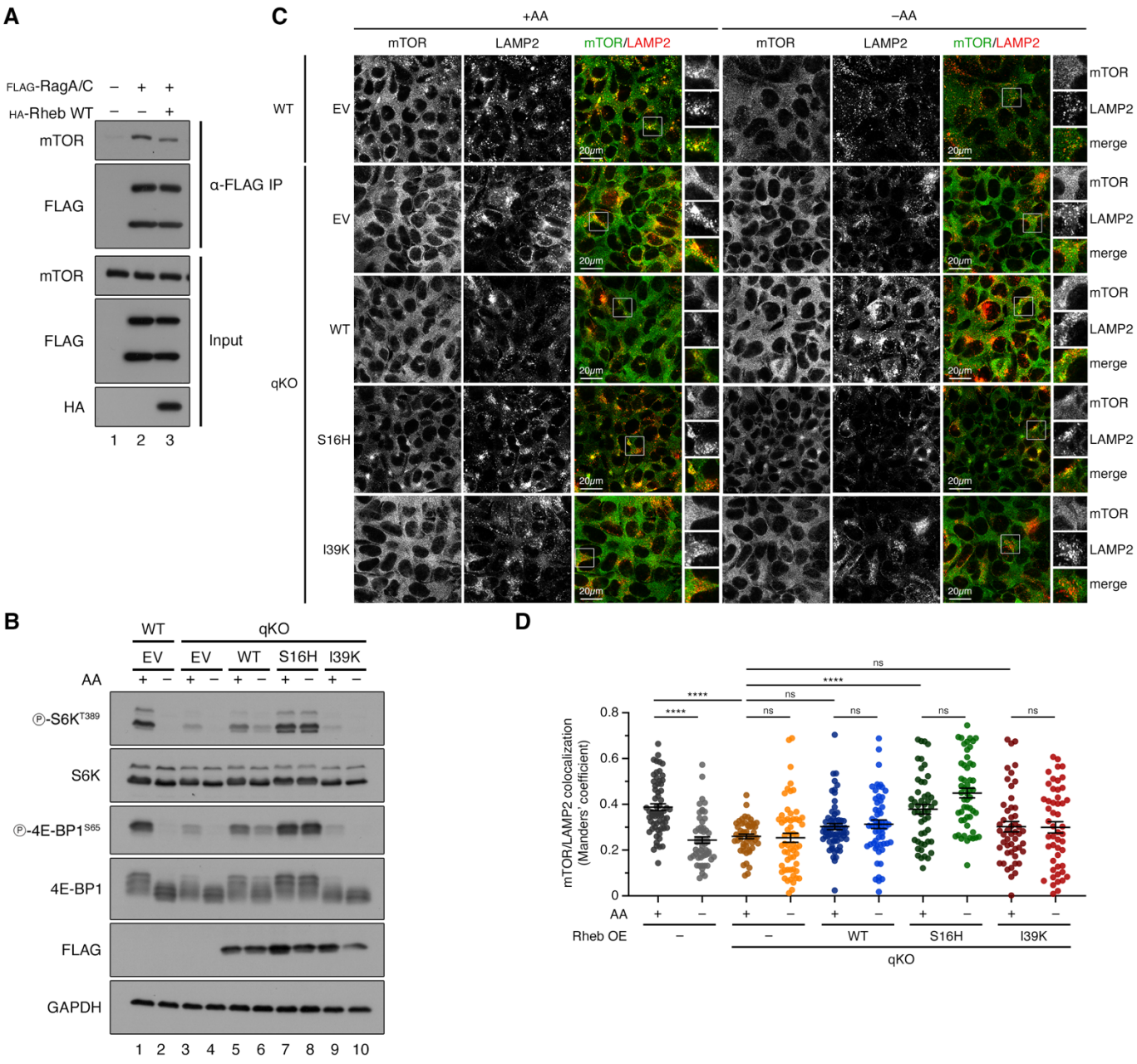

Figure 3. Rheb drives mTORC1 lysosomal retention in the absence of Rag GTPases.

(A) Co-immunoprecipitation of transiently expressed FLAG-tagged RagA/C and HA-tagged Rheb WT in WT HEK293FT cells. The input and IP samples were analyzed by immunoblotting using antibodies against the indicated proteins.

(B) Immunoblots with lysates from WT or Rag A-D quadruple knockout (qKO) HEK293FT cells stably expressing FLAG-tagged WT, active (S16H) or inactive (I39K) Rheb, treated with media containing (+AA) or lacking (-AA) amino acids for 1 hour,

using confocal microscopy and probed with different antibodies, as indicated. Cells transfected with an empty vector (EV) used as control.

(C-D) Colocalization analysis of mTOR with LAMP2 (lysosomal marker) in WT or Rag A-D quadruple knockout (qKO) HEK293FT cells stably expressing FLAG-tagged WT, active (S16H) or inactive (I39K) Rheb, treated with media containing (+AA) or lacking (-AA) amino acids for 1 hour, using confocal microscopy. Cells transfected with an empty vector (EV) used as control. Magnified insets shown to the right (C). Quantification of colocalization in (D). n = 50-60 individual cells from 3 independent fields per condition.

Scale bars = 20 μm. P: phosphorylated form. Data in graphs shown as mean ± SEM. **** $p < 0.0001$, ns: non-significant.

A

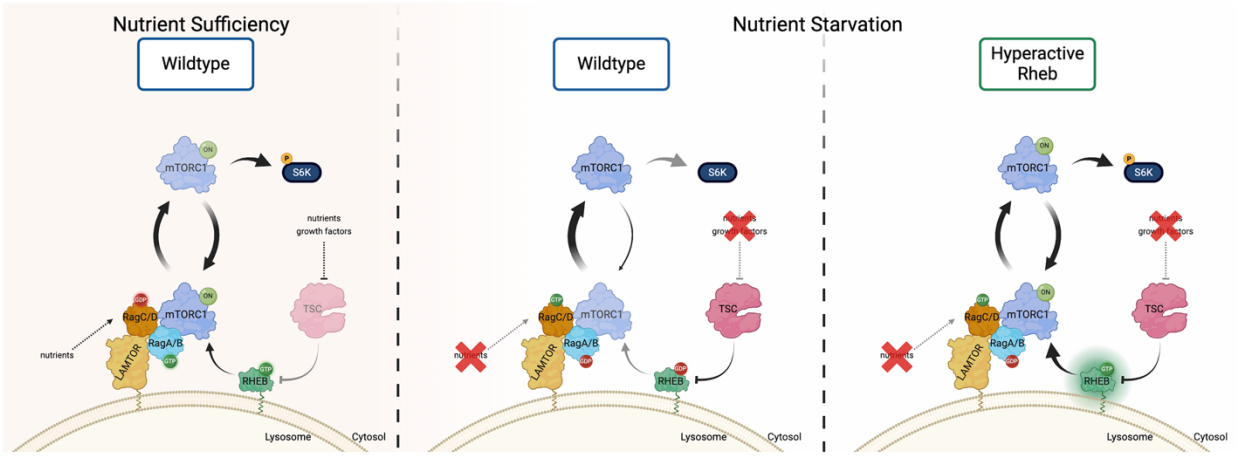

Figure 4. Hyperactive Rheb retains mTOR at the lysosomal surface even upon nutrient starvation.

(A) Proposed model of the secondary role of hyperactive Rheb in serving as an alternate lysosomal anchor for mTORC1. Under nutrient sufficiency, mTORC1 is recruited to the lysosomal surface primarily by the Rags where it is activated by Rheb, allowing phosphorylation of downstream targets such as S6K. This recruitment is suppressed upon nutrient starvation. However, when Rheb is hyperactive (due to its overexpression or TSC dysfunction) it actively tethers mTOR to lysosomes and allows for continued signaling even upon starvation.

Methods

Cell culture

All cell lines were grown at 37 °C, 5% CO2. Human female embryonic kidney HEK293FT cells (#R70007, Invitrogen; RRID: CVCL_6911) were cultured in high-glucose Dulbecco's Modified Eagle Medium (DMEM) (#41965039, Gibco), supplemented with 10% fetal bovine serum (FBS) (#F7524, Sigma; #P30-3306, PAN-Biotech; #FBS.HP.0500, Bio&SELL). All media were supplemented with 1x Penicillin-Streptomycin (#15140122, Gibco; #P4333-100ML, Sigma).

HEK293FT cells were purchased from Invitrogen at the initiation of the project. The identity of the HEK293FT cells was validated by the Multiplex human Cell Line Authentication test (Multiplexion GmbH), which uses a single nucleotide polymorphism (SNP) typing approach, and was performed as described at www.multiplexion.de. No commonly misidentified cell lines were used in this study. All cell lines were regularly tested for *Mycoplasma* contamination, using a PCR-based approach and were confirmed to be *Mycoplasma*-free.

Cell culture treatments

Amino acid (AA) starvation experiments were performed as described previously [12,26]. In brief, custom-made starvation media were formulated according to the Gibco recipe for high-glucose DMEM, specifically omitting all amino acids. The media were filtered through a 0.22-µm filter device and tested for proper pH and osmolality before use. For the respective AA-replete (+AA) treatment media, commercially available high-glucose DMEM was used (#41965039, Gibco). All treatment media were supplemented with 10% dialyzed FBS (dFBS) and 1x Penicillin-Streptomycin (#15140122, Gibco; #P4333-100ML, Sigma). For this purpose, FBS was dialyzed against 1x PBS through 3,500 MWCO dialysis tubing. For basal (+AA) conditions, the culture media were replaced with +AA treatment media 60 min before lysis or fixation. For amino-acid starvation (-AA), culture media were replaced with starvation media for 1 hour, unless otherwise indicated in the figure legends. For glucose starvation experiments, cells were cultured for 1 hour in glucose-free DMEM (#11966025, Gibco) supplemented with 10% dFBS and 1x Penicillin-Streptomycin. For the respective control wells, the culture media were replaced with high-glucose DMEM containing

10% dFBS and 1x Penicillin-Streptomycin at the beginning of the experiment.

To inhibit mTOR kinase activity, Torin1 (#4247, Tocris Bioscience) was added in the culture media to a final concentration of 250 nM for 1 hour. For all drug treatments, DMSO (#4720.1, Roth) was used as vehicle control.

Antibodies

The H4B4 antibody against LAMP2 was obtained from the Developmental Studies Hybridoma Bank, created by the NICHD of the NIH and maintained at The University of Iowa, Department of Biology. H4B4 was deposited to the DSHB by August, J.T. / Hildreth, J.E.K. (DSHB Hybridoma Product H4B4) [27].

Plasmids and Molecular Cloning

For transient overexpression, Rheb constructs were cloned in a pcDNA3-FLAG backbone. FLAG-hRheb-WT was amplified from human cDNA using appropriate primers and cloned between EcoRI/NotI sites of a pcDNA3-FLAG empty vector. FLAG-hRheb-S16H, FLAG-hRheb-I39K, and FLAG-hRheb-C181S were cloned by site-directed mutagenesis using appropriate primers using pcDNA3-FLAG-hRheb-WT as the template. FLAG-hRheb-S16H/C181S was cloned by introducing the C181S mutation in FLAG-hRheb-S16H using appropriate primers. A pcDNA3-FLAG-Luciferase construct was used as a vector control.

The pcDNA3-HA-hRheb-WT construct was sub-cloned from pcDNA3-FLAG-hRheb-WT to pcDNA3-HA vector between EcoRI/NotI restriction sites using appropriate primers. pcDNA3-HA-hRagA WT and pcDNA3-HA-hRagC WT constructs were cloned by PCR amplification of the Rag CDS (described in [24,28]).

For stable overexpression, FLAG-hRheb-WT, FLAG-hRheb-S16H, FLAG-hRheb-I39K constructs were sub-cloned into a pITR-TTP-puro vector (described in [29,30]) between PvuII and NotI restriction sites. The respective empty pITR vector (pITR-EV) was used in control transfections. All restriction enzymes were purchased from Fermentas/Thermo Scientific. The integrity of all constructs was verified by sequencing.

Plasmid DNA transfections

Plasmid DNA transfections in HEK293FT cells were performed using Effectene transfection reagent (#301425, QIAGEN), according to the manufacturer's instructions. For Rag and Rheb co-transfections, equal amounts of each plasmid were transfected.

Generation of stable cell lines

The polyclonal HEK293FT WT or Rag qKO cell lines stably expressing the various Rheb constructs were generated using a doxycycline-inducible sleeping-beauty-based transposon system [29,30]. In brief, Wt or Rag qKO cells were transfected with pITR-FLAG-Rheb expression constructs (see 'Plasmid' section above) in a 10:1 ratio together with the transposase-expressing pCMV-Trp vector. Thirty-six to 40 hours post transfection, cells were selected with 2 µg/ml puromycin (#A1113803, Thermo Fisher Scientific). The polyclonal cell lines were subsequently maintained in media containing the selection agents. Doxycycline-induced expression from the integrated transposon was checked by treating the cells overnight with 2 µg/mL doxycycline (#9891, Sigma). For experiments, all cell lines were plated for experiments in the presence of 1 µg/mL doxycycline, in order to achieve overexpression.

Cell lysis and immunoblotting

For standard SDS-PAGE and immunoblotting experiments, cells from one well of a 6-well plate were treated as indicated in the figures and lysed in 300 µl of ice-cold Triton lysis buffer (50 mM Tris pH 7.5, 1% Triton X-100, 150 mM NaCl, 50 mM NaF, 2 mM Na-vanadate, 0.011 gr/ml beta-glycerophosphate), supplemented with 1x PhosSTOP phosphatase inhibitors (#04906837001, Roche) and 1x cOmplete protease inhibitors (#11697498001, Roche), for 10 minutes on ice. Lysates were clarified by centrifugation (15000 rpm, 10 min, 4 °C) and supernatants transferred to a new tube. Protein concentration was determined using a Protein Assay Dye Reagent (#5000006, Bio-Rad). Normalized samples were boiled in 1x SDS sample buffer for 5 min at 95 °C (6x SDS sample buffer: 350 mM Tris-HCl pH 6.8, 30% glycerol, 600 mM DTT, 12.8% SDS, 0.12% bromophenol blue).

Protein samples were subjected to electrophoretic separation on SDS-PAGE and

analysed by standard Western blotting techniques. In brief, proteins were transferred to nitrocellulose membranes (#10600002 or #10600001, Amersham) and stained with 0.2% Ponceau solution (#33427-01, Serva) to confirm equal loading. Membranes were blocked with 5% skim milk powder (#42590, Serva) in TBS-T [1x TBS, 0.1% Tween-20 (#A1389, AppliChem)] for 1 hour at room temperature, washed three times for 5 min with TBS-T and then incubated with primary antibodies [1:1000 in TBS-T, 5% bovine serum albumin (BSA; #10735086001, Roche; #8076, Carl Roth)] overnight at 4 °C. The next day, membranes were washed three times for 5 min with TBS-T and incubated with the appropriate HRP-conjugated secondary antibodies (1:10000 in 5% milk in TBS-T) for 1 hour at room temperature. Signals were detected by enhanced chemiluminescence (ECL), using ECL Western Blotting Substrate (#W1015, Promega); or SuperSignal West Femto Substrate (#34095, Thermo Scientific) for weaker signals. Immunoblot images were captured on films (#28906835, GE Healthcare; #4741019289, Fujifilm). Blots were scanned for figure preparation.

Co-immunoprecipitation (co-IP)

For co-immunoprecipitation experiments, cells of one well of a 6-well plate were lysed in 300 µl CHAPS IP buffer (50 mM Tris pH 7.5, 0.3% CHAPS, 150 mM NaCl, 50 mM NaF, 2 mM Na-vanadate, 0.011 gr/ml beta-glycerophosphate) supplemented with 1x PhosSTOP phosphatase inhibitors (#04906837001, Roche) and 1x cOmplete protease inhibitors (#11697498001, Roche) for 10 minutes on ice. Samples were clarified by centrifugation (15000 rpm, 10 min, 4 °C) and a portion of the samples was taken as input. 30 µl of pre-washed anti-FLAG-M2 Affinity Gel (#A2220, Sigma) were added to the remaining volume of the supernatants and the IP samples were incubated at 4 °C on a rotating mixer for 2 h. After incubation, beads were washed four times with CHAPS IP wash buffer (50 mM Tris pH 7.5, 0.3% CHAPS, 150 mM NaCl, 50 mM NaF) and boiled in 2x SDS loading buffer. Samples were analysed by SDS-PAGE and the presence of co-immunoprecipitated proteins was detected by immunoblotting with appropriate specific antibodies.

Immunofluorescence and confocal microscopy

Immunofluorescence/confocal microscopy experiments were performed as described previously [12,31]. In brief, cells were seeded on glass coverslips coated with 0.1%

Gelatin (#G1393, Sigma) or 0.1% Poly-L-Lysine (#sc-286689, Santa Cruz Biotechnology), treated as described in the figure legends, and fixed with 4% paraformaldehyde (PFA) (#28908, Thermo Scientific) in 1x PBS (10 min, room temperature), followed by a permeabilization step with PBT (1x PBS, 0.1 % Tween-20) for 20 min. Cells were blocked in BBT (1x PBS, 0.1% Tween-20, 1% BSA) for 45 minutes. Staining with anti-mTOR (#2983, Cell Signaling Technology) and anti-LAMP2 (#H4B4, Developmental Studies Hybridoma Bank) primary antibodies diluted 1:200 in BBT solution was performed for 2h at room temperature. After staining with primary antibodies, coverslips were washed three times with PBT and then stained with highly cross-adsorbed fluorescent secondary antibodies (Donkey anti-Rabbit Alexa Fluor 488, Donkey anti-Mouse Alexa Fluor 594; both from Jackson ImmunoResearch) diluted 1:400 in BBT for 1 hour. Nuclei were stained with DAPI (#A1001, VWR) (1:2000 in PBT) for 10 min and coverslips were washed two times for 10 min with PBT solution before mounting on glass slides with Fluoromount-G (#00-4958-02, Invitrogen). All images were acquired on an SP8 Leica confocal microscope (TCS SP8 X or TCS SP8 DLS, Leica Microsystems) using a 40x oil objective lens. Image acquisition was performed using the LAS X software (Leica Microsystems). Images from single channels are shown in grayscale, whereas in merged images, Alexa Fluor 488 is shown in green and Alexa Fluor 594 in red. Brightness and contrast were adjusted for visualization purposes using Fiji (https://imagej.net/software/fiji/downloads) [32]. Alterations were applied to the entire image, keeping the parameters identical between all images of the same channel in each panel.

Quantification of colocalization

Colocalization analysis in confocal microscopy experiments was performed as in [26,31], using the Coloc2 plugin of the Fiji software [32]. On average, 50-60 individual cells from 3-5 independent representative images per condition acquired from one representative experiment (out of 3 independent replicate experiments as indicated in the figure legends) were used to calculate Manders' colocalization coefficient (MCC) with automatic Costes thresholding [33-35]. Outlines of individual cells were traced, excluding the area corresponding to the cell nucleus, to generate the region of interest (ROI) used for calculating the MCC to prevent false-positive colocalization due to automatic signal adjustments. MCC and PCC are defined as a part of the signal of

interest (mTOR), which overlaps with a second signal (LAMP2).

Statistical analysis

Statistical analysis and presentation of quantification data was performed using GraphPad Prism (versions 9 and 10). All relevant information on the statistical details of experiments is provided in the figure legends. Information on quantifications for each method is also provided in the respective Methods section. Data in all graphs are shown as mean ± SEM. For graphs with only two conditions shown (Fig. 1J and Fig. S5D-F), significance was calculated using Student's t-test (unpaired, two-tailed). For all other graphs, significance for the indicated pairwise comparisons was calculated using one-way ANOVA with *post hoc* Tukey's multiple comparisons test. Sample sizes (n) and significance values are indicated in figure legends (* $p < 0.05$, ** $p < 0.01$, *** $p < 0.001$, **** $p < 0.0001$, ns: non-significant).

All findings were reproducible over multiple independent experiments, within a reasonable degree of variability between replicates. For most experiments, at least three independent replicates were performed. The sample size for microscopy experiments (number of individual cells used in quantifications) is provided in the respective figure legends. No statistical method was used to predetermine sample size, which was determined in accordance with standard practices in the field. No data were excluded from the analyses. The experiments were not randomized, and the investigators were not blinded to allocation during experiments and outcome assessment.

Acknowledgements

We thank all members of the Demetriades lab for critical discussions; Andreas Lamprakis for support with cell culture and Jiyoung Pan for support with cloning; and the MPI-AGE FACS & Imaging Core Facility for support with confocal microscopy. AA received support by the Cologne Graduate School of Ageing Research. CD is funded by the European Research Council (ERC) under the European Union's Horizon 2020 research and innovation programme (grant agreement No 757729), and by the Max Planck Society. Parts of this work were supported by the Deutsche Forschungsgemeinschaft (DFG, German Research Foundation) through the Research Unit Grant FOR2722 (DE 3170/1-1; Project No 384170921) to CD. Models in figures created with BioRender.com.

Author Contributions

Experimental work: A.A., S.K.; data analysis: A.A., S.K.; project design, conceptualization: A.A., C.D.; supervision: C.D.; funding acquisition: C.D.; figure preparation: A.A.; manuscript draft: A.A. All authors approved the final version of the manuscript and agree on the content and conclusions.

Declaration of Interests

The authors declare no competing interests.

Data availability

The data that support the findings of this study (uncropped immunoblots, microscopy pictures, molecular dynamics) are available from the corresponding author upon reasonable request.

Code availability

No code was generated in this study.

Additional Information

Supplemental Information (Supplemental Figures S1-S2) is available for this paper.

References

1. Hein, M.Y., Peng, D., Todorova, V., McCarthy, F., Kim, K., Liu, C., Savy, L., Januel, C., Baltazar-Nunez, R., Sekhar, M., et al. (2024). Global organelle profiling reveals subcellular localization and remodeling at proteome scale. Cell. 10.1016/j.cell.2024.11.028.

2. Hung, M.C., and Link, W. (2011). Protein localization in disease and therapy. J Cell Sci *124*, 3381-3392. 10.1242/jcs.089110.

3. Gonzalez, A., and Hall, M.N. (2017). Nutrient sensing and TOR signaling in yeast and mammals. EMBO J *36*, 397-408. 10.15252/embj.201696010.

4. Rabanal-Ruiz, Y., and Korolchuk, V.I. (2018). mTORC1 and Nutrient Homeostasis: The Central Role of the Lysosome. Int J Mol Sci *19*. 10.3390/ijms19030818.

5. Fernandes, S.A., and Demetriades, C. (2021). The Multifaceted Role of Nutrient Sensing and mTORC1 Signaling in Physiology and Aging. Front Aging *2*, 707372. 10.3389/fragi.2021.707372.

6. Liu, G.Y., and Sabatini, D.M. (2020). mTOR at the nexus of nutrition, growth, ageing and disease. Nat Rev Mol Cell Biol *21*, 183-203. 10.1038/s41580-019-0199-y.

7. Menon, S., Dibble, C.C., Talbott, G., Hoxhaj, G., Valvezan, A.J., Takahashi, H., Cantley, L.C., and Manning, B.D. (2014). Spatial control of the TSC complex integrates insulin and nutrient regulation of mTORC1 at the lysosome. Cell *156*, 771-785. 10.1016/j.cell.2013.11.049.

8. Sancak, Y., Peterson, T.R., Shaul, Y.D., Lindquist, R.A., Thoreen, C.C., Bar-Peled, L., and Sabatini, D.M. (2008). The Rag GTPases bind raptor and mediate amino acid signaling to mTORC1. Science *320*, 1496-1501. 10.1126/science.1157535.

9. Sancak, Y., Bar-Peled, L., Zoncu, R., Markhard, A.L., Nada, S., and Sabatini, D.M. (2010). Ragulator-Rag complex targets mTORC1 to the lysosomal surface and is necessary for its activation by amino acids. Cell *141*, 290-303. 10.1016/j.cell.2010.02.024.

10. Tee, A.R., Manning, B.D., Roux, P.P., Cantley, L.C., and Blenis, J. (2003). Tuberous sclerosis complex gene products, Tuberin and Hamartin, control mTOR signaling by acting as a GTPase-activating protein complex toward Rheb. Curr Biol *13*, 1259-1268. 10.1016/s0960-9822(03)00506-2.

11. Inoki, K., Li, Y., Xu, T., and Guan, K.L. (2003). Rheb GTPase is a direct target of TSC2 GAP activity and regulates mTOR signaling. Genes Dev *17*, 1829-1834. 10.1101/gad.1110003.

12. Demetriades, C., Doumpas, N., and Teleman, A.A. (2014). Regulation of TORC1 in

response to amino acid starvation via lysosomal recruitment of TSC2. Cell *156*, 786-799. 10.1016/j.cell.2014.01.024.

13. Fernandes, S.A., Angelidaki, D.D., Nuchel, J., Pan, J., Gollwitzer, P., Elkis, Y., Artoni, F., Wilhelm, S., Kovacevic-Sarmiento, M., and Demetriades, C. (2024). Spatial and functional separation of mTORC1 signalling in response to different amino acid sources. Nat Cell Biol *26*, 1918-1933. 10.1038/s41556-024-01523-7.

14. Alesi, N., Akl, E.W., Khabibullin, D., Liu, H.J., Nidhiry, A.S., Garner, E.R., Filippakis, H., Lam, H.C., Shi, W., Viswanathan, S.R., et al. (2021). TSC2 regulates lysosome biogenesis via a non-canonical RAGC and TFEB-dependent mechanism. Nat Commun *12*, 4245. 10.1038/s41467-021-24499-6.

15. Alesi, N., Khabibullin, D., Rosenthal, D.M., Akl, E.W., Cory, P.M., Alchoueiry, M., Salem, S., Daou, M., Gibbons, W.F., Chen, J.A., et al. (2024). TFEB drives mTORC1 hyperactivation and kidney disease in Tuberous Sclerosis Complex. Nat Commun *15*, 406. 10.1038/s41467-023-44229-4.

16. Dai, X., Jiang, C., Jiang, Q., Fang, L., Yu, H., Guo, J., Yan, P., Chi, F., Zhang, T., Inuzuka, H., et al. (2023). AMPK-dependent phosphorylation of the GATOR2 component WDR24 suppresses glucose-mediated mTORC1 activation. Nat Metab *5*, 265-276. 10.1038/s42255-022-00732-4.

17. Efeyan, A., Zoncu, R., Chang, S., Gumper, I., Snitkin, H., Wolfson, R.L., Kirak, O., Sabatini, D.D., and Sabatini, D.M. (2013). Regulation of mTORC1 by the Rag GTPases is necessary for neonatal autophagy and survival. Nature *493*, 679-683. 10.1038/nature11745.

18. Inoki, K., Zhu, T., and Guan, K.L. (2003). TSC2 mediates cellular energy response to control cell growth and survival. Cell *115*, 577-590. 10.1016/s0092-8674(03)00929-2.

19. Gwinn, D.M., Shackelford, D.B., Egan, D.F., Mihaylova, M.M., Mery, A., Vasquez, D.S., Turk, B.E., and Shaw, R.J. (2008). AMPK phosphorylation of raptor mediates a metabolic checkpoint. Mol Cell *30*, 214-226. 10.1016/j.molcel.2008.03.003.

20. Malik, N., Ferreira, B.I., Hollstein, P.E., Curtis, S.D., Trefts, E., Weiser Novak, S., Yu, J., Gilson, R., Hellberg, K., Fang, L., et al. (2023). Induction of lysosomal and mitochondrial biogenesis by AMPK phosphorylation of FNIP1. Science *380*, eabj5559. 10.1126/science.abj5559.

21. Yu, Y., Li, S., Xu, X., Li, Y., Guan, K., Arnold, E., and Ding, J. (2005). Structural basis for the unique biological function of small GTPase RHEB. J Biol Chem *280*, 17093-17100. 10.1074/jbc.M501253200.

22. Angarola, B., and Ferguson, S.M. (2019). Weak membrane interactions allow Rheb to activate mTORC1 signaling without major lysosome enrichment. Mol Biol Cell *30*, 2750-2760. 10.1091/mbc.E19-03-0146.

23. Lawrence, R.E., Cho, K.F., Rappold, R., Thrun, A., Tofaute, M., Kim, D.J., Moldavski, O., Hurley, J.H., and Zoncu, R. (2018). A nutrient-induced affinity switch controls mTORC1 activation by its Rag GTPase-Ragulator lysosomal scaffold. Nat Cell Biol *20*, 1052-1063. 10.1038/s41556-018-0148-6.

24. Gollwitzer, P., Grutzmacher, N., Wilhelm, S., Kummel, D., and Demetriades, C. (2022). A Rag GTPase dimer code defines the regulation of mTORC1 by amino acids. Nat Cell Biol *24*, 1394-1406. 10.1038/s41556-022-00976-y.

25. Long, X., Ortiz-Vega, S., Lin, Y., and Avruch, J. (2005). Rheb binding to mammalian target of rapamycin (mTOR) is regulated by amino acid sufficiency. J Biol Chem *280*, 23433-23436. 10.1074/jbc.C500169200.

26. Demetriades, C., Plescher, M., and Teleman, A.A. (2016). Lysosomal recruitment of TSC2 is a universal response to cellular stress. Nat Commun *7*, 10662. 10.1038/ncomms10662.

27. Mane, S.M., Marzella, L., Bainton, D.F., Holt, V.K., Cha, Y., Hildreth, J.E., and August, J.T. (1989). Purification and characterization of human lysosomal membrane glycoproteins. Arch Biochem Biophys *268*, 360-378. 10.1016/0003-9861(89)90597-3.

28. Bryk, B., Hahn, K., Cohen, S.M., and Teleman, A.A. (2010). MAP4K3 regulates body size and metabolism in Drosophila. Dev Biol *344*, 150-157. 10.1016/j.ydbio.2010.04.027.

29. Kowarz, E., Loscher, D., and Marschalek, R. (2015). Optimized Sleeping Beauty transposons rapidly generate stable transgenic cell lines. Biotechnol J *10*, 647-653. 10.1002/biot.201400821.

30. Nuchel, J., Tauber, M., Nolte, J.L., Morgelin, M., Turk, C., Eckes, B., Demetriades, C., and Plomann, M. (2021). An mTORC1-GRASP55 signaling axis controls unconventional secretion to reshape the extracellular proteome upon stress. Mol Cell. 10.1016/j.molcel.2021.06.017.

31. Fitzian, K., Bruckner, A., Brohee, L., Zech, R., Antoni, C., Kiontke, S., Gasper, R., Linard Matos, A.L., Beel, S., Wilhelm, S., et al. (2021). TSC1 binding to lysosomal PIPs is required for TSC complex translocation and mTORC1 regulation. Mol Cell *81*, 2705-2721 e2708. 10.1016/j.molcel.2021.04.019.

32. Schindelin, J., Arganda-Carreras, I., Frise, E., Kaynig, V., Longair, M., Pietzsch, T., Preibisch, S., Rueden, C., Saalfeld, S., Schmid, B., et al. (2012). Fiji: an open-source platform for biological-image analysis. Nat Methods *9*, 676-682. 10.1038/nmeth.2019.

33. Manders, E.M.M., Verbeek, F.J., and Aten, J.A. (1993). Measurement of co-localization of objects in dual-colour confocal images. J Microsc *169*, 375-382. 10.1111/j.1365-2818.1993.tb03313.x.

34. Costes, S.V., Daelemans, D., Cho, E.H., Dobbin, Z., Pavlakis, G., and Lockett, S. (2004). Automatic and quantitative measurement of protein-protein colocalization in live cells. Biophys J *86*, 3993-4003. 10.1529/biophysj.103.038422.

35. Dunn, K.W., Kamocka, M.M., and McDonald, J.H. (2011). A practical guide to evaluating colocalization in biological microscopy. Am J Physiol Cell Physiol *300*, C723-742. 10.1152/ajpcell.00462.2010.

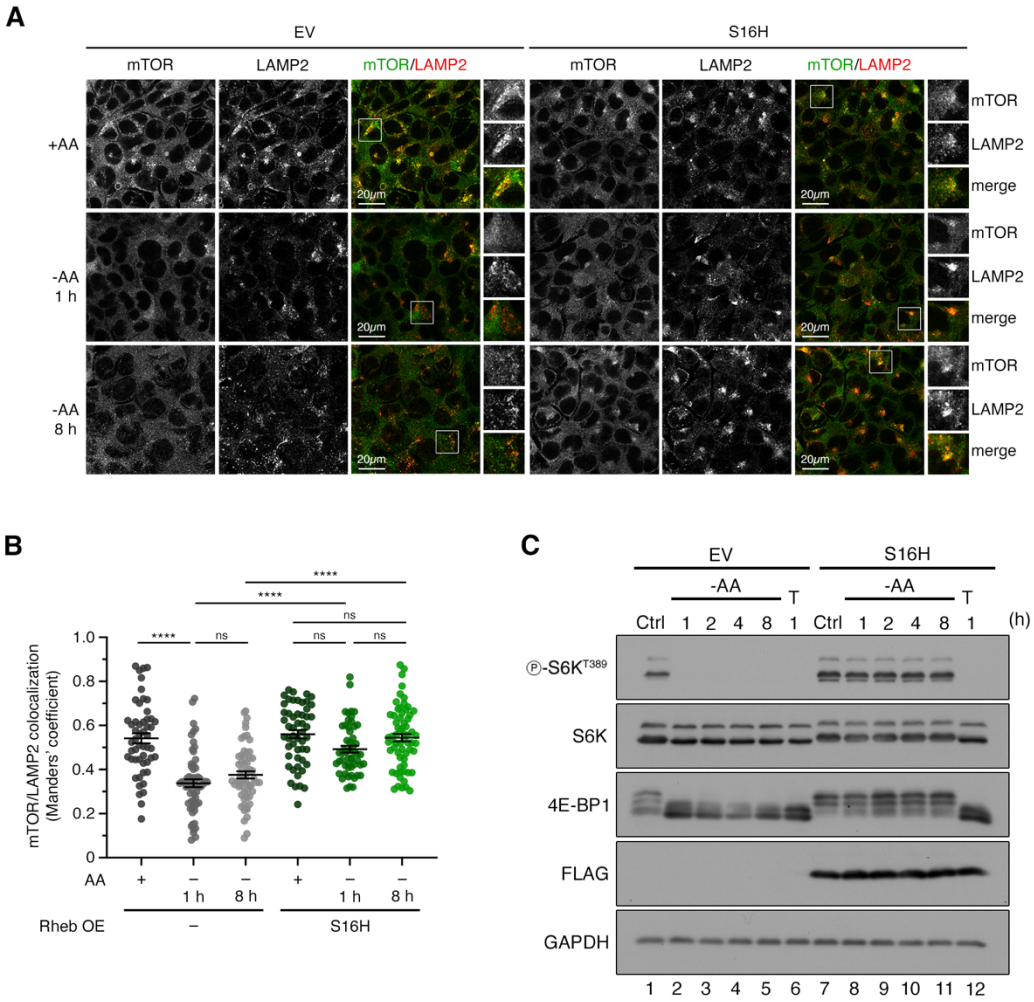

Figure S1. Overexpression of Rheb renders mTORC1 localization and activity insensitive to prolonged amino acid starvation.

(A-B) Colocalization analysis of mTOR with LAMP2 (lysosomal marker) in WT HEK293FT cells stably expressing FLAG-tagged active (S16H) Rheb, treated with media containing (+AA) or lacking (-AA) amino acids for the indicated duration, using confocal microscopy. Cells transfected with an empty vector (EV) used as control. Magnified insets shown to the right (A). Quantification of colocalization in (B). n = 50-60 individual cells from 3 independent fields per condition.

(C) Immunoblots with lysates from WT HEK293FT cells stably expressing FLAG-tagged active (S16H) Rheb (or EV as a control), treated with media containing (+AA) or lacking (-AA) amino acids for different times (1-8 hours), and probed with different antibodies, as indicated. Torin1 (T) treatment (250 nM, 1 h) was used as a control.

Scale bars = 20 μm. P: phosphorylated form. Data in graphs shown as mean ± SEM. **** $p < 0.0001$, ns: non-significant.

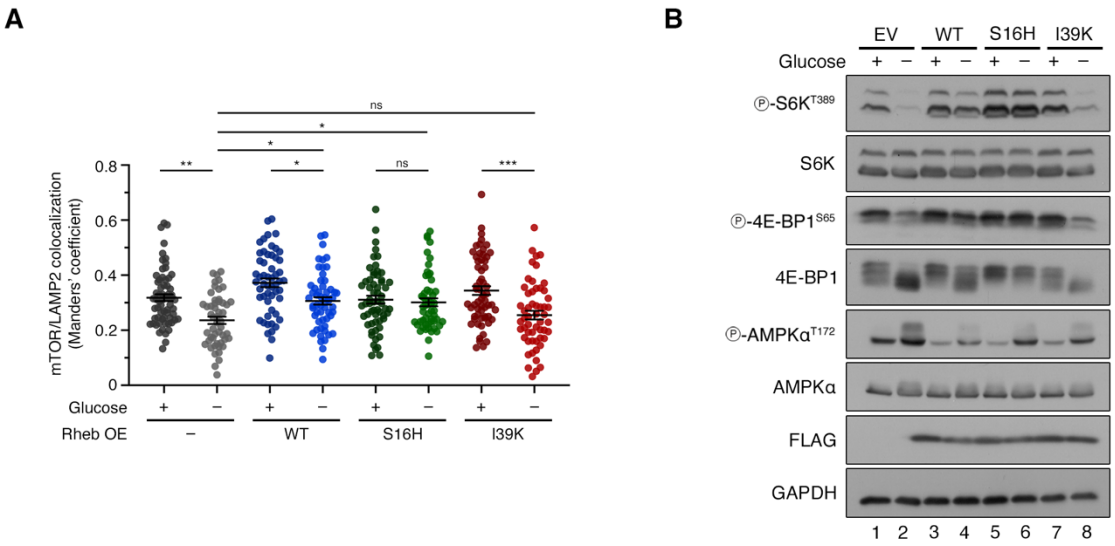

Figure S2. Overexpression of Rheb desensitizes mTORC1 localization and activity to glucose starvation.

(A) Quantification of colocalization analysis of mTOR with LAMP2 (lysosomal marker) in WT HEK293FT cells stably expressing FLAG-tagged WT, active (S16H), or inactive (I39K) Rheb, treated with media containing or lacking glucose for 1 hour, using confocal microscopy. Cells transfected with an empty vector (EV) used as control. n = 50-60 individual cells from 3 independent fields per condition.

(C) Immunoblots with lysates from WT HEK293FT cells stably expressing FLAG-tagged WT, active (S16H), or inactive (I39K) Rheb, treated with media containing or lacking glucose for 1 hour, and probed with different antibodies, as indicated.

P: phosphorylated form. Data in graphs shown as mean ± SEM. * $p < 0.05$, ** $p < 0.01$, *** $p < 0.001$, ns: non-significant.

3 Discussion

Cells employ several sophisticated strategies to spatially and temporally regulate the activity of proteins, such as rapid changes in their amount through synthesis and/or degradation, regulatory feedback loops for attenuating or upregulating their activity to meet cellular requirements, post-translational modifications that possess the ability to alter their structure and/or function or dynamic changes in their spatial distribution. The central role of the mTORC1 signaling pathway in integrating environmental cues to maintain a balance between anabolic and catabolic programs of the cell as well as the detrimental consequences of mTORC1 dysregulation, highlight the need for such fine-tuning mechanisms to exist. This thesis examines the intricate link between mTORC1 activity and localization, and illuminates two novel molecular principles that govern both mTORC1 localization and signaling:

(1) mTORC1 autoregulates its lysosomal presence via its intrinsic activity

(2) Hyperactive RHEB serves as a secondary tether for mTORC1 at lysosomes

3.1 mTORC1 activity licenses its own release from the lysosomal surface

Within cells, mTORC1 is primarily distributed between the cytosol and lysosomes. According to the common consensus in the field, when nutrients are sufficient, an elaborate lysosomal machinery functions to recruit mTORC1 to the lysosomal surface for activation. In brief, sensing of nutrient sufficiency by a complex network of upstream sensors ultimately leads to the active conformation of the Rag GTPases, whereby they gain a higher affinity for mTORC1 and recruit it to the lysosomal surface. In contrast, when nutrients are scarce, mTORC1 remains cytosolic due to reduced affinity of the Rag GTPases when in their inactive conformation. At the lysosomal surface, mTORC1 comes in close proximity to another small GTPase, Rheb, that allosterically induces a conformational change in the catalytic cleft of mTORC1, thereby leading to its activation and kinase activity toward its downstream substrates. In more than a decade of research since the initial finding of mTORC1 at lysosomes, a large amount of effort has led to the development of a lysosome-centric model with details of how mTORC1 is recruited and activated at

lysosomes. However, mTORC1 is not static on lysosomes upon its recruitment; in fact, under conditions of prolonged nutrient sufficiency, it continuously cycles on and off lysosomes, but the mechanistic underpinnings of how it is released were thus far unknown. Based on the findings in Chapter 1 of the Results section, I demonstrated that mTORC1 activity controls its own release by regulating the nucleotide-binding of RagA.

Using pharmacological or genetic down-regulation of mTORC1 as a means to capture a static picture of an otherwise dynamic protein, I observed increased enrichment of mTORC1 at lysosomes, indicating that intact mTORC1 activity is a prerequisite for normal shuttling of the complex on/off lysosomes. This was contrary to the prior notion of a linear causality between mTORC1 localization and activity, wherein the former dictates the latter. As per the predominant model, a widespread perception was that mTORC1 was 'active' only when on lysosomes and 'inactive' when cytosolic. However, my findings showcasing the accumulation of inactive complexes at the lysosomal membrane counter this premise. The aberrant retention of inactive mTOR on lysosomes was dominant over the effect that amino acid or glucose starvation or lysosomal dysfunction otherwise has on its localization, causing mTOR to prevail at the organelle rather than become diffused and cytosolic in distribution.

I experimentally eliminated the possibility that the enhanced lysosomal enrichment of mTOR was an outcome of increased recruitment of mTORC1 to lysosomes, and confirmed the hypothesis that mTORC1 inhibition prohibited its release from the lysosomal surface. What necessitates the release of mTORC1 from the lysosomal surface under basal conditions? Although the lysosomal surface is the chief site of mTORC1 activation, several substrates of mTORC1 are located elsewhere in the cell [104]. Moreover, cycling of the complex on/off lysosomes in nutrient sufficiency has been detected and its activity has also been measured in several different cellular compartments [21,105]. Together with my experimental findings, these data support the notion that mTORC1 is recruited to lysosomes for activation and subsequently released to encounter and exert its activity toward non-lysosomal substrates elsewhere in the cell. Given the cellular resources that are expended in recruiting mTORC1 to lysosomes, it is also reasonable that a checkpoint system is in place to prevent delocalization of mTORC1 prior to its activation, which would then be a futile cycle.

Concomitant with an effect on mTOR localization, mTORC1 signaling was also affected upon pharmacological inhibition of mTORC1 (by Rapamycin) or use of a genetic model of downregulated mTORC1 (RHEB knockout cells). Strikingly, whereas S6K phosphorylation declined upon mTORC1 downregulation, TFEB phosphorylation was augmented. Technically, the opposing responses can be attributed to the differences in the nature of the two substrates: while S6K is a Rapamycin-sensitive, RHEB-dependent substrate of mTORC1, TFEB is Rapamycin-insensitive and RHEB-independent. From a cell biological standpoint, these results indicate a clear distinction between mTORC1 activity towards non-lysosomal, canonical substrates such as S6K and lysosomal, non-canonical substrates such as TFEB. While lysosomal TFEB exhibited enhanced phosphorylation, as a direct outcome of the enhanced lysosomal enrichment of mTORC1, S6K phosphorylation was compromised, signifying the critical role of mTORC1 in triggering its own release from lysosomes to enable its activity toward substrates present at other cellular locations. It is worth noting that the contradictory effect of perturbation of mTORC1 signaling on S6K and TFEB has also been reported previously in the case of cells with a non-functional TSC complex, which will be discussed in further detail.

A recent publication from our lab demonstrated the existence of spatially distinct mTORC1 entities that also exhibit functional separation, by virtue of targeting diverse substrates at different subcellular locations. For instance, cytosolic activity of mTORC1 is largely directed toward the regulation of *de novo* protein synthesis, by phosphorylation of substrates such as S6K and 4EBP1; on the other hand, lysosomal activity of mTORC1 primarily suppresses lysosomal biogenesis and autophagy, by phosphorylation and inactivation of TFEB and TFE3. While these entities operate in a self-contained system, with local AA production likely stimulating compartmentalized activity of mTORC1 through thus far unidentified mechanisms, the different populations are not entirely disconnected and flux from one into the other [106]. The mechanism of autoregulation of lysosomal mTORC1 that has been put forth in this thesis is positioned at a unique signaling node in the cell. Therefore, I propose the release of mTORC1 as a decision point that determines the balance between lysosomal and non-lysosomal activities of mTORC1 to fulfill the physiological demands of the cell. In such a case, higher residence time of mTORC1 on lysosomes due to greater retention could promote more lysosomal activity whereas lower residence time achieved by faster release

could correspond to more non-lysosomal activities of the complex, while still engaging the lysosomal recruitment machinery.

Mechanistically, I demonstrated that the lysosomal retention of inactive mTORC1 is brought about by locking of the Rag GTPases in their active conformation, in which RagA is GTP-bound and RagC is GDP-bound. The Rag dimer has been shown to exhibit functional separation, with the smaller Rags driving mTORC1 localization, while the larger Rags drive TFEB/TFE3 recruitment and phosphorylation. Indeed, even the inactivation of mTORC1 primarily impacted the nucleotide loading status of RagA, locking it in the active conformation, which in turn prevented mTORC1 release from the lysosomal surface; in comparison, RagC activation state was not critical for this event. However, considering the fact that one GTP-bound subunit prohibits GTP-binding of the other within a Rag dimer [83], and the continued ability of mTORC1 to phosphorylate TFEB/TFE3 upon Rapamycin treatment or in RHEB KO cells, it is probable that RagC is in the GDP-bound state as it is indispensable for mTORC1-dependent TFEB phosphorylation [99,107]. The effect of mTORC1 inhibition on the RagA activation state was further assessed using NPRL3 KO cells, which lack a functional GATOR1 complex and therefore contain RagA/B fixed in their active conformation. In these cells, mTORC1 localization was not affected upon pharmacological inhibition, thus confirming that a switch in the RagA nucleotide loading was essential to release activated mTORC1 from lysosomes.

While the effect of mTORC1 inhibition on the upstream GATOR1-RagA axis was clear, the precise molecular mechanism(s), i.e. the downstream target(s) of mTORC1 kinase activity remain elusive. Taking into account the rapid effect of mTORC1 inhibition on its localization, it is conceivable that a local signaling event continuously occurs on the lysosomal landscape, and that it affects the existing lysosomal machinery in a manner that initial recruitment of the complex is unaffected. Notably, a publication in the same issue of Molecular Cell from the Zwartkruis lab identified a Rapamycin-sensitive phosphosite on DEPDC5, a component of the GATOR1 complex. Moreover, use of 'The Kinase Library', a kinase prediction algorithm, revealed several putative mTOR phosphosites on two of the three member proteins of the GATOR1 complex: DEPDC5 and NPRL3 (see Appendix A) [108].

GATOR1 is a logical candidate for the feedback regulation of mTORC1 since its GAP activity

toward RagA is required for the switch from the active, GTP-loaded state (higher affinity for mTORC1) to the inactive, GDP-loaded state (lower affinity for mTORC1). GATOR1 binds to the Rag GTPases in two different effector modes: (1) the inhibitory mode in which DEPDC5 contacts RagA and suppresses its intrinsic GTPase activity, causing RagA to remain in the GTP-bound state, and (2) the GAP mode in which a catalytic arginine finger of the NPRL2-NPRL3 dimer interacts with RagA to stimulate GTPase activity. The mechanism underlying the switch between the inhibitory mode to the GAP mode, which is necessary for GATOR1 to carry out its function as a negative regulator of mTORC1, as well as its biological relevance is yet to be determined. A plausible hypothesis is that mTORC1 dictates this switch, enabling its own release by indirectly impacting RagA nucleotide loading via GATOR1.

Previously, the Rag GTPase paralogues (RagA and RagB, and RagC and RagD) were considered to be functionally equivalent due to their high sequence homology. However, more recent work described the differences between the proteins and their functioning in the mTORC1 pathway: RagA and RagB vary in the signaling response generated upon amino acid depletion, whereas RagC and RagD differ in their binding affinity to p18/LAMTOR1, thus differentially affecting mTOR localization and TFEB/TFE3 phosphorylation. In light of these studies, it would be interesting to expand the results of this thesis and assess the effect of mTORC1 inhibition on its lysosomal localization in cells reconstituted with RagA/D, RagB/C or RagB/D-containing dimers (the present work utilized cells reconstituted with RagA/C). Of particular interest are the findings from Teleman lab which demonstrated that compared to RagA, RagB conferred resistance to AA starvation by inhibiting GATOR1 via its interaction with DEPDC5. This particularly resonates with the hypothesis stated previously regarding mTORC1-mediated regulation of GATOR1, and could be informative in the search for the precise molecular mechanism of mTORC1 cycling.

In addition to GATOR1, which functions as a GAP toward RagA/B, another candidate whose involvement in this process of releasing mTORC1 from lysosomes is worth exploring is SLC38A9, which acts as non-canonical GEF for RagA [42,48]. In such a scenario, mTORC1 phosphorylation may regulate the cytosolic N-terminal tail of SLC38A9 which has been shown to block GDP-to-GTP exchange of RagA in coordination with the lysosomal FLCN complex (LFC) [48]. Interestingly, ‘The Kinase Library’ predicted an mTOR-dependent

phosphosite within the cytoplasmic tail of SLC38A9 (see Appendix A) [108]. Moreover, an mTORC1-dependent effect on the functioning of SLC38A9 as a lysosomal amino acid transporter has been observed previously [109], further supporting this hypothesis.

I demonstrated that mTORC1 does not passively exit the lysosomal landscape; rather its release from lysosomes is an active process mediated by Rag GTPases by virtue of affecting their binding to mTORC1. Another layer of complexity is added when considering that the Rag-LAMTOR interface has also been shown to respond to nutrient cues, with RagA-GTP promoting destabilization of the interaction to attenuate mTORC1 signaling [21]. Thus, the extent of lysosomal localization of mTOR is the cumulative output of both Rag-mTOR and Rag-LAMTOR interactions. Although I established that mTORC1 inhibition caused its lysosomal enrichment through locking of RagA in the GTP-bound state, no significant change in RagC lysosomal localization was observed, suggesting that mTORC1 activity does not impinge on Rag-LAMTOR binding. A possible explanation for this discrepancy is the stoichiometry of mTORC1 and Rags: Rag dimers are found to be in excess in the cell in comparison to mTORC1 complexes [110], which could explain why despite strong Rag-mediated lysosomal enrichment of mTORC1, there was no observable difference in RagC localization.

3.2 Hyperactive Rheb acts as a lysosomal tether for mTORC1

The TSC-Rheb axis upstream of mTORC1 is a potent regulator of its activity, with Rheb directly interacting with mTOR on the lysosomal membrane to stimulate its catalytic activity [66,74,111]. The TSC complex lies upstream of Rheb, promoting its GTPase activity and GDP-bound state in response to several starvation or stress stimuli, and hence is one of the strongest negative regulators of mTORC1 activity. Through the findings in Chapter 2 of the Results section, I demonstrated that the TSC-Rheb axis not only impacts on mTORC1 activity but also its localization.

Using overexpression of different Rheb mutants as a proxy for its hyperactivation, I attempted to understand how Rheb hyperactivation affects mTORC1 localization and activity. Overexpression of WT or S16H (active) mutant demonstrated the capacity to desensitize mTORC1 to amino acid or glucose starvation, while overexpression of I39K (inactive) mutant was lacking in this respect. Rheb has been shown to predominantly favor

its GTP-bound state *in vivo* due to low intrinsic GTPase activity as well as higher levels of cellular GTP pools [112,113]; therefore, it is understandable why WT overexpression is sufficient to induce a phenotype similar to that of S16H. Arguably, the small but consistent difference between WT and S16H may stem from the nature of the mutant: the higher GTP-loading of S16H is attributed to resistance to TSC2 GAP activity [114,115], while WT remains susceptible to TSC action. On the other hand, the I39K inactive mutant of Rheb does not differ from WT in terms of GTP-loading, but its binding to mTOR is impaired due to a mutation in the Switch I region of the protein [116]. This indicates that the localization phenotype of mTORC1 is reliant on intact Rheb activity, by virtue of its nucleotide loading status as well as direct binding to mTOR.

In order to test which molecular properties of hyperactive Rheb are critical for mediating lysosomal anchoring of mTORC1, I assessed the ability of a farnesylation-deficient mutant of Rheb (C181S) [117] to retain mTORC1 localization and function upon amino acid deprivation. The C181S mutant has been shown to have slightly lower levels of GTP-loading compared to WT Rheb [116]; therefore, to clearly distinguish between nucleotide binding versus endomembrane anchoring properties of Rheb and the requirement of each to mediate the effect on mTOR localization, I generated the C181S mutant in the background of S16H active mutant. Despite having presumably higher GTP-binding, the S16H/C181S mutant failed to tether mTOR to lysosomes in nutrient starvation, indicating that farnesylation of hyperactive Rheb is indispensable for an effect on lysosomal mTORC1. This is in line with previous findings emphasizing its importance to Rheb, enabling it to activate mTOR at lysosomes [59,60,118].

The direct interaction between Rheb and mTOR has been previously reported to be independent of the nucleotide loading status of Rheb, although critical for its activity [116,119,120]. However, Rheb hyperactivity did have an effect on Rag-mTORC1 binding: Rheb overexpression counterintuitively decreased the association of mTOR with the RAGs, possibly triggering instability in their interaction. A possible hypothesis is that Rheb hyperactivity shifts the balance from Rag- to Rheb-dominant lysosomal tethering of mTORC1. It would be necessary to verify this finding in a TSC1/2 KO model, to ascertain whether this was an outcome of sequestration of mTORC1 away from available Rag binding surfaces due to high expression levels of Rheb, or if it can be recapitulated in a Rheb

hyperactive system with no increase in protein abundance.

In cells lacking the Rag GTPases, hyperactive Rheb still displayed the ability to sustain mTORC1 activity in the absence of amino acids. An interesting point of distinction was that, unlike in WT cells, in qKO cells WT Rheb did not display similar resistance to starvation as S16H. A possible explanation is that in the absence of the Rags there may be greater Rheb-dependent lysosomal localization of the TSC complex upon AA starvation, which can sterically inhibit Rheb-mTOR interaction [77].

Even more striking was the observation that in the absence of the Rags, hyperactive Rheb was sufficient to trigger lysosomal localization of mTORC1, suggesting that in the absence of intact lysosomal recruitment machinery, Rheb itself co-opts as a recruiting factor. A prior study had shown that exogenously supplied PA (phosphatidic acid) in the form of vesicles can induce lysosomal translocation of mTORC1 in a Rag- and Rheb-independent manner [121]. Further study is required to determine whether such a mechanism can occur in a cell-autonomous manner, downstream of Rheb hyperactivity. Additionally, AA-induced polyubiquitination of Rheb was found to enable lysosomal localization and activation of mTORC1 in Rag/Ragulator-deficient cells [122]. How Rheb ubiquitination interplays with its activation state, and whether this mechanism lies downstream of Rheb activity or in a parallel regulatory pathway remains to be elucidated.

The paradoxical regulation of lysosomal substrates (TFEB, TFE3) versus non-lysosomal substrates (S6K, 4E-BP1) of mTORC1, alluded to in the previous section, has been reported previously in the context of TSC1/2 knockouts [101,107]. Indeed, in line with these findings, I observed that overexpression of WT or active Rheb led to the same puzzling hypophosphorylation of TFEB and TFE3, while exhibiting hyperphosphorylation of S6K and 4E-BP1, implying that the effect observed in TSC KO cells is due to TSC GAP activity, or lack thereof, and not due to a GAP-independent phenomenon. In TSC KO, the FLCN-RagC axis has been implicated as the underlying cause for abolished TFEB phosphorylation, due to improper substrate recruitment to the lysosomal surface where mTOR is appropriately—rather, excessively localized [107,123]. It is noteworthy to mention that TFEB hypophosphorylation also persists in the presence of activating mTOR mutations, but the underlying cause is the aberrantly non-lysosomal localization of the kinase [124]. Whether

Rheb overexpression similarly impinges on FLCN-RagC, acting as yet another potential junction where Rags and Rheb branches overlap, remains to be seen. It is tempting to speculate that hyperactivity of Rheb may be affecting the formation of the lysosomal mTORC1-TFEB-Rag-Ragulator megacomplex, recently shown to involve a non-canonical Rag-Ragulator module and a requisite for TFEB phosphorylation [99], thus tipping the scales toward phosphorylation of cytosolic substrates as in the case of TSC KO.

Extending this line of thought further, a question that begs to be answered is why there is a disconnect between kinase localization and substrate phosphorylation in the case of hyperactive Rheb models, i.e., mTORC1 is enriched at lysosomes, even upon AA or glucose deprivation, but this is accompanied by phosphorylation of its cytosolic substrates. The lack of proper localization of TFEB/TFE3 for mTORC1 phosphorylation, mentioned above, still does not explain how Rheb-tethered lysosomally-activated mTORC1 exerts its activity on substrates located elsewhere. Several intriguing possibilities emerge, but there is no clear consensus to date: prior studies have contended that proximity to a Rheb-containing membrane is a pre-requisite for mTORC1 to remain catalytically active after its initial activation [21,125], yet it is conceivable that after the initial Rheb-mediated activation on lysosomes mTORC1 still retains its active conformation and functionality, for reasons enlisted further. Firstly, although my experiments, in line with previous findings, revealed that farnesylation and endomembrane anchorage of Rheb is necessary for mTORC1 activation, the farnesylation moiety has been shown to endow Rheb with the property of transiently interacting with endomembranes [61]. Targeting of Rheb to a specific endomembrane, thus prohibiting its dynamicity, has resulted in conflicting data in terms of its activatory potential toward mTORC1 [61,126]. This opens up the possibility for Rheb to leave the membrane in complex with mTORC1 after activating it, thus preserving its catalytic conformation. Further, farnesylation of Rheb has been shown to be dispensable for nuclear mTORC1 activity [126], again allowing for a mechanism in which activated mTORC1, in complex with Rheb, leaves lysosomes and exerts its activity in a subcellular location devoid of endomembrane anchorage. Secondly, PLD1 (Phospholipase D1) has been proposed to be an effector of Rheb that activates mTORC1 by locally generating PA at lysosomes [127-129]; PA is a phospholipid that can bind to the FRB domain of mTOR and has been shown to promote mTORC1 activity and stability [130-132]. Thus, it is conceivable that Rheb-induced PA

acts as an activating placeholder for Rheb and allows sustained activity of mTORC1 after it leaves the lysosomal surface [133].

The above ideas pertain to the population of mTORC1 that is activated at lysosomes, and subsequently released to meet its substrates elsewhere, as described in Results, Chapter 1. However, spatially distinct pools of mTORC1 that can be activated locally were recently shown to exist [106]. It is likely that these pools are also activated locally by Rheb, whose enrichment has been detected on several endomembranes beside lysosomes, such as Golgi, ER, peroxisomes, and mitochondria [60,61,118,134,135]. It is plausible that one or more pools of Rheb synergize to bring about lysosomal localization when hyperactive, considering that Rheb dynamically shuttles on and off endomembranes, or that inter-organelle contact sites play an essential role in bridging the interaction between lysosomal mTORC1 and Rheb located at a different endomembrane. Alternatively, perhaps the small but distinctly present pool of lysosomal Rheb is the only pool that has the capacity to retain mTORC1 because it works in collaboration with one or more participating proteins to mediate this effect. Further investigation is required to distinguish between these possibilities.

3.3 Summary

In Chapter 1, I showed that when mTORC1 activity is downregulated, either through pharmacological or genetic manipulation, it prevents the appropriate release of mTORC1 from lysosomes via a 'molecular switch' mechanism that involves the GATOR1-RagA axis, and is independent of Rheb (as it occurs even in RHEB KO cells). The lysosomal retention of mTORC1 increases activity toward its lysosomal substrates such as TFEB and TFE3 and decreases it toward non-lysosomal substrates such as S6K and 4E-BP1. In Chapter 2, I demonstrated that when the TSC-Rheb axis is hyperactive, either due to TSC loss-of-function or Rheb overexpression, mTORC1 is enriched at lysosomes in a manner independent of the Rag proteins, but dependent on Rheb, which causes hypophosphorylation of lysosomal substrates and hyperphosphorylation of non-lysosomal substrates. At the outset, these two sets of findings may appear contradictory. On the one hand, mTORC1 inhibition leads to its accumulation at the lysosomal surface; on the other hand, hyperactive mTORC1 also displays enhanced lysosomal localization. While at a superficial level this conundrum is apparent, upon closer inspection of the molecular

machinations at play, it begins to resolve itself.

By use of specific inhibitors of mTORC1, I concluded that it is the intrinsic catalytic activity of mTOR that is the driving force behind its release as it cycles on/off lysosomes. This was corroborated in an independent study from the Zwartkruis lab using base-edited kinase-dead or activating point mutants of mTOR, which were found to increase or decrease its lysosomal occupancy, respectively [124]. In direct contrast to the reduced lysosomal presence of activating mutants of mTOR, mTORC1 that is hyperactive due to inputs from the TSC-Rheb axis is found more enriched at lysosomes. Thus, the mode of mTORC1 activation (or suppression) is a crucial factor that defines its behavior. Importantly, catalytic inhibition of mTORC1 in TSC2 KO cells further enhances the lysosomal localization of mTOR [124] (see also Appendix B*)*, indicating that both mechanisms that govern localization are not mutually exclusive events.

Using Rheb overexpression as a surrogate for cells lacking a functional TSC, I illustrated that it is the activity of Rheb that triggers the forced lysosomal retention of mTOR. This further increases signaling toward downstream targets like S6K and 4E-BP1, while reducing signaling toward TFEB and TFE3. A simple explanation is that the former are Rheb-dependent substrates, while the latter are Rheb-independent. However, in addition to this categorization, an important consideration is that other molecular machineries are also altered in mTORC1 hyperactive models such as TSC loss-of-function, as elaborated on previously.

An interesting concept worth exploring is that it is the interplay between the two GTPases—Rags and Rheb— that directs the activity of mTORC1, by affecting its mode of lysosomal anchoring. Rag KO cells have fully abrogated signaling toward TFEB/TFE3, with little to no effect on S6K and 4E-BP1 [106]; whereas, RHEB KO cells have dramatically reduced levels of activity toward S6K and 4E-BP1, and heightened signaling toward TFEB/TFE3. Considering that the different spatially separated populations of mTORC1 are not fully disjunct, it is conceivable that the Rag GTPases keep mTORC1 activity focused on its lysosomal substrates, by actively controlling not just lysosomal recruitment but also release, whereas Rheb-dominated tethering promotes mTORC1 activity toward its non-lysosomal substrates. This likely allow cells to re-direct their metabolic programs in response to

nutrient cues or environmental stressors in a modular fashion.

In conclusion, this thesis contributes to existing knowledge about mTORC1 localization and activity, and how one influences the other to impart tighter regulation and fine-tuning of signaling. The findings shed new light on the existing model of the Rags and Rheb GTPases forming a 'coincidence detector' to activate mTORC1 by elucidating further functional overlap between the two axes, and emphasizing the amenable balance that should exist between the two upstream arms to synergistically regulate mTORC1 function.

3.4 Outlook

The insights gained from this thesis contribute to our understanding of the complexities of mTORC1 signaling, giving rise to lines of questioning and concepts that may be applied to other contexts. Below are some perspectives on how the findings of this thesis may be furthered and expanded.

The molecular underpinnings of the lysosomal enrichment of mTORC1 upon its inhibition have not been fully elucidated. Considering the mild but consistent differences in the effect of Rapamycin and Torin1 treatments on mTORC1 localization, it stands to reason that both Rapamycin-sensitive and Rapamycin-insensitive sites/substrates on lysosomes act in concert to regulate the dynamic shuttling of mTORC1 on and off lysosomes. This also hints at several different components of the lysosomal landscape being involved in a mTORC1-driven multisite phosphorylation to orchestrate its release. Characterization of the lysosomal mTORC1-dependent phosphoproteome is relevant, not only for comprehensively studying the details entailed in this mechanism, but also for the identification of novel mTORC1 lysosomal substrates. The molecular logic of the phenotype suggests that the involved mTORC1 targets are not dependent on amino acid presence or absence (if they were, lysosomal localization would take place in conditions of amino acid starvation), but sensitive to catalytic activity of mTORC1. This property can be harnessed when using proteomics approaches, for instance by comparing inhibitor-treated and -untreated samples in combination with amino acid starvation, as this would help the identification of low abundance but biologically relevant phosphosites that may otherwise be masked due to bulk phosphorylation in the samples. Further, techniques such as lysosomal phosphoproteomics can also be employed to enrich for the lysosomal

proteome, as it constitutes a small fraction of the total proteome, which would also help overcome technical issues associated with protein abundance.

Identification of the lysosomal 'signaling checkpoint' places mTORC1 at a unique position to strike a balance between its lysosomal and non-lysosomal activities, which equips cells with the potential to dynamically monitor intracellular processes to maintain homeostasis. A recent study from our lab showed that spatially distinct mTORC1 entities exist, which respond to different amino acid sources, with exogenous amino acids influencing mTORC1-dependent effects on anabolic processes such as translation, while lysosomal amino acids primarily promoting mTORC1-driven inhibition of catabolic processes such as lysosomal biogenesis and autophagy [106]. Indeed, one can envision scenarios in which cells switch their nutrition source while requiring cellular processes to carry on uninterrupted.

Studies on early embryogenesis have reported the transition from naïve to primed pluripotency entails increasing eIF4E-dependent translation (more cytosolic activity of mTORC1) and more nuclear exclusion of TFEB (more lysosomal activity of mTORC1) to exit pluripotency [136,137]. This critical transition happens against the backdrop of shifting amino acid sources from extracellular protein uptake to exogenous amino acids [138]. How mTORC1 maintains its balancing act, and whether the above-mentioned signaling checkpoint has a role to play in this transition are interesting topics that can be addressed by future studies.

I showed experimentally that cells with downregulated mTORC1 were unable to upregulate TFEB-dependent transcription or lysosomal biogenesis in response to prolonged glucose starvation, indicating that cells with mTORC1 inhibition may be unable to cope with nutrient stress. Applying this to a disease setting could mean higher efficacy of rapalogs when used against cancers that give rise to poorly vascularized tumors that are nutrient-depleted. However, it is important to note that in K-Ras-driven cancers, which exhibit induced macropinocytosis-mediated uptake of extracellular proteins, rapamycin had the opposite effect [139]. In fact, it benefited tumor survival by inhibiting mTORC1, releasing the inhibition on utilization of endocytosed proteins as a nutrient source. Thus, mTORC1 inhibitors based on rapamycin as therapeutic drugs must be used with caution and with a clear understanding of the genetic background of the disease.

In Rheb overexpressing cells, mTORC1 accumulations that colocalized at lysosomes were qualitatively observed to be more perinuclear in distribution. The positioning of lysosomes within cells has been found to be associated with their function, which in turn regulates mTORC1 signaling [140,141]. Further, a recent preprint suggested that in addition to Rheb-mediated activation of mTORC1, engagement with the lysosomal membrane itself allows for full activation of the complex [125], suggesting that different sizes of lysosomes, which have different membrane curvatures, could directly impact mTORC1 activation. Altered PA incorporation in membranes has also been suggested to affect membrane curvature [142], and thus its regulation could be an alternative means by which hyperactive Rheb boosts mTORC1 signaling. Overall, the crosstalk between hyperactive Rheb and lysosomal size, position, or identity, and how this translates to altered mTORC1 localization and activity needs to be elucidated further.

As the name implies, Rheb (Ras homolog enriched in brain) is found to be highly expressed in certain regions of the brain, such as cerebral cortex and hippocampus [143]. The finding that Rheb overexpression triggers desensitization to amino acids and glucose starvation, coupled with the fact that both glucose and branched chain amino acids (BCAA) are uptaken and utilized by different cell populations in the brain [144], raises the intriguing hypothesis that it is an additional strategy that spares the brain from entering a mode of starvation when either of the metabolites are low.

In a more pathophysiological context, glioblastoma cells, one of the most aggressive and common types of cancer in the brain are also found to highly express Rheb [145-148]. Further, cancers with genomic aberrations in Rheb are primarily due to copy number amplifications [149-151]. It would be of importance to assess how increased Rheb abundance impacts mTORC1 localization and activity, and whether this correlates with better or worse prognosis in these disease contexts.

4 Appendix A

Protein	Phosphosite	Rank of mTOR
DEPDC5	S445	1
	S503	32
	S579	21
	S833	1
	S1333	42
NPRL3	S189	35
	S476	23
RagC	S15	1
	S86	7
	T394	34
FLCN	S62	30
	S73	32
	S298	41
	S571	36
FNIP1	S174	29
	S214	34
	S296	38
FNIP2	S115	14
	S149	1
	S216	26
	S723	8
SLC38A9	S99	1

Table 1 enlisting several proteins involved in the mTORC1 signaling pathway with phosphosites for which mTOR highly ranked (>50) as a putative kinase based on the kinase prediction tool: The Kinase Library [108].

5 Appendix B

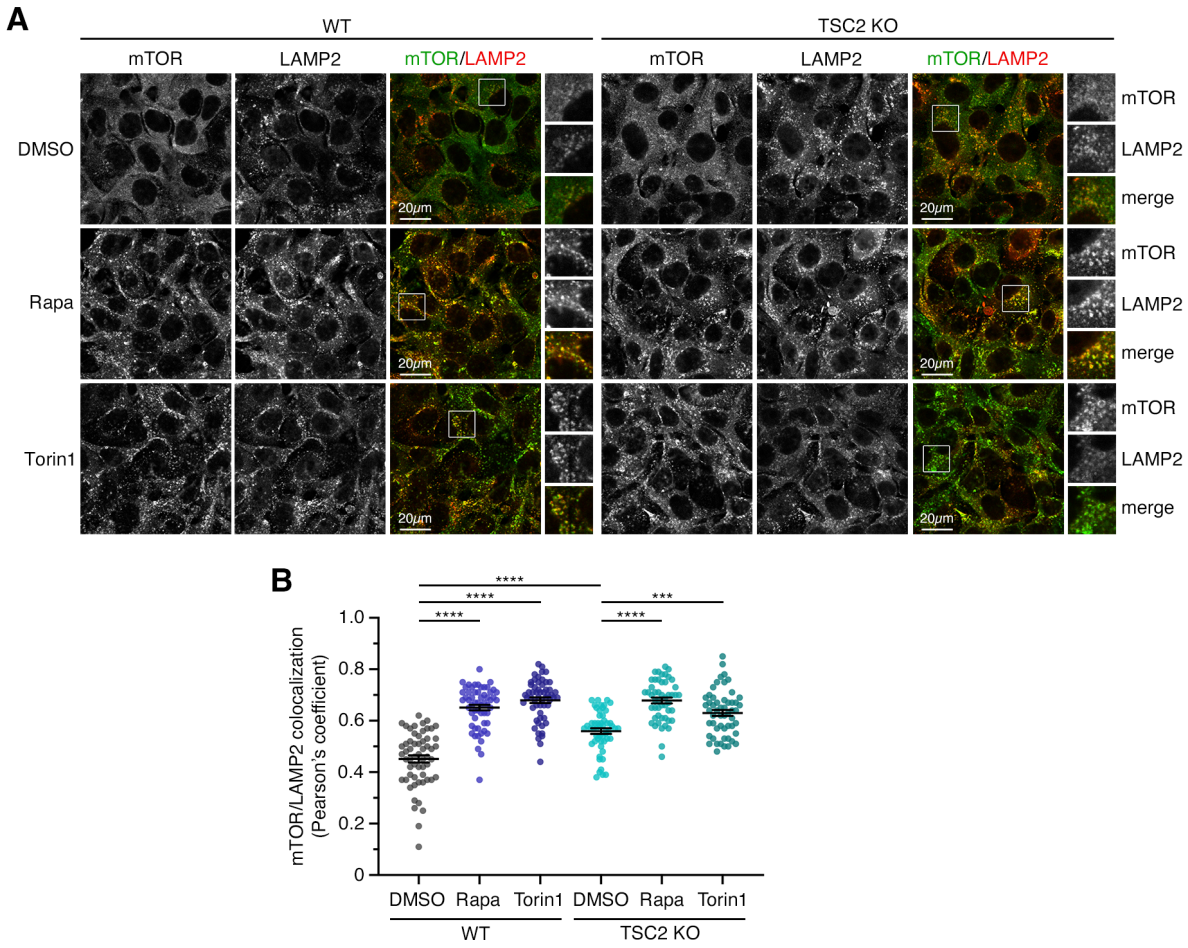

Figure 3. Pharmacological inhibition of mTORC1 further enhances the lysosomal presence of mTOR in TSC2 KO cells

(A-B) Colocalization analysis of mTOR with LAMP2 (lysosomal marker) in WT and TSC2 KO HEK293FT cells, treated with DMSO (vehicle), rapamycin (Rapa, 20 nM), or Torin1 (250 nM) for 1 h, using confocal microscopy. Scale bars = 20 μm. Magnified insets shown to the right (A). Quantification of colocalization in (B). Data shown as mean ± SEM. *** $p < 0.001$, **** $p < 0.0001$.

6 References

1. Chantranupong, L., Wolfson, R.L., and Sabatini, D.M. (2015). Nutrient-Sensing Mechanisms across Evolution. Cell *161*, 67-83. 10.1016/j.cell.2015.02.041.

2. Fernandes, S.A., and Demetriades, C. (2021). The Multifaceted Role of Nutrient Sensing and mTORC1 Signaling in Physiology and Aging. Front Aging *2*, 707372. 10.3389/fragi.2021.707372.

3. Liu, G.Y., and Sabatini, D.M. (2020). mTOR at the nexus of nutrition, growth, ageing and disease. Nat Rev Mol Cell Biol *21*, 183-203. 10.1038/s41580-019-0199-y.

4. Goul, C., Peruzzo, R., and Zoncu, R. (2023). The molecular basis of nutrient sensing and signalling by mTORC1 in metabolism regulation and disease. Nat Rev Mol Cell Biol *24*, 857-875. 10.1038/s41580-023-00641-8.

5. Heitman, J., Movva, N.R., and Hall, M.N. (1991). Targets for cell cycle arrest by the immunosuppressant rapamycin in yeast. Science *253*, 905-909. 10.1126/science.1715094.

6. Yang, H., Rudge, D.G., Koos, J.D., Vaidialingam, B., Yang, H.J., and Pavletich, N.P. (2013). mTOR kinase structure, mechanism and regulation. Nature *497*, 217-223. 10.1038/nature12122.

7. Guertin, D.A., Guntur, K.V., Bell, G.W., Thoreen, C.C., and Sabatini, D.M. (2006). Functional genomics identifies TOR-regulated genes that control growth and division. Curr Biol *16*, 958-970. 10.1016/j.cub.2006.03.084.

8. Peterson, T.R., Laplante, M., Thoreen, C.C., Sancak, Y., Kang, S.A., Kuehl, W.M., Gray, N.S., and Sabatini, D.M. (2009). DEPTOR is an mTOR inhibitor frequently overexpressed in multiple myeloma cells and required for their survival. Cell *137*, 873-886. 10.1016/j.cell.2009.03.046.

9. Walchli, M., Berneiser, K., Mangia, F., Imseng, S., Craigie, L.M., Stuttfeld, E., Hall, M.N., and Maier, T. (2021). Regulation of human mTOR complexes by DEPTOR. Elife *10*. 10.7554/eLife.70871.

10. Gao, D., Inuzuka, H., Tan, M.K., Fukushima, H., Locasale, J.W., Liu, P., Wan, L., Zhai, B., Chin, Y.R., Shaik, S., et al. (2011). mTOR drives its own activation via SCF(betaTrCP)-dependent degradation of the mTOR inhibitor DEPTOR. Mol Cell *44*, 290-303. 10.1016/j.molcel.2011.08.030.

11. Sancak, Y., Thoreen, C.C., Peterson, T.R., Lindquist, R.A., Kang, S.A., Spooner, E., Carr, S.A., and Sabatini, D.M. (2007). PRAS40 is an insulin-regulated inhibitor of the mTORC1 protein kinase. Mol Cell *25*, 903-915. 10.1016/j.molcel.2007.03.003.

12. Yang, H., Jiang, X., Li, B., Yang, H.J., Miller, M., Yang, A., Dhar, A., and Pavletich, N.P. (2017). Mechanisms of mTORC1 activation by RHEB and inhibition by PRAS40. Nature *552*, 368-373. 10.1038/nature25023.

13. Oshiro, N., Takahashi, R., Yoshino, K., Tanimura, K., Nakashima, A., Eguchi, S., Miyamoto, T., Hara, K., Takehana, K., Avruch, J., et al. (2007). The proline-rich Akt substrate of 40 kDa (PRAS40) is a physiological substrate of mammalian target of rapamycin complex 1. J Biol Chem *282*, 20329-20339. 10.1074/jbc.M702636200.

14. Sarbassov, D.D., Ali, S.M., Kim, D.H., Guertin, D.A., Latek, R.R., Erdjument-Bromage, H., Tempst, P., and Sabatini, D.M. (2004). Rictor, a novel binding partner of mTOR, defines a rapamycin-insensitive and raptor-independent pathway that regulates the cytoskeleton. Curr Biol *14*, 1296-1302. 10.1016/j.cub.2004.06.054.

15. Jacinto, E., Loewith, R., Schmidt, A., Lin, S., Ruegg, M.A., Hall, A., and Hall, M.N. (2004). Mammalian TOR complex 2 controls the actin cytoskeleton and is rapamycin insensitive. Nat Cell Biol *6*, 1122-1128. 10.1038/ncb1183.

16. Stuttfeld, E., Aylett, C.H., Imseng, S., Boehringer, D., Scaiola, A., Sauer, E., Hall, M.N., Maier, T., and Ban, N. (2018). Architecture of the human mTORC2 core complex. Elife *7*. 10.7554/eLife.33101.

17. Aylett, C.H., Sauer, E., Imseng, S., Boehringer, D., Hall, M.N., Ban, N., and Maier, T. (2016). Architecture of human mTOR complex 1. Science *351*, 48-52. 10.1126/science.aaa3870.

18. Yip, C.K., Murata, K., Walz, T., Sabatini, D.M., and Kang, S.A. (2010). Structure of the human mTOR complex I and its implications for rapamycin inhibition. Mol Cell *38*, 768-774. 10.1016/j.molcel.2010.05.017.

19. Battaglioni, S., Benjamin, D., Walchli, M., Maier, T., and Hall, M.N. (2022). mTOR substrate phosphorylation in growth control. Cell *185*, 1814-1836. 10.1016/j.cell.2022.04.013.

20. Sancak, Y., Peterson, T.R., Shaul, Y.D., Lindquist, R.A., Thoreen, C.C., Bar-Peled, L., and Sabatini, D.M. (2008). The Rag GTPases bind raptor and mediate amino acid signaling to mTORC1. Science *320*, 1496-1501. 10.1126/science.1157535.

21. Lawrence, R.E., Cho, K.F., Rappold, R., Thrun, A., Tofaute, M., Kim, D.J., Moldavski, O., Hurley, J.H., and Zoncu, R. (2018). A nutrient-induced affinity switch controls mTORC1 activation by its Rag GTPase-Ragulator lysosomal scaffold. Nat Cell Biol *20*, 1052-1063. 10.1038/s41556-018-0148-6.

22. Liu, X., and Zheng, X.F. (2007). Endoplasmic reticulum and Golgi localization sequences for mammalian target of rapamycin. Mol Biol Cell *18*, 1073-1082. 10.1091/mbc.e06-05-0406.

23. Ramanathan, A., and Schreiber, S.L. (2009). Direct control of mitochondrial function by mTOR. Proc Natl Acad Sci U S A *106*, 22229-22232. 10.1073/pnas.0912074106.

24. Schieke, S.M., Phillips, D., McCoy, J.P., Jr., Aponte, A.M., Shen, R.F., Balaban, R.S., and Finkel, T. (2006). The mammalian target of rapamycin (mTOR) pathway regulates mitochondrial oxygen consumption and oxidative capacity. J Biol Chem *281*, 27643-27652. 10.1074/jbc.M603536200.

25. Giguere, V. (2018). Canonical signaling and nuclear activity of mTOR-a teamwork effort to regulate metabolism and cell growth. FEBS J *285*, 1572-1588. 10.1111/febs.14384.

26. Zhang, X., Shu, L., Hosoi, H., Murti, K.G., and Houghton, P.J. (2002). Predominant nuclear localization of mammalian target of rapamycin in normal and malignant cells in culture. J Biol Chem *277*, 28127-28134. 10.1074/jbc.M202625200.

27. Bachmann, R.A., Kim, J.H., Wu, A.L., Park, I.H., and Chen, J. (2006). A nuclear transport signal in mammalian target of rapamycin is critical for its cytoplasmic signaling to S6 kinase 1. J Biol Chem *281*, 7357-7363. 10.1074/jbc.M512218200.

28. Audet-Walsh, E., Dufour, C.R., Yee, T., Zouanat, F.Z., Yan, M., Kalloghlian, G., Vernier, M., Caron, M., Bourque, G., Scarlata, E., et al. (2017). Nuclear mTOR acts as a transcriptional integrator of the androgen signaling pathway in prostate cancer. Genes Dev *31*, 1228-1242. 10.1101/gad.299958.117.

29. Rabanal-Ruiz, Y., Byron, A., Wirth, A., Madsen, R., Sedlackova, L., Hewitt, G., Nelson, G., Stingele, J., Wills, J.C., Zhang, T., et al. (2021). mTORC1 activity is supported by spatial association with focal adhesions. J Cell Biol *220*. 10.1083/jcb.202004010.

30. Vezina, C., Kudelski, A., and Sehgal, S.N. (1975). Rapamycin (AY-22,989), a new antifungal antibiotic. I. Taxonomy of the producing streptomycete and isolation of the active principle. J Antibiot (Tokyo) *28*, 721-726. 10.7164/antibiotics.28.721.

31. Martel, R.R., Klicius, J., and Galet, S. (1977). Inhibition of the immune response by rapamycin, a new antifungal antibiotic. Can J Physiol Pharmacol *55*, 48-51. 10.1139/y77-007.

32. Kang, S.A., Pacold, M.E., Cervantes, C.L., Lim, D., Lou, H.J., Ottina, K., Gray, N.S., Turk, B.E., Yaffe, M.B., and Sabatini, D.M. (2013). mTORC1 phosphorylation sites encode their sensitivity to starvation and rapamycin. Science *341*, 1236566. 10.1126/science.1236566.

33. Thoreen, C.C., Chantranupong, L., Keys, H.R., Wang, T., Gray, N.S., and Sabatini, D.M. (2012). A unifying model for mTORC1-mediated regulation of mRNA translation. Nature *485*, 109-113. 10.1038/nature11083.

34. Kim, E., Goraksha-Hicks, P., Li, L., Neufeld, T.P., and Guan, K.L. (2008). Regulation of TORC1 by Rag GTPases in nutrient response. Nat Cell Biol *10*, 935-945. 10.1038/ncb1753.

35. Sekiguchi, T., Hirose, E., Nakashima, N., Ii, M., and Nishimoto, T. (2001). Novel G

proteins, Rag C and Rag D, interact with GTP-binding proteins, Rag A and Rag B. J Biol Chem *276*, 7246-7257. 10.1074/jbc.M004389200.

36. Gollwitzer, P., Grutzmacher, N., Wilhelm, S., Kummel, D., and Demetriades, C. (2022). A Rag GTPase dimer code defines the regulation of mTORC1 by amino acids. Nat Cell Biol *24*, 1394-1406. 10.1038/s41556-022-00976-y.

37. Figlia, G., Muller, S., Hagenston, A.M., Kleber, S., Roiuk, M., Quast, J.P., Ten Bosch, N., Carvajal Ibanez, D., Mauceri, D., Martin-Villalba, A., and Teleman, A.A. (2022). Brain-enriched RagB isoforms regulate the dynamics of mTORC1 activity through GATOR1 inhibition. Nat Cell Biol *24*, 1407-1421. 10.1038/s41556-022-00977-x.

38. Sancak, Y., Bar-Peled, L., Zoncu, R., Markhard, A.L., Nada, S., and Sabatini, D.M. (2010). Ragulator-Rag complex targets mTORC1 to the lysosomal surface and is necessary for its activation by amino acids. Cell *141*, 290-303. 10.1016/j.cell.2010.02.024.

39. Nada, S., Hondo, A., Kasai, A., Koike, M., Saito, K., Uchiyama, Y., and Okada, M. (2009). The novel lipid raft adaptor p18 controls endosome dynamics by anchoring the MEK-ERK pathway to late endosomes. EMBO J *28*, 477-489. 10.1038/emboj.2008.308.

40. Sanders, S.S., De Simone, F.I., and Thomas, G.M. (2019). mTORC1 Signaling Is Palmitoylation-Dependent in Hippocampal Neurons and Non-neuronal Cells and Involves Dynamic Palmitoylation of LAMTOR1 and mTOR. Front Cell Neurosci *13*, 115. 10.3389/fncel.2019.00115.

41. Bar-Peled, L., Schweitzer, L.D., Zoncu, R., and Sabatini, D.M. (2012). Ragulator is a GEF for the rag GTPases that signal amino acid levels to mTORC1. Cell *150*, 1196-1208. 10.1016/j.cell.2012.07.032.

42. Shen, K., and Sabatini, D.M. (2018). Ragulator and SLC38A9 activate the Rag GTPases through noncanonical GEF mechanisms. Proc Natl Acad Sci U S A *115*, 9545-9550. 10.1073/pnas.1811727115.

43. Jung, J., Genau, H.M., and Behrends, C. (2015). Amino Acid-Dependent mTORC1 Regulation by the Lysosomal Membrane Protein SLC38A9. Mol Cell Biol *35*, 2479-2494. 10.1128/MCB.00125-15.

44. Rebsamen, M., Pochini, L., Stasyk, T., de Araujo, M.E., Galluccio, M., Kandasamy, R.K., Snijder, B., Fauster, A., Rudashevskaya, E.L., Bruckner, M., et al. (2015). SLC38A9 is a component of the lysosomal amino acid sensing machinery that controls mTORC1. Nature *519*, 477-481. 10.1038/nature14107.

45. Wang, S., Tsun, Z.Y., Wolfson, R.L., Shen, K., Wyant, G.A., Plovanich, M.E., Yuan, E.D., Jones, T.D., Chantranupong, L., Comb, W., et al. (2015). Metabolism. Lysosomal amino acid transporter SLC38A9 signals arginine sufficiency to mTORC1. Science *347*, 188-194. 10.1126/science.1257132.

46. Wyant, G.A., Abu-Remaileh, M., Wolfson, R.L., Chen, W.W., Freinkman, E., Danai, L.V., Vander Heiden, M.G., and Sabatini, D.M. (2017). mTORC1 Activator SLC38A9 Is Required to Efflux Essential Amino Acids from Lysosomes and Use Protein as a Nutrient. Cell *171*, 642-654 e612. 10.1016/j.cell.2017.09.046.

47. Lei, H.T., Ma, J., Sanchez Martinez, S., and Gonen, T. (2018). Crystal structure of arginine-bound lysosomal transporter SLC38A9 in the cytosol-open state. Nat Struct Mol Biol *25*, 522-527. 10.1038/s41594-018-0072-2.

48. Fromm, S.A., Lawrence, R.E., and Hurley, J.H. (2020). Structural mechanism for amino acid-dependent Rag GTPase nucleotide state switching by SLC38A9. Nat Struct Mol Biol *27*, 1017-1023. 10.1038/s41594-020-0490-9.

49. Song, Q., Meng, B., Xu, H., and Mao, Z. (2020). The emerging roles of vacuolar-type ATPase-dependent Lysosomal acidification in neurodegenerative diseases. Transl Neurodegener *9*, 17. 10.1186/s40035-020-00196-0.

50. Zoncu, R., Bar-Peled, L., Efeyan, A., Wang, S., Sancak, Y., and Sabatini, D.M. (2011). mTORC1 senses lysosomal amino acids through an inside-out mechanism that requires the vacuolar H(+)-ATPase. Science *334*, 678-683. 10.1126/science.1207056.

51. Chung, C.Y., Shin, H.R., Berdan, C.A., Ford, B., Ward, C.C., Olzmann, J.A., Zoncu, R., and Nomura, D.K. (2019). Covalent targeting of the vacuolar H(+)-ATPase activates autophagy via mTORC1 inhibition. Nat Chem Biol *15*, 776-785. 10.1038/s41589-019-0308-4.

52. Bar-Peled, L., Chantranupong, L., Cherniack, A.D., Chen, W.W., Ottina, K.A., Grabiner, B.C., Spear, E.D., Carter, S.L., Meyerson, M., and Sabatini, D.M. (2013). A Tumor suppressor complex with GAP activity for the Rag GTPases that signal amino acid sufficiency to mTORC1. Science *340*, 1100-1106. 10.1126/science.1232044.

53. Egri, S.B., Ouch, C., Chou, H.T., Yu, Z., Song, K., Xu, C., and Shen, K. (2022). Cryo-EM structures of the human GATOR1-Rag-Ragulator complex reveal a spatial-constraint regulated GAP mechanism. Mol Cell *82*, 1836-1849 e1835. 10.1016/j.molcel.2022.03.002.

54. Jiang, C., Dai, X., He, S., Zhou, H., Fang, L., Guo, J., Liu, S., Zhang, T., Pan, W., Yu, H., et al. (2023). Ring domains are essential for GATOR2-dependent mTORC1 activation. Mol Cell *83*, 74-89 e79. 10.1016/j.molcel.2022.11.021.

55. Wolfson, R.L., Chantranupong, L., Wyant, G.A., Gu, X., Orozco, J.M., Shen, K., Condon, K.J., Petri, S., Kedir, J., Scaria, S.M., et al. (2017). KICSTOR recruits GATOR1 to the lysosome and is necessary for nutrients to regulate mTORC1. Nature *543*, 438-442. 10.1038/nature21423.

56. Zhao, T., Guan, Y., Xu, C., Wang, D., Guan, J., and Liu, Y. (2023). VWCE modulates amino acid-dependent mTOR signaling and coordinates with KICSTOR to recruit GATOR1 to the lysosomes. Nat Commun *14*, 8464. 10.1038/s41467-023-44241-8.

57. Yu, Y., Li, S., Xu, X., Li, Y., Guan, K., Arnold, E., and Ding, J. (2005). Structural basis for the unique biological function of small GTPase RHEB. J Biol Chem *280*, 17093-17100. 10.1074/jbc.M501253200.

58. Hancock, J.F., Paterson, H., and Marshall, C.J. (1990). A polybasic domain or palmitoylation is required in addition to the CAAX motif to localize p21ras to the plasma membrane. Cell *63*, 133-139. 10.1016/0092-8674(90)90294-o.

59. Basso, A.D., Mirza, A., Liu, G., Long, B.J., Bishop, W.R., and Kirschmeier, P. (2005). The farnesyl transferase inhibitor (FTI) SCH66336 (lonafarnib) inhibits Rheb farnesylation and mTOR signaling. Role in FTI enhancement of taxane and tamoxifen anti-tumor activity. J Biol Chem *280*, 31101-31108. 10.1074/jbc.M503763200.

60. Hanker, A.B., Mitin, N., Wilder, R.S., Henske, E.P., Tamanoi, F., Cox, A.D., and Der, C.J. (2010). Differential requirement of CAAX-mediated posttranslational processing for Rheb localization and signaling. Oncogene *29*, 380-391. 10.1038/onc.2009.336.

61. Angarola, B., and Ferguson, S.M. (2019). Weak membrane interactions allow Rheb to activate mTORC1 signaling without major lysosome enrichment. Mol Biol Cell *30*, 2750-2760. 10.1091/mbc.E19-03-0146.

62. Sato, T., Nakashima, A., Guo, L., and Tamanoi, F. (2009). Specific activation of mTORC1 by Rheb G-protein in vitro involves enhanced recruitment of its substrate protein. J Biol Chem *284*, 12783-12791. 10.1074/jbc.M809207200.

63. Tabancay, A.P., Jr., Gau, C.L., Machado, I.M., Uhlmann, E.J., Gutmann, D.H., Guo, L., and Tamanoi, F. (2003). Identification of dominant negative mutants of Rheb GTPase and their use to implicate the involvement of human Rheb in the activation of p70S6K. J Biol Chem *278*, 39921-39930. 10.1074/jbc.M306553200.

64. Hansmann, P., Bruckner, A., Kiontke, S., Berkenfeld, B., Seebohm, G., Brouillard, P., Vikkula, M., Jansen, F.E., Nellist, M., Oeckinghaus, A., and Kummel, D. (2020). Structure of the TSC2 GAP Domain: Mechanistic Insight into Catalysis and Pathogenic Mutations. Structure *28*, 933-942 e934. 10.1016/j.str.2020.05.008.

65. Yang, H., Yu, Z., Chen, X., Li, J., Li, N., Cheng, J., Gao, N., Yuan, H.X., Ye, D., Guan, K.L., and Xu, Y. (2021). Structural insights into TSC complex assembly and GAP activity on Rheb. Nat Commun *12*, 339. 10.1038/s41467-020-20522-4.

66. Garami, A., Zwartkruis, F.J., Nobukuni, T., Joaquin, M., Roccio, M., Stocker, H., Kozma, S.C., Hafen, E., Bos, J.L., and Thomas, G. (2003). Insulin activation of Rheb, a mediator of mTOR/S6K/4E-BP signaling, is inhibited by TSC1 and 2. Mol Cell *11*, 1457-1466. 10.1016/s1097-2765(03)00220-x.

67. Inoki, K., Li, Y., Xu, T., and Guan, K.L. (2003). Rheb GTPase is a direct target of TSC2 GAP activity and regulates mTOR signaling. Genes Dev *17*, 1829-1834. 10.1101/gad.1110003.

68. Chong-Kopera, H., Inoki, K., Li, Y., Zhu, T., Garcia-Gonzalo, F.R., Rosa, J.L., and Guan,

K.L. (2006). TSC1 stabilizes TSC2 by inhibiting the interaction between TSC2 and the HERC1 ubiquitin ligase. J Biol Chem *281*, 8313-8316. 10.1074/jbc.C500451200.

69. Woodford, M.R., Sager, R.A., Marris, E., Dunn, D.M., Blanden, A.R., Murphy, R.L., Rensing, N., Shapiro, O., Panaretou, B., Prodromou, C., et al. (2017). Tumor suppressor Tsc1 is a new Hsp90 co-chaperone that facilitates folding of kinase and non-kinase clients. EMBO J *36*, 3650-3665. 10.15252/embj.201796700.

70. Gai, Z., Chu, W., Deng, W., Li, W., Li, H., He, A., Nellist, M., and Wu, G. (2016). Structure of the TBC1D7-TSC1 complex reveals that TBC1D7 stabilizes dimerization of the TSC1 C-terminal coiled coil region. J Mol Cell Biol *8*, 411-425. 10.1093/jmcb/mjw001.

71. Duvel, K., Yecies, J.L., Menon, S., Raman, P., Lipovsky, A.I., Souza, A.L., Triantafellow, E., Ma, Q., Gorski, R., Cleaver, S., et al. (2010). Activation of a metabolic gene regulatory network downstream of mTOR complex 1. Mol Cell *39*, 171-183. 10.1016/j.molcel.2010.06.022.

72. Valvezan, A.J., and Manning, B.D. (2019). Molecular logic of mTORC1 signalling as a metabolic rheostat. Nat Metab *1*, 321-333. 10.1038/s42255-019-0038-7.

73. Demetriades, C., Plescher, M., and Teleman, A.A. (2016). Lysosomal recruitment of TSC2 is a universal response to cellular stress. Nat Commun *7*, 10662. 10.1038/ncomms10662.

74. Tee, A.R., Manning, B.D., Roux, P.P., Cantley, L.C., and Blenis, J. (2003). Tuberous sclerosis complex gene products, Tuberin and Hamartin, control mTOR signaling by acting as a GTPase-activating protein complex toward Rheb. Curr Biol *13*, 1259-1268. 10.1016/s0960-9822(03)00506-2.

75. Roux, P.P., Ballif, B.A., Anjum, R., Gygi, S.P., and Blenis, J. (2004). Tumor-promoting phorbol esters and activated Ras inactivate the tuberous sclerosis tumor suppressor complex via p90 ribosomal S6 kinase. Proc Natl Acad Sci U S A *101*, 13489-13494. 10.1073/pnas.0405659101.

76. Menon, S., Dibble, C.C., Talbott, G., Hoxhaj, G., Valvezan, A.J., Takahashi, H., Cantley, L.C., and Manning, B.D. (2014). Spatial control of the TSC complex integrates insulin and nutrient regulation of mTORC1 at the lysosome. Cell *156*, 771-785. 10.1016/j.cell.2013.11.049.

77. Carroll, B., Maetzel, D., Maddocks, O.D., Otten, G., Ratcliff, M., Smith, G.R., Dunlop, E.A., Passos, J.F., Davies, O.R., Jaenisch, R., et al. (2016). Control of TSC2-Rheb signaling axis by arginine regulates mTORC1 activity. Elife *5*. 10.7554/eLife.11058.

78. Demetriades, C., Doumpas, N., and Teleman, A.A. (2014). Regulation of TORC1 in response to amino acid starvation via lysosomal recruitment of TSC2. Cell *156*, 786-799. 10.1016/j.cell.2014.01.024.

79. Fitzian, K., Bruckner, A., Brohee, L., Zech, R., Antoni, C., Kiontke, S., Gasper, R.,

Linard Matos, A.L., Beel, S., Wilhelm, S., et al. (2021). TSC1 binding to lysosomal PIPs is required for TSC complex translocation and mTORC1 regulation. Mol Cell *81*, 2705-2721 e2708. 10.1016/j.molcel.2021.04.019.

80. Prentzell, M.T., Rehbein, U., Cadena Sandoval, M., De Meulemeester, A.S., Baumeister, R., Brohee, L., Berdel, B., Bockwoldt, M., Carroll, B., Chowdhury, S.R., et al. (2021). G3BPs tether the TSC complex to lysosomes and suppress mTORC1 signaling. Cell *184*, 655-674 e627. 10.1016/j.cell.2020.12.024.

81. Bayly-Jones, C., Lupton, C.J., D'Andrea, L., Chang, Y.G., Jones, G.D., Steele, J.R., Venugopal, H., Schittenhelm, R.B., Halls, M.L., and Ellisdon, A.M. (2024). Structure of the human TSC:WIPI3 lysosomal recruitment complex. Sci Adv *10*, eadr5807. 10.1126/sciadv.adr5807.

82. Chantranupong, L., Wolfson, R.L., Orozco, J.M., Saxton, R.A., Scaria, S.M., Bar-Peled, L., Spooner, E., Isasa, M., Gygi, S.P., and Sabatini, D.M. (2014). The Sestrins interact with GATOR2 to negatively regulate the amino-acid-sensing pathway upstream of mTORC1. Cell Rep *9*, 1-8. 10.1016/j.celrep.2014.09.014.

83. Shen, K., Choe, A., and Sabatini, D.M. (2017). Intersubunit Crosstalk in the Rag GTPase Heterodimer Enables mTORC1 to Respond Rapidly to Amino Acid Availability. Mol Cell *68*, 552-565 e558. 10.1016/j.molcel.2017.09.026.

84. Meng, J., and Ferguson, S.M. (2018). GATOR1-dependent recruitment of FLCN-FNIP to lysosomes coordinates Rag GTPase heterodimer nucleotide status in response to amino acids. J Cell Biol *217*, 2765-2776. 10.1083/jcb.201712177.

85. Hardie, D.G., Ross, F.A., and Hawley, S.A. (2012). AMPK: a nutrient and energy sensor that maintains energy homeostasis. Nat Rev Mol Cell Biol *13*, 251-262. 10.1038/nrm3311.

86. Gwinn, D.M., Shackelford, D.B., Egan, D.F., Mihaylova, M.M., Mery, A., Vasquez, D.S., Turk, B.E., and Shaw, R.J. (2008). AMPK phosphorylation of raptor mediates a metabolic checkpoint. Mol Cell *30*, 214-226. 10.1016/j.molcel.2008.03.003.

87. Dai, X., Jiang, C., Jiang, Q., Fang, L., Yu, H., Guo, J., Yan, P., Chi, F., Zhang, T., Inuzuka, H., et al. (2023). AMPK-dependent phosphorylation of the GATOR2 component WDR24 suppresses glucose-mediated mTORC1 activation. Nat Metab *5*, 265-276. 10.1038/s42255-022-00732-4.

88. Orozco, J.M., Krawczyk, P.A., Scaria, S.M., Cangelosi, A.L., Chan, S.H., Kunchok, T., Lewis, C.A., and Sabatini, D.M. (2020). Dihydroxyacetone phosphate signals glucose availability to mTORC1. Nat Metab *2*, 893-901. 10.1038/s42255-020-0250-5.

89. Li, M., Zhang, C.S., Feng, J.W., Wei, X., Zhang, C., Xie, C., Wu, Y., Hawley, S.A., Atrih, A., Lamont, D.J., et al. (2021). Aldolase is a sensor for both low and high glucose, linking to AMPK and mTORC1. Cell Res *31*, 478-481. 10.1038/s41422-020-00456-8.

90. Kovacina, K.S., Park, G.Y., Bae, S.S., Guzzetta, A.W., Schaefer, E., Birnbaum, M.J., and Roth, R.A. (2003). Identification of a proline-rich Akt substrate as a 14-3-3 binding partner. J Biol Chem *278*, 10189-10194. 10.1074/jbc.M210837200.

91. Shah, O.J., Wang, Z., and Hunter, T. (2004). Inappropriate activation of the TSC/Rheb/mTOR/S6K cassette induces IRS1/2 depletion, insulin resistance, and cell survival deficiencies. Curr Biol *14*, 1650-1656. 10.1016/j.cub.2004.08.026.

92. Yu, Y., Yoon, S.O., Poulogiannis, G., Yang, Q., Ma, X.M., Villen, J., Kubica, N., Hoffman, G.R., Cantley, L.C., Gygi, S.P., and Blenis, J. (2011). Phosphoproteomic analysis identifies Grb10 as an mTORC1 substrate that negatively regulates insulin signaling. Science *332*, 1322-1326. 10.1126/science.1199484.

93. Gingras, A.C., Gygi, S.P., Raught, B., Polakiewicz, R.D., Abraham, R.T., Hoekstra, M.F., Aebersold, R., and Sonenberg, N. (1999). Regulation of 4E-BP1 phosphorylation: a novel two-step mechanism. Genes Dev *13*, 1422-1437. 10.1101/gad.13.11.1422.

94. Fuentes, P., Pelletier, J., Martinez-Herraez, C., Diez-Obrero, V., Iannizzotto, F., Rubio, T., Garcia-Cajide, M., Menoyo, S., Moreno, V., Salazar, R., et al. (2021). The 40S-LARP1 complex reprograms the cellular translatome upon mTOR inhibition to preserve the protein synthetic capacity. Sci Adv *7*, eabg9275. 10.1126/sciadv.abg9275.

95. Saba, J.A., Huang, Z., Schole, K.L., Ye, X., Bhatt, S.D., Li, Y., Timp, W., Cheng, J., and Green, R. (2024). LARP1 binds ribosomes and TOP mRNAs in repressed complexes. EMBO J *43*, 6555-6572. 10.1038/s44318-024-00294-z.

96. Moustafa-Kamal, M., Kucharski, T.J., El-Assaad, W., Abbas, Y.M., Gandin, V., Nagar, B., Pelletier, J., Topisirovic, I., and Teodoro, J.G. (2020). The mTORC1/S6K/PDCD4/eIF4A Axis Determines Outcome of Mitotic Arrest. Cell Rep *33*, 108230. 10.1016/j.celrep.2020.108230.

97. Dorrello, N.V., Peschiaroli, A., Guardavaccaro, D., Colburn, N.H., Sherman, N.E., and Pagano, M. (2006). S6K1- and betaTRCP-mediated degradation of PDCD4 promotes protein translation and cell growth. Science *314*, 467-471. 10.1126/science.1130276.

98. Napolitano, G., Di Malta, C., Esposito, A., de Araujo, M.E.G., Pece, S., Bertalot, G., Matarese, M., Benedetti, V., Zampelli, A., Stasyk, T., et al. (2020). A substrate-specific mTORC1 pathway underlies Birt-Hogg-Dube syndrome. Nature *585*, 597-602. 10.1038/s41586-020-2444-0.

99. Cui, Z., Napolitano, G., de Araujo, M.E.G., Esposito, A., Monfregola, J., Huber, L.A., Ballabio, A., and Hurley, J.H. (2023). Structure of the lysosomal mTORC1-TFEB-Rag-Ragulator megacomplex. Nature *614*, 572-579. 10.1038/s41586-022-05652-7.

100. Puertollano, R., Ferguson, S.M., Brugarolas, J., and Ballabio, A. (2018). The complex relationship between TFEB transcription factor phosphorylation and subcellular localization. EMBO J *37*. 10.15252/embj.201798804.

101. Alesi, N., Khabibullin, D., Rosenthal, D.M., Akl, E.W., Cory, P.M., Alchoueiry, M., Salem, S., Daou, M., Gibbons, W.F., Chen, J.A., et al. (2024). TFEB drives mTORC1 hyperactivation and kidney disease in Tuberous Sclerosis Complex. Nat Commun *15*, 406. 10.1038/s41467-023-44229-4.

102. Roczniak-Ferguson, A., Petit, C.S., Froehlich, F., Qian, S., Ky, J., Angarola, B., Walther, T.C., and Ferguson, S.M. (2012). The transcription factor TFEB links mTORC1 signaling to transcriptional control of lysosome homeostasis. Sci Signal *5*, ra42. 10.1126/scisignal.2002790.

103. Ganley, I.G., Lam du, H., Wang, J., Ding, X., Chen, S., and Jiang, X. (2009). ULK1.ATG13.FIP200 complex mediates mTOR signaling and is essential for autophagy. J Biol Chem *284*, 12297-12305. 10.1074/jbc.M900573200.

104. Nuchel, J., Tauber, M., Nolte, J.L., Morgelin, M., Turk, C., Eckes, B., Demetriades, C., and Plomann, M. (2021). An mTORC1-GRASP55 signaling axis controls unconventional secretion to reshape the extracellular proteome upon stress. Mol Cell *81*, 3275-3293 e3212. 10.1016/j.molcel.2021.06.017.

105. Zhou, X., Li, S., and Zhang, J. (2016). Tracking the Activity of mTORC1 in Living Cells Using Genetically Encoded FRET-based Biosensor TORCAR. Curr Protoc Chem Biol *8*, 225-233. 10.1002/cpch.11.

106. Fernandes, S.A., Angelidaki, D.D., Nuchel, J., Pan, J., Gollwitzer, P., Elkis, Y., Artoni, F., Wilhelm, S., Kovacevic-Sarmiento, M., and Demetriades, C. (2024). Spatial and functional separation of mTORC1 signalling in response to different amino acid sources. Nat Cell Biol *26*, 1918-1933. 10.1038/s41556-024-01523-7.

107. Alesi, N., Akl, E.W., Khabibullin, D., Liu, H.J., Nidhiry, A.S., Garner, E.R., Filippakis, H., Lam, H.C., Shi, W., Viswanathan, S.R., et al. (2021). TSC2 regulates lysosome biogenesis via a non-canonical RAGC and TFEB-dependent mechanism. Nat Commun *12*, 4245. 10.1038/s41467-021-24499-6.

108. Johnson, J.L., Yaron, T.M., Huntsman, E.M., Kerelsky, A., Song, J., Regev, A., Lin, T.Y., Liberatore, K., Cizin, D.M., Cohen, B.M., et al. (2023). An atlas of substrate specificities for the human serine/threonine kinome. Nature *613*, 759-766. 10.1038/s41586-022-05575-3.

109. Abu-Remaileh, M., Wyant, G.A., Kim, C., Laqtom, N.N., Abbasi, M., Chan, S.H., Freinkman, E., and Sabatini, D.M. (2017). Lysosomal metabolomics reveals V-ATPase- and mTOR-dependent regulation of amino acid efflux from lysosomes. Science *358*, 807-813. 10.1126/science.aan6298.

110. Kulak, N.A., Pichler, G., Paron, I., Nagaraj, N., and Mann, M. (2014). Minimal, encapsulated proteomic-sample processing applied to copy-number estimation in eukaryotic cells. Nat Methods *11*, 319-324. 10.1038/nmeth.2834.

111. Zhang, Y., Gao, X., Saucedo, L.J., Ru, B., Edgar, B.A., and Pan, D. (2003). Rheb is a direct target of the tuberous sclerosis tumour suppressor proteins. Nat Cell Biol *5*,

578-581. 10.1038/ncb999.

112. Parmar, N., and Tamanoi, F. (2010). Rheb G-Proteins and the Activation of mTORC1. Enzymes *27*, 39-56. 10.1016/S1874-6047(10)27003-8.

113. Traut, T.W. (1994). Physiological concentrations of purines and pyrimidines. Mol Cell Biochem *140*, 1-22. 10.1007/BF00928361.

114. Yan, L., Findlay, G.M., Jones, R., Procter, J., Cao, Y., and Lamb, R.F. (2006). Hyperactivation of mammalian target of rapamycin (mTOR) signaling by a gain-of-function mutant of the Rheb GTPase. J Biol Chem *281*, 19793-19797. 10.1074/jbc.C600028200.

115. Deng, L., Chen, L., Zhao, L., Xu, Y., Peng, X., Wang, X., Ding, L., Jin, J., Teng, H., Wang, Y., et al. (2019). Ubiquitination of Rheb governs growth factor-induced mTORC1 activation. Cell Res *29*, 136-150. 10.1038/s41422-018-0120-9.

116. Long, X., Lin, Y., Ortiz-Vega, S., Yonezawa, K., and Avruch, J. (2005). Rheb binds and regulates the mTOR kinase. Curr Biol *15*, 702-713. 10.1016/j.cub.2005.02.053.

117. Takahashi, K., Nakagawa, M., Young, S.G., and Yamanaka, S. (2005). Differential membrane localization of ERas and Rheb, two Ras-related proteins involved in the phosphatidylinositol 3-kinase/mTOR pathway. J Biol Chem *280*, 32768-32774. 10.1074/jbc.M506280200.

118. Buerger, C., DeVries, B., and Stambolic, V. (2006). Localization of Rheb to the endomembrane is critical for its signaling function. Biochem Biophys Res Commun *344*, 869-880. 10.1016/j.bbrc.2006.03.220.

119. Long, X., Ortiz-Vega, S., Lin, Y., and Avruch, J. (2005). Rheb binding to mammalian target of rapamycin (mTOR) is regulated by amino acid sufficiency. J Biol Chem *280*, 23433-23436. 10.1074/jbc.C500169200.

120. Smith, E.M., Finn, S.G., Tee, A.R., Browne, G.J., and Proud, C.G. (2005). The tuberous sclerosis protein TSC2 is not required for the regulation of the mammalian target of rapamycin by amino acids and certain cellular stresses. J Biol Chem *280*, 18717-18727. 10.1074/jbc.M414499200.

121. Frias, M.A., Mukhopadhyay, S., Lehman, E., Walasek, A., Utter, M., Menon, D., and Foster, D.A. (2020). Phosphatidic acid drives mTORC1 lysosomal translocation in the absence of amino acids. J Biol Chem *295*, 263-274. 10.1074/jbc.RA119.010892.

122. Yao, Y., Hong, S., Ikeda, T., Mori, H., MacDougald, O.A., Nada, S., Okada, M., and Inoki, K. (2020). Amino Acids Enhance Polyubiquitination of Rheb and Its Binding to mTORC1 by Blocking Lysosomal ATXN3 Deubiquitinase Activity. Mol Cell *80*, 437-451 e436. 10.1016/j.molcel.2020.10.004.

123. Asrani, K., Woo, J., Mendes, A.A., Schaffer, E., Vidotto, T., Villanueva, C.R., Feng, K., Oliveira, L., Murali, S., Liu, H.B., et al. (2022). An mTORC1-mediated negative

feedback loop constrains amino acid-induced FLCN-Rag activation in renal cells with TSC2 loss. Nat Commun *13*, 6808. 10.1038/s41467-022-34617-7.

124. Zwakenberg, S., Westland, D., van Es, R.M., Rehmann, H., Anink, J., Ciapaite, J., Bosma, M., Stelloo, E., Liv, N., Sobrevals Alcaraz, P., et al. (2024). mTORC1 restricts TFE3 activity by auto-regulating its presence on lysosomes. Mol Cell *84*, 4368-4384 e4366. 10.1016/j.molcel.2024.10.009.

125. Cui, Z., Esposito, A., Napolitano, G., Ballabio, A., and Hurley, J.H. (2024). Structural basis for growth factor and nutrient signal integration on the lysosomal membrane by mTORC1. bioRxiv. 10.1101/2024.11.15.623810.

126. Zhong, Y., Zhou, X., Guan, K.L., and Zhang, J. (2022). Rheb regulates nuclear mTORC1 activity independent of farnesylation. Cell Chem Biol *29*, 1037-1045 e1034. 10.1016/j.chembiol.2022.02.006.

127. Sun, Y., Fang, Y., Yoon, M.S., Zhang, C., Roccio, M., Zwartkruis, F.J., Armstrong, M., Brown, H.A., and Chen, J. (2008). Phospholipase D1 is an effector of Rheb in the mTOR pathway. Proc Natl Acad Sci U S A *105*, 8286-8291. 10.1073/pnas.0712268105.

128. Fang, Y., Vilella-Bach, M., Bachmann, R., Flanigan, A., and Chen, J. (2001). Phosphatidic acid-mediated mitogenic activation of mTOR signaling. Science *294*, 1942-1945. 10.1126/science.1066015.

129. Bernfeld, E., Menon, D., Vaghela, V., Zerin, I., Faruque, P., Frias, M.A., and Foster, D.A. (2018). Phospholipase D-dependent mTOR complex 1 (mTORC1) activation by glutamine. J Biol Chem *293*, 16390-16401. 10.1074/jbc.RA118.004972.

130. Rodriguez Camargo, D.C., Link, N.M., and Dames, S.A. (2012). The FKBP-rapamycin binding domain of human TOR undergoes strong conformational changes in the presence of membrane mimetics with and without the regulator phosphatidic acid. Biochemistry *51*, 4909-4921. 10.1021/bi3002133.

131. Toschi, A., Lee, E., Xu, L., Garcia, A., Gadir, N., and Foster, D.A. (2009). Regulation of mTORC1 and mTORC2 complex assembly by phosphatidic acid: competition with rapamycin. Mol Cell Biol *29*, 1411-1420. 10.1128/MCB.00782-08.

132. Veverka, V., Crabbe, T., Bird, I., Lennie, G., Muskett, F.W., Taylor, R.J., and Carr, M.D. (2008). Structural characterization of the interaction of mTOR with phosphatidic acid and a novel class of inhibitor: compelling evidence for a central role of the FRB domain in small molecule-mediated regulation of mTOR. Oncogene *27*, 585-595. 10.1038/sj.onc.1210693.

133. Frias, M.A., Hatipoglu, A., and Foster, D.A. (2023). Regulation of mTOR by phosphatidic acid. Trends Endocrinol Metab *34*, 170-180. 10.1016/j.tem.2023.01.004.

134. Hao, F., Kondo, K., Itoh, T., Ikari, S., Nada, S., Okada, M., and Noda, T. (2018). Rheb

localized on the Golgi membrane activates lysosome-localized mTORC1 at the Golgi-lysosome contact site. J Cell Sci *131*. 10.1242/jcs.208017.

135. Zhang, J., Kim, J., Alexander, A., Cai, S., Tripathi, D.N., Dere, R., Tee, A.R., Tait-Mulder, J., Di Nardo, A., Han, J.M., et al. (2013). A tuberous sclerosis complex signalling node at the peroxisome regulates mTORC1 and autophagy in response to ROS. Nat Cell Biol *15*, 1186-1196. 10.1038/ncb2822.

136. Chen, C., Zhang, X., Wang, Y., Chen, X., Chen, W., Dan, S., She, S., Hu, W., Dai, J., Hu, J., et al. (2022). Translational and post-translational control of human naive versus primed pluripotency. iScience *25*, 103645. 10.1016/j.isci.2021.103645.

137. Betschinger, J., Nichols, J., Dietmann, S., Corrin, P.D., Paddison, P.J., and Smith, A. (2013). Exit from pluripotency is gated by intracellular redistribution of the bHLH transcription factor Tfe3. Cell *153*, 335-347. 10.1016/j.cell.2013.03.012.

138. Todorova, P.K., Jackson, B.T., Garg, V., Paras, K.I., Brunner, J.S., Bridgeman, A.E., Chen, Y., Baksh, S.C., Yan, J., Hadjantonakis, A.K., and Finley, L.W.S. (2024). Amino acid intake strategies define pluripotent cell states. Nat Metab *6*, 127-140. 10.1038/s42255-023-00940-6.

139. Palm, W., Park, Y., Wright, K., Pavlova, N.N., Tuveson, D.A., and Thompson, C.B. (2015). The Utilization of Extracellular Proteins as Nutrients Is Suppressed by mTORC1. Cell *162*, 259-270. 10.1016/j.cell.2015.06.017.

140. Korolchuk, V.I., Saiki, S., Lichtenberg, M., Siddiqi, F.H., Roberts, E.A., Imarisio, S., Jahreiss, L., Sarkar, S., Futter, M., Menzies, F.M., et al. (2011). Lysosomal positioning coordinates cellular nutrient responses. Nat Cell Biol *13*, 453-460. 10.1038/ncb2204.

141. Ebner, M., Puchkov, D., Lopez-Ortega, O., Muthukottiappan, P., Su, Y., Schmied, C., Zillmann, S., Nikonenko, I., Koddebusch, J., Dornan, G.L., et al. (2023). Nutrient-regulated control of lysosome function by signaling lipid conversion. Cell *186*, 5328-5346 e5326. 10.1016/j.cell.2023.09.027.

142. Bills, B.L., and Knowles, M.K. (2022). Phosphatidic Acid Accumulates at Areas of Curvature in Tubulated Lipid Bilayers and Liposomes. Biomolecules *12*. 10.3390/biom12111707.

143. Yamagata, K., Sanders, L.K., Kaufmann, W.E., Yee, W., Barnes, C.A., Nathans, D., and Worley, P.F. (1994). rheb, a growth factor- and synaptic activity-regulated gene, encodes a novel Ras-related protein. J Biol Chem *269*, 16333-16339.

144. Sweatt, A.J., Garcia-Espinosa, M.A., Wallin, R., and Hutson, S.M. (2004). Branched-chain amino acids and neurotransmitter metabolism: expression of cytosolic branched-chain aminotransferase (BCATc) in the cerebellum and hippocampus. J Comp Neurol *477*, 360-370. 10.1002/cne.20200.

145. Uhlen, M., Fagerberg, L., Hallstrom, B.M., Lindskog, C., Oksvold, P., Mardinoglu, A.,

Sivertsson, A., Kampf, C., Sjostedt, E., Asplund, A., et al. (2015). Proteomics. Tissue-based map of the human proteome. Science *347*, 1260419. 10.1126/science.1260419.

146. Thul, P.J., Akesson, L., Wiking, M., Mahdessian, D., Geladaki, A., Ait Blal, H., Alm, T., Asplund, A., Bjork, L., Breckels, L.M., et al. (2017). A subcellular map of the human proteome. Science *356*. 10.1126/science.aal3321.

147. Sjostedt, E., Zhong, W., Fagerberg, L., Karlsson, M., Mitsios, N., Adori, C., Oksvold, P., Edfors, F., Limiszewska, A., Hikmet, F., et al. (2020). An atlas of the protein-coding genes in the human, pig, and mouse brain. Science *367*. 10.1126/science.aay5947.

148. Karlsson, M., Zhang, C., Mear, L., Zhong, W., Digre, A., Katona, B., Sjostedt, E., Butler, L., Odeberg, J., Dusart, P., et al. (2021). A single-cell type transcriptomics map of human tissues. Sci Adv *7*. 10.1126/sciadv.abh2169.

149. Cerami, E., Gao, J., Dogrusoz, U., Gross, B.E., Sumer, S.O., Aksoy, B.A., Jacobsen, A., Byrne, C.J., Heuer, M.L., Larsson, E., et al. (2012). The cBio cancer genomics portal: an open platform for exploring multidimensional cancer genomics data. Cancer Discov *2*, 401-404. 10.1158/2159-8290.CD-12-0095.

150. Gao, J., Aksoy, B.A., Dogrusoz, U., Dresdner, G., Gross, B., Sumer, S.O., Sun, Y., Jacobsen, A., Sinha, R., Larsson, E., et al. (2013). Integrative analysis of complex cancer genomics and clinical profiles using the cBioPortal. Sci Signal *6*, pl1. 10.1126/scisignal.2004088.

151. de Bruijn, I., Kundra, R., Mastrogiacomo, B., Tran, T.N., Sikina, L., Mazor, T., Li, X., Ochoa, A., Zhao, G., Lai, B., et al. (2023). Analysis and Visualization of Longitudinal Genomic and Clinical Data from the AACR Project GENIE Biopharma Collaborative in cBioPortal. Cancer Res *83*, 3861-3867. 10.1158/0008-5472.CAN-23-0816.

7 List of Abbreviations

4E-BP1	4E-binding protein 1
AA	amino acids
AMPK	5'-AMP-activated protein kinase
ATG13	autophagy-related protein 13
ATG14	autophagy-related protein 14
BSA	bovine serum albumin
CASTOR1/2	cytosolic arginine sensor for mTORC1
CDK1	cyclin-dependent kinase 1
cDNA	complementary DNA
CLEAR	coordinated lysosomal expression and regulation
DEPDC5	DEP domain-containing 5
DEPTOR	DEP-domain-containing mTOR-interacting protein
dFBS	dialyzed FBS
DMEM	Dulbecco’s modified eagle medium
DTT	dithiothreitol
eIF4A	eukaryotic initiation factor 4A
eIF4B	eukaryotic initiation factor 4B
eIF4E	eukaryotic initiation factor 4E
eIF4G	eukaryotic initiation factor 4G

ERK1/2	extracellular signal-regulated kinases
FAT	FRAP, ATM, TRRAP
FBS	fetal bovine serum
FIP200	200-kDa FAK family kinase-interacting protein
FKBP12	FK506-binding protein 12
FLCN	folliculin
FNIP1/2	FLCN-interacting proteins 1 and 2
FOXO	forkhead box proteins
FRB	FKBP-Rapamycin-binding
G3BPs	Ras GTPase-activating protein-binding proteins
GAP	GTPase-activating protein domain
GAPDH	glyceraldehyde-3-phosphate dehydrogenase
GATOR1	GAP activity towards Rags 1
GATOR2	GAP activity towards Rags 2
GDP	guanosine diphosphate
GEF	guanine exchange factors
GF	growth factors
GRB10	growth factor receptor-bound protein 10
GTP	guanosine triphosphate
HA	hemagglutinin
HEAT	Huntingtin, EF3, PP2A, TOR1

HEK	human embryonic kidney
IPTG	isopropyl-β-D-thiogalactopyranoside
IRS1/2	insulin receptor substrate 1/2
ITFG2	integrin-α FG-GAP repeat containing 2
IVK	*in vitro* kinase assay
KO	knockout
KPTN	Kaptin
LOH	loss-of-heterozygosity
MEFs	murine embryonic fibroblasts
MEK	mitogen-activated protein kinase kinase
MIOS	meiosis regulator for oocyte development
mLST8	mammalian lethal with SEC13 protein 8
mSIN1	mammalian stress-activated protein kinase-interacting protein 1
mTOR	mechanistic target of Rapamycin
mTORC1	mTOR Complex 1
mTORC2	mTOR Complex 2
NaF	sodium fluoride
NPRL2	nitrogen permease regulator-like 2
NPRL3	nitrogen permease regulator-like 3
P/S	penicillin-streptomycin
PCR	polymerase chain reaction

PDPK1	phosphoinositide-dependent protein kinase 1
PH	pleckstrin-homology
PI3K	phosphatidylinositol 3-kinase
PIK3CA	phosphatidylinositol 3-kinase catalytic subunit
PIP	phosphatidylinositol phosphate
PIP2	phosphatidylinositol (4,5)-trisphosphate
PIP3	phosphatidylinositol (3,4,5)-trisphosphate
PKB/AKT	protein kinase B
PP	protein phosphatase
PRAS40	proline-rich AKT substrate 40 kDa
PTEN	phosphatidylinositol 3,4,5-trisphosphate 3-phosphatase and dual-specificity protein phosphatase
RAF	rapidly accelerated fibrosarcoma
RAGs	Ras-related GTP-binding proteins
RAPTOR	regulatory-associated protein of mTOR
RAS	rat sarcoma
RHEB	Ras-homolog enriched in brain
RICTOR	rapamycin-independent companion of mTOR
RPS6	ribosomal protein S6
RSK1/2	p90 ribosomal S6 kinases 1/2
RT-qPCR	reverse transcription quantitative real-time PCR

S6	ribosomal protein S6
S6K1	p70 S6 Kinase 1
SD	standard deviation
SDS-PAGE	sodium dodecyl sulphate polyacrylamide gel electrophoresis
SEC13	sec13 homolog nuclear pore and COPII coat complex component
SEH1L	seh1 like nucleoporin
SEM	standard error of the mean
SGK1	serine/threonine-protein kinase SGK1
siRNAs	small interfering RNAs
SLC38A9	sodium-coupled neutral amino acid transporter 9
SZT2	C12orf66 and seizure threshold 2
TBC1D7	TBC1 domain family member 7
TFE3	transcription factor E3
TFEB	transcription factor EB
TOP	terminal oligopyrimidine tract
TOS	TOR signaling motifs
TSC	tuberous sclerosis complex
TSC1	tuberous sclerosis complex 1
TSC2	tuberous sclerosis complex 2
ULK1	serine/threonine-protein kinase ULK1
WDR24	WD repeat domain 24

WDR59	WD repeat domain 59
WT	wild-type